

On Observables in Supersymmetric Gauge Theories

Robert Mooney

A thesis submitted in partial fulfillment of the
requirements of the Degree of
Doctor of Philosophy

Thesis Supervisor
Andreas Brandhuber

Centre for Research in String Theory
School of Physics and Astronomy
Queen Mary, University of London
Mile End Road, London, E14NS

September 2014

Abstract

There has been great progress in recent years in the understanding of the mathematical structure of scattering amplitudes in Quantum Field Theory as well as the development of powerful methods for their calculation, particularly in the arena of $\mathcal{N} = 4$ Super Yang-Mills where hidden and manifest symmetries lead to striking simplifications. In this thesis, we will discuss the extensions of such methods away from the case of on-shell amplitudes in conformal $\mathcal{N} = 4$.

After introducing the necessary mathematical background and physical setting, we consider in Chapter Three the form factors of BPS operators in $\mathcal{N} = 4$ Super Yang-Mills. These objects have several physical applications, and share many properties with scattering amplitudes. However, they are off-shell, which makes them a natural starting point to set out in the direction of correlation functions. After demonstrating the computation of form factors by BCFW recursion and unitarity based methods, we go on to show how the scalar form factor can be supersymmetrised to encompass the full stress-tensor multiplet.

In Chapter Four, we discuss the Sudakov form factor in ABJM Theory. This object, which first appears at two loops and controls the IR divergences of the theory, is computed by generalised unitarity. In particular, we note that the maximal transcendentality of three dimensional integrals is related to particular triple cuts.

Finally, in Chapter Five we consider massive amplitudes on the Coulomb Branch of $\mathcal{N} = 4$ at one loop. Here we find that vertex cut conditions inherited from the embedding of the theory in String Theory lead to a restricted class of massive integrals.

Contents

1	Introduction	8
2	Scattering Amplitudes and Other Observables	12
2.1	Colour Ordering and the Planar Limit	12
2.2	The Spinor Helicity Formalism	14
2.3	Computing Amplitudes at Tree Level	17
2.3.1	The BCFW Recursion Relations	18
2.3.2	The MHV Vertex Expansion	22
2.4	Computing Amplitudes at Loop Level	24
2.4.1	The Unitarity Based Method	25
2.4.2	Examples	26
2.4.3	Generalized Unitarity	30
2.5	Methods for Evaluating Feynman Integrals	31
2.5.1	Reduction to Master Integrals	31
2.5.2	Feynman Parameters	36
2.5.3	Mellin-Barnes	38

2.5.4	Infrared Divergences	41
2.6	Wilson Loops	44
2.6.1	Divergences and Renormalization	45
2.6.2	Lightlike Contours	46
2.7	Form Factors	48
3	Computable Models	52
3.1	Superconformal Symmetry	52
3.1.1	Conformal Transformations	53
3.1.2	Conformal Primaries	55
3.1.3	Correlation Functions	56
3.1.4	Superconformal Symmetry	57
3.1.5	Classical and Quantum CFTs	59
3.2	$\mathcal{N} = 4$ Super Yang-Mills	60
3.2.1	Superamplitudes	62
3.2.2	Amplitudes on The Coulomb Branch	65
3.2.3	BPS Operators	68
3.2.4	Form Factors	68
3.2.5	Hidden Symmetries and Dualities	72
3.3	ABJM Theory	77
3.3.1	The Spinor Helicity Formalism in Three Dimensions	79
3.3.2	Superamplitudes	81

3.3.3	The Four-Point Amplitude at One and Two Loops	82
3.3.4	Colour Ordering	85
3.3.5	Half-BPS operators	86
4	Super Form Factors in $\mathcal{N} = 4$ Super Yang-Mills	89
4.1	Tree-level methods	90
4.1.1	MHV diagrams	90
4.1.2	Recursion relations	93
4.2	Supersymmetric form factors and Ward identities	105
4.2.1	Form factor of the chiral stress-tensor multiplet operator . . .	106
4.2.2	Examples	110
4.2.3	Form factor of the complete stress-tensor multiplet	114
4.3	Supersymmetric methods	117
4.3.1	Supersymmetric MHV rules	117
4.3.2	Supersymmetric recursion relations	119
4.3.3	Supersymmetric unitarity-based method	120
4.3.4	Examples	123
4.3.5	Higher-loop diagrams	127
5	The Sudakov Form Factor in ABJM	131
5.1	The complete one-loop amplitude	132
5.1.1	Results	132
5.1.2	Symmetry properties of the one-loop amplitude	133

5.1.3	Derivation of the complete one-loop amplitude from cuts . . .	133
5.2	The Sudakov form factor at one and two loops	136
5.2.1	One-loop form factor in ABJM	137
5.2.2	Two-loop form factor in ABJM	138
5.3	Maximally transcendental integrals in 3d	147
6	Massive Amplitudes on the Coulomb Branch	150
6.1	One-Loop 4-Point Integrand from Unitarity	150
6.1.1	Three-Vertex Cuts and the Basis of Integrals	153
6.1.2	Coefficients	154
6.2	Higher Point Amplitudes	155
6.3	The Two-Loop Integrand	156
A	A Menagerie of Integral Functions	158
A.1	Massless Scalar Box Functions	158
A.2	Scalar Triangles	159
A.3	Transcendental Integrals In Three Dimensions	160
A.4	Massive Boxes in Four Dimensions	162
B	Material Ancillary to Chapters 4 and 5	165
B.1	Vanishing of form factors at large z	165
B.1.1	Bosonic form factors	165
B.1.2	Supersymmetric form factors	166

B.2	Dual MHV rules	168
B.3	Properties of the box integral in ABJM	170
B.3.1	Rotation by 90°	170
B.3.2	An identity for the s -channel cuts of $I(1, 2, 3, 4)$ and $I(1, 2, 4, 3)$	172

Declaration

I hereby declare that the material presented in this thesis is my work, except where stated otherwise, and is the result of collaborations with Andreas Brandhuber, Omer Gurdogan, Dimitrios Korres, Gabriele Travaglini and Gang Yang.

Chapter 1

Introduction

Although the venerable formalism of Feynman diagrams remains a useful tool in many contexts, it does not respect the physical symmetries of the theory in question at each intermediate step of the calculation. This causes particular issues in non-Abelian gauge theories, where one must sum up vast numbers of diagrams to recover results expressed as simple gauge invariant expressions. There has been tremendous progress in recent years in understanding the structure of scattering amplitudes in such theories and in perturbative quantum gravity by the use of new methods in which physical symmetries are manifest throughout.

The central plank thereof, the unitarity based method, is not a new idea; indeed, it was at the heart of the old S-matrix theory [1]. That program failed on account of its fundamentalism; far more data is required to construct the full S-matrix. However, in the 1990s a key development was made through the work of Bern, Dixon, Dunbar and Kosower [2] who realised that by combining unitarity with known facts deriving from the Feynman rules and dimensional regularization one could construct one-loop (and higher) amplitudes from tree-level ones. It would take a decade for the state of the art at tree level to catch up, beginning with the work of Witten [3] on the twistor space

structure of scattering amplitudes which led to a flurry of interest from Theorists and subsequently the development of MHV diagrams [4] and recursive on-shell methods [5] for the construction of tree-level amplitudes.

These have been applied to gauge theory, and have been absolutely critical in computing QCD background processes at the LHC, where the automated BlackHat [6] code has enabled a vast array of one-loop amplitudes to be computed. In a completely orthogonal direction, the discovery of colour-kinematic duality [7] has enabled a detailed appraisal of the UV behaviour of the S-matrix of several supergravity theories.

In $\mathcal{N} = 4$ Super-Yang-Mills we have gone much further. In addition to the significant computational aid provided by maximal supersymmetry, application of these methods has led to the discovery of hidden symmetries of the S-matrix that are completely invisible at the level of the Lagrangian. In particular, dual superconformal symmetry [8] not only strongly constrains scattering amplitudes but suggests a beautiful internal duality (or triality) also incorporating Wilson loops [9] [10] and certain correlation functions [11].

In parallel programs of research, a Grassmannian formalism [12] [13] based on on-shell diagrams has been developed to compute in principle the complete S-matrix integrand; while the number-theoretic properties of the theory have been exploited via the symbol map to compute loop amplitudes directly without reference to Feynman integrals [14]. These developments have uncovered relations to many areas of mathematics including the theory of motives and cluster algebras. The relation of these on-shell properties to the integrability observed for the correlation functions of certain operators remains an intriguing question.

Exciting as these developments are, a key question is the following: how much is dependent on the particular qualities of the $\mathcal{N} = 4$ S-Matrix? If we consider other theories, or off-shell quantities, do we expect any of these properties to survive? If so,

which? Rather than being ambitious in this regard, we here confine ourselves to the minimal departure from the familiar realm. Form factors are in some sense a minimal departure from on-shell scattering amplitudes; indeed, they may be regarded as the amplitudes arising from coupling to off-shell currents. By restricting ourselves to the case of BPS operators we avoid the presence of ultraviolet singularities which may complicate our analysis. They also can be regarded as building blocks for correlation functions in the context of generalized unitarity, a direction which has been fruitfully explored by [15]. By considering amplitudes on the Coulomb Branch of the theory, we leave the realm of massless particles and remove the formerly vital crutch of conformal symmetry, but do so in a highly controlled way which allows us to still exploit much of what we have left behind.

ABJM Theory at first glance seems a very different arena to any Yang-Mills theory since in a Chern-Simons-Matter Theory in $(2 + 1)$ -dimensions the dynamical degrees of freedom do not include the gauge field, but consist of (bi-)fundamental matter. However, it bears the same relation to M -Theory that $\mathcal{N} = 4$ bears to Type IIB String Theory; and has a fairly straightforward holographic dual on $AdS_4 \times CP^3$. In this sense the theories can be said to be cousins and like its cousin ABJM Theory exhibits many remarkable properties in its S-matrix including a form of dual superconformal symmetry. It provides a fascinating parallel laboratory for the study of scattering amplitudes.

The outline of this thesis is as follows. In Chapter Two we review modern methods for the computation of scattering amplitudes and introduce other observables of interest. In Chapter Three we review the superconformal theories in which these methods reveal startling hidden structures that both motivate and enable our work. These provide a foundation for what follows. In Chapter Four we discuss results concerning the form factors of $\mathcal{N} = 4$ sYM, in particular their supersymmetric extension and a

large class of solutions to their tree-level recursion relation, largely following [16]. In Chapter Five we switch to ABJM Theory and in particular the computation of the Sudakov form factor which was presented in [17]. Finally, in Chapter Six, we return to $\mathcal{N} = 4$, this time on the Coulomb Branch, to examine the one-loop amplitudes with massive external states.

Chapter 2

Scattering Amplitudes and Other Observables

In this chapter our focus is on the description of the modern methods for computing scattering amplitudes and other observables to which they are related. Our approach is to be so far as possible agnostic with respect to the particular theory with which we work, although our examples (being the simplest cases) are principally drawn from $\mathcal{N} = 4$ sYM. We work here principally in four dimensions in dimensional regularization, although much what is said is valid in any number of dimensions (see 3.3.1 for the three dimensional formalism).

2.1 Colour Ordering and the Planar Limit

The structure of scattering amplitudes is more clearly elucidated if they are decomposed into smaller gauge-invariant objects with a particular cyclic ordering of external legs [18]. This not only describes the dependence of the amplitude on group-theoretic data, but these objects are also analytically simpler than the full amplitude since

their poles and branch cuts can only arise in channels formed from cyclically adjacent momenta.

In an $SU(N)$ gauge theory, gluons (and their superpartners) transform in the adjoint representation carrying the index $a = 1, \dots, N^2 - 1$; if there is (anti-)fundamental matter (quarks) in the theory they carry (anti-)fundamental indices $i(\bar{j}) = 1, \dots, N$. From the Feynman rules we see that the three-gluon vertex produces a factor of the structure constant f^{abc} , and the four-point vertex contributes a contraction of two structure constants. The three-point gluon-quark-antiquark vertex carries a factor of the gauge group generator $(T^a)_{i\bar{j}}$. Propagators in colour space take the form of delta functions contracting their endpoints; a gluon propagator carries δ_{ab} and a quark propagator carries $\delta^{\bar{j}i}$. We may then replace the structure constants which appear with generators using the defining relation

$$f^{abc} = -\frac{i}{\sqrt{2}} \text{Tr}[T^a, [T^b, T^c]] \quad (2.1.1)$$

which will leave us with a long string of traces. These can be simplified by application of the identity

$$(T^a)_{i\bar{j}_1} (T^a)_{i\bar{j}_2} = \delta_{i\bar{j}_1}^{\bar{j}_2} \delta_{i\bar{j}_2}^{\bar{j}_1} - \frac{1}{N} \delta_{i\bar{j}_1}^{\bar{j}_1} \delta_{i\bar{j}_2}^{\bar{j}_2} \quad (2.1.2)$$

where summation over the adjoint index is implicit. In this way all structure constants may be written as sums over single-traces of generators. We may write the full amplitude as a sum over colour ordered partial amplitudes multiplied by a colour trace, which for a purely gluonic amplitude at tree level takes the form:

$$\mathcal{A}_n^{(0)}(p_i, h_i, a_i) = \sum_{\sigma \in S_n/Z_n} \text{Tr}(T^{a_{\sigma(1)}} \dots T^{a_{\sigma(n)}}) A_n^{(0)}(\sigma(1)^{h_{\sigma(1)}}, \dots, \sigma(n)^{h_{\sigma(n)}}). \quad (2.1.3)$$

The partial amplitudes A_n depend on the cyclic ordering of the external momenta and contain all the kinematic dependence of the amplitude. All the colour dependence is contained in the sum over traces, which must avoid double-counting the cyclic permutations which leave the trace invariant.

Beyond tree level, the colour structure is enriched by the presence of multi-trace structures. For instance, at one loop the colour decomposition takes the form

$$\begin{aligned}
\mathcal{A}^{(1)}(1, \dots, n) &= \mathcal{A}_P^{(1)} + \mathcal{A}_{NP}^{(1)} \\
&= N \sum_{\sigma \in S_n/Z_n} \text{Tr}(T^{a_{\sigma 1}} \dots T^{a_{\sigma n}}) A_{n;1}^{(1)}(1, \dots, n) \\
&\quad + \sum_{\sigma \in S_n/S_{n;c}} \sum_{c=2}^{n/2+1} \text{Tr}(T^{a_{\sigma 1}} \dots T^{a_{\sigma c-1}}) \text{Tr}(T^{a_{\sigma c} a_{\sigma n}}) A_{n;c}(1, \dots, n). \quad (2.1.4)
\end{aligned}$$

Note that in the limit $N \rightarrow \infty$ the single trace term dominates producing a large simplification. This regime, called the *planar limit*, will be the principle focus of our subsequent study.

2.2 The Spinor Helicity Formalism

In order to solve any problem in an efficient way, it is necessary to use an efficient notation. For scattering amplitudes involving massless particles, this is accomplished by exploiting the properties of spinors to implicitly impose the on-shell mass condition $p_i^2 = 0$. Our discussion here largely follows that of [3].

Recall that the complexified Lorentz Group is locally isomorphic to $SL(2) \times SL(2)$, whose finite dimensional representations are classified by the integers (p, q) . Spinors in the $(1/2, 0)$ are written λ_α , and those in the $(0, 1/2)$ as $\tilde{\lambda}_{\dot{\alpha}}$. Spinor indices are raised and lowered with $\epsilon_{\alpha\beta}$ and it's inverse, and likewise for dotted indices. Hence, we can define the Lorentz invariant spinor products:

$$\langle ij \rangle = \epsilon_{\alpha\beta} \lambda_i^\alpha \lambda_j^\beta \quad (2.2.1)$$

$$[ij] = \epsilon_{\dot{\alpha}\dot{\beta}} \tilde{\lambda}_i^{\dot{\alpha}} \tilde{\lambda}_j^{\dot{\beta}} \quad (2.2.2)$$

in terms of which we will write scattering amplitudes. Note that these are antisymmetric; $\langle ij \rangle = -\langle ji \rangle$ and that parity conjugation exchanges λ_α and $\tilde{\lambda}_{\dot{\alpha}}$.

Since spinors are two dimensional objects, we can write

$$\lambda_k = a\lambda_i + b\lambda_j. \quad (2.2.3)$$

Contracting with either λ_i or λ_j allows us to solve for the coefficients a, b to find:

$$\lambda_k = \frac{\langle kj \rangle \lambda_i + \langle ik \rangle \lambda_j}{\langle ij \rangle}. \quad (2.2.4)$$

Contracting with a fourth spinor λ_l we obtain the Schouten identity:

$$\langle ij \rangle \langle kl \rangle = \langle ik \rangle \langle jl \rangle + \langle il \rangle \langle kj \rangle. \quad (2.2.5)$$

The vector representation of the Lorentz group is $(1/2, 1/2)$. Therefore, a momentum vector p_μ can be mapped to a bispinor through the Pauli Matrices σ_μ with $\sigma_0 = \mathbf{1}$.

$$p_{\alpha\dot{\alpha}} = \sigma_{\alpha\dot{\alpha}}^\mu p_\mu \quad (2.2.6)$$

and $p^2 = \det(p_{\alpha\dot{\alpha}})$. As the rank of a 2×2 matrix is at most 2, it follows that lightlike momenta can be written in terms of left and right-handed Weyl spinors as

$$p_{\alpha\dot{\alpha}} = \lambda_\alpha \tilde{\lambda}_{\dot{\alpha}}. \quad (2.2.7)$$

Note that while specifying $\lambda, \tilde{\lambda}$ determines p_μ , the inverse is true only up to a scaling $\lambda \rightarrow t\lambda, \tilde{\lambda} \rightarrow t^{-1}\tilde{\lambda}$.

Kinematic invariants can now be written in terms of these spinors as:

$$s_{ij} = (p_i + p_j)^2 = \langle ij \rangle [ji]. \quad (2.2.8)$$

In colour-ordered amplitudes, one encounters only invariants formed from groups of cyclically adjacent momenta, and in an n -particle amplitude $n + 1 = 1$ implicitly. We can also construct Lorentz invariant quantities by contracting spinors with momentum bispinors in the following way:

$$\langle i|P|j \rangle = \lambda_i^\alpha P_\alpha^{\dot{\alpha}} \tilde{\lambda}_{j\dot{\alpha}} \quad (2.2.9)$$

where P is not necessarily lightlike. We also note that cyclic strings of spinor products can be reduced to traces:

$$\langle ij \rangle [jk] \dots \langle lm \rangle [mi] = \text{tr}_+(ijk \dots lm) \quad (2.2.10)$$

with $\text{tr}_+(\dots) = \text{tr}((1 - \gamma_5) \dots)$.

We have now dealt with an efficient notation for the momentum dependence of scattering amplitudes. For particles with spin, however, the amplitude must also be a function of the helicities of external states. Given a momentum and a helicity, it is not in general possible to specify a polarization vector uniquely; however, given a particular decomposition $p_{\alpha\dot{\alpha}} = \lambda_\alpha \tilde{\lambda}_{\dot{\alpha}}$ we can write

$$\begin{aligned} \epsilon_{\alpha\dot{\alpha}}^- &= \frac{\lambda_\alpha \tilde{\mu}_{\dot{\alpha}}}{[\lambda\mu]} \\ \epsilon_{\alpha\dot{\alpha}}^+ &= \frac{\mu_\alpha \tilde{\lambda}_{\dot{\alpha}}}{\langle \lambda\mu \rangle} \end{aligned} \quad (2.2.11)$$

where μ is an arbitrary reference spinor. Note that ϵ^\pm is invariant under rescalings of μ , while the action $\mu \rightarrow \mu + c$ corresponds to a gauge transformation. Hence, we can safely write the amplitude $\hat{A}(\lambda_i, \tilde{\lambda}_i, h_i)$ as a function of the spinor variables and helicities, satisfying n auxiliary conditions

$$\left(\lambda_i^\alpha \frac{\partial}{\partial \lambda_i^\alpha} - \tilde{\lambda}_i^{\dot{\alpha}} \frac{\partial}{\partial \tilde{\lambda}_i^{\dot{\alpha}}} \right) \hat{A}(\lambda_i, \tilde{\lambda}_i, h_i) = -2h_i \hat{A}(\lambda_i, \tilde{\lambda}_i, h_i). \quad (2.2.12)$$

At three points, this is in fact enough to determine the amplitudes. We make an ansatz of the form

$$A(1^{h_1}, 2^{h_2}, 3^{h_3}) \propto \langle 12 \rangle^{a_1} \langle 23 \rangle^{a_2} \langle 31 \rangle^{a_3} \quad (2.2.13)$$

and solve to find

$$A(h_1, h_2, h_3) \propto \langle 12 \rangle^{h_3 - h_1 - h_2} \langle 23 \rangle^{h_2 - h_1 - h_3} \langle 31 \rangle^{h_1 - h_2 - h_3}. \quad (2.2.14)$$

Taking the case of two negative and one positive helicity gluon, this gives us the first of the famous Parke-Taylor amplitudes:

$$A(1^-, 2^-, 3^+) = \frac{\langle 12 \rangle^3}{\langle 23 \rangle \langle 31 \rangle}. \quad (2.2.15)$$

Note that we could also consider an ansatz with all square brackets. In this case, we would find a negative mass dimension which cannot be generated by a local Lagrangian, so it must be discarded. However, in the $(++-)$ case this solution has the correct dimension and is retained.

2.3 Computing Amplitudes at Tree Level

Equipped with this notation, we would now like to compute the amplitudes of physical processes. Although all the information of perturbative field theory is contained in the textbook Feynman diagram expansion, for amplitudes involving many particles its computational complexity grows alarmingly quickly

External Legs	4	5	6	7	8	9	10
Diagrams	4	25	220	2485	34300	559405	10525900

Further, each of these terms can be extremely complex, carrying complicated tensor structures, and are not independent of each other as the Feynman rules are off-shell and do not manifest gauge symmetry term by term, only in the final result. However, given these issues, it was long observed that the final expressions for amplitudes are strikingly simple. In particular, for the so-called MHV amplitude:

$$A(1^+, \dots, i^-, \dots, j^-, n^+) = \frac{\langle ij \rangle^4}{\langle 12 \rangle \langle 23 \rangle \dots \langle n1 \rangle} \quad (2.3.1)$$

conjectured by Parke and Taylor [19] and proven by Berends and Giele [20]. This apparent simplicity suggests the existence of an underlying structure, which began to be understood with the work of Witten [3] on the twistor space structure of MHV amplitudes. This led to the development of the MHV vertex expansion [4], in which MHV amplitudes form the building blocks of larger structures, and subsequently to

the fully recursive formalism of BCFW [21] [5]. Since the former method can be derived from the latter, we shall forsake the historical development and describe it first.

2.3.1 The BCFW Recursion Relations

In order to seed the recursion relation from three points we must work in complex momenta; and the techniques of complex analysis will prove a powerful weapon. We define a complex shift of momenta $[i, j\rangle$ by:

$$\begin{aligned}\lambda_i &\rightarrow \lambda_i - z\lambda_j \\ \tilde{\lambda}_j &\rightarrow \tilde{\lambda}_j + z\tilde{\lambda}_i\end{aligned}\tag{2.3.2}$$

with $z \in \mathbb{C}$. The amplitude is still on-shell, and momentum conservation is still satisfied. This promotes the amplitude to a function $A(z)$ of z , and leaves it open to the powerful techniques of complex analysis. If we restrict ourselves to tree level amplitudes, the analytic structure is necessarily very simple, being limited to poles where an internal propagator goes on-shell, with no branch cuts. This requires:

$$(P + z\lambda_i\tilde{\lambda}_j)^2 = P^2 + 2z\langle i|P|j\rangle = 0\tag{2.3.3}$$

and so the poles in z are all simple and located away from the origin at

$$z_P = \frac{P^2}{2\langle i|P|j\rangle}\tag{2.3.4}$$

. Now consider the contour integral

$$\mathcal{C} = \frac{1}{2\pi i} \oint_{\mathcal{C}} dz \frac{A(z)}{z}\tag{2.3.5}$$

where \mathcal{C} is a circle at infinity in the complex z plane. The integral captures all of the poles z_P , plus the pole at $z = 0$ which corresponds to the physical amplitude,

provided $A(z)$ vanishes as $z \rightarrow \infty$. So we can write the physical amplitudes as a sum over residues:

$$A(0) = \sum_{z_P} \text{Res} \left[\frac{A(z)}{z} \right]. \quad (2.3.6)$$

As is well known, when a propagator goes on-shell the amplitude factorises into a product of two sub-amplitudes:

$$A(z) \rightarrow \hat{A}_L(z) \frac{i}{\hat{P}^2(z)} \hat{A}_R(z). \quad (2.3.7)$$

Using 2.3.4 we can remove the z -dependence from the propagator and write:

$$A(1, \dots, n) = \sum_{h_P} \sum_{i,j} A_L(i, \dots, j, P) \frac{1}{P_{ij}^2} A_R(P, i+1, \dots, j-1) \quad (2.3.8)$$

where we have used the notation $P_{ij} = p_i + p_{i+1} + \dots + p_j$. Now, if we know lower point tree amplitudes, we can construct higher point ones directly and recursively without use of Feynman diagrams.

Examples

The seed for any tree level recursion in Yang-Mills Theory is the three-point MHV amplitude $A(1^-, 2^-, 3^+)$. For real momenta (hence physical processes) this vanishes, since λ and $\tilde{\lambda}$ are related by conjugation. For complex momenta, we can proceed to compute from the Feynman rules that:

$$A_3 = \frac{1}{\sqrt{2}} (\epsilon_1 \cdot (p_2 - p_3) \epsilon_2^- \cdot \epsilon_3^+ + \epsilon_2 \cdot (p_3 - p_1) \epsilon_1^- \cdot \epsilon_3^+ + \epsilon_3 \cdot (p_1 - p_2) \epsilon_1^- \cdot \epsilon_2^+). \quad (2.3.9)$$

Choosing the reference momenta $\mu_1 = \mu_2$ and $\mu_3 = p_1$ reduces the expression to one term:

$$\begin{aligned} A_3 &= i\sqrt{2} \epsilon_2^- \cdot \epsilon_3^+ \epsilon_1^- \cdot p_2 \\ &= \frac{\langle 12 \rangle^4}{\langle 12 \rangle \langle 23 \rangle \langle 31 \rangle}. \end{aligned} \quad (2.3.10)$$

Note that this expression is consistent with the spinor weight condition 2.2.12, which can be used to derive the three-point amplitude.

To illustrate, the use of the recursion relations, we use first the four-point MHV amplitude $A(1^-, 2^-, 3^+, 4^+)$. There is only one diagram in the $[1, 2\rangle$ shift,

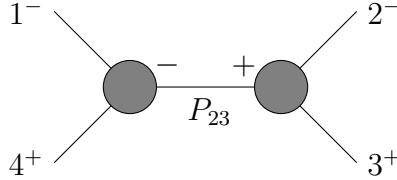


Figure 2.1: The only class of diagram for MHV amplitudes in BCFW recursion.

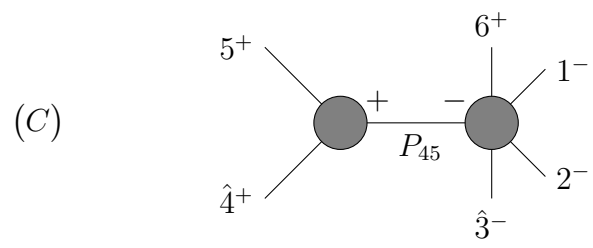
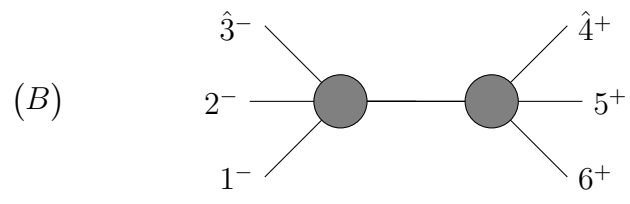
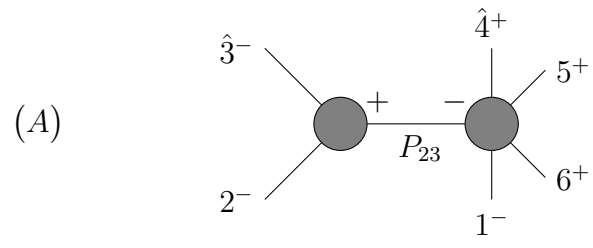
$$\begin{aligned}
 A_4 &= \frac{\langle 1\hat{P} \rangle^3}{\langle \hat{P}4 \rangle \langle 41 \rangle} \frac{1}{\langle 32 \rangle [23]} \frac{[3\hat{P}]^3}{[\hat{P}2][23]} \\
 &= \frac{\langle 1|\hat{P}|3 \rangle^3}{\langle 4|\hat{P}|2 \rangle \langle 41 \rangle \langle 32 \rangle [23]^2} \\
 &= \frac{\langle 12 \rangle^3}{\langle 23 \rangle \langle 34 \rangle \langle 41 \rangle}
 \end{aligned} \tag{2.3.11}$$

One can then continue to add three-point vertices to inductively construct the all- n MHV amplitude.

Our second example is less trivial, the six-point NMHV amplitude $A(1^-, 2^-, 3^-, 4^+, 5^+, 6^+)$. We use a $[3, 4\rangle$ shift, which gives three diagrams: Diagram (B) vanishes since there is no non-zero helicity configuration for the internal leg, and diagram (C) is related to diagram (A) by conjugation. Hence, (A) is the only diagram that requires calculation.

$$(A) = \frac{\langle 23 \rangle^3}{\langle 3\hat{P} \rangle \langle \hat{P}2 \rangle} \frac{1}{\langle 23 \rangle [32]} \frac{\langle 1\hat{P} \rangle^3}{\langle \hat{P}4 \rangle \langle \hat{4}5 \rangle \langle 56 \rangle \langle 61 \rangle} \tag{2.3.12}$$

Note that unlike in the MHV case, the holomorphically shifted momentum appears in a holomorphic spinor product. Hence we need to solve for z_{23} such that $\hat{P}_{23} = [2\hat{3}]\langle \hat{3}2 \rangle$



is on shell. This gives us

$$z = -\frac{[23]}{[24]} \quad (2.3.13)$$

Also,

$$\langle k\hat{P} \rangle = \frac{\langle k|2+3|4\rangle}{[\hat{P}4]} \quad (2.3.14)$$

Now we have

$$(A) = \frac{\langle 1|2+3|4\rangle^3}{[24][34]P_{24}^2} \frac{1}{\langle \hat{4}5 \rangle \langle 56 \rangle \langle 61 \rangle} \quad (2.3.15)$$

$$= \frac{1}{P_{24}^2} \frac{\langle 1|2+3|4\rangle^3}{[23][34]\langle 56 \rangle \langle 61 \rangle \langle 5|3+4|2\rangle} \quad (2.3.16)$$

Combining with (C), we find

$$A(1^-, 2^-, 3^-, 4^+, 5^+, 6^+) = \frac{1}{\langle 5|3+4|2\rangle} \left(\frac{1}{P_{24}} \frac{\langle 1|2+3|4\rangle^3}{[23][34]\langle 56 \rangle \langle 61 \rangle} + \frac{1}{P_{46}} \frac{\langle 3|4+5|6\rangle^3}{[61][12]\langle 34 \rangle \langle 45 \rangle} \right) \quad (2.3.17)$$

2.3.2 The MHV Vertex Expansion

In this useful technique, MHV amplitudes are promoted to the status of interaction vertices joined by off-shell propagators $1/P^2$ to form amplitudes with generic helicity configurations. This is accomplished by writing the internal momenta in terms of a reference spinor

$$\lambda_{P\alpha} = P_{\alpha\dot{\alpha}}\eta^{\dot{\alpha}} \quad (2.3.18)$$

so that the spinor brackets take the form

$$\langle iP \rangle = \langle i|P|\eta \rangle. \quad (2.3.19)$$

Though first derived by considering the twistor space structure of tree amplitudes by Cachazo, Svrcek and Witten, we can most readily arrive at this method from the BCFW relation by considering the multiline shift [22]

$$|i\rangle \rightarrow |i\rangle, \quad |i] \rightarrow |i] + zc_i|\eta] \quad (2.3.20)$$

where $\sum_{i=1}^n c_i |i\rangle = 0$. Using this shift, we see that an NMHV amplitude can be written as a sum over MHV amplitudes

$$A^{\text{NMHV}} = \sum_i A_L^{\text{MHV}}(1, 2, \dots, \hat{P}) \frac{1}{P^2} A_R^{\text{MHV}}(-\hat{P}_i, \dots, n-1, n) \quad (2.3.21)$$

where \hat{P} is shifted by the reference spinor according to 2.3.18, and because the shift is holomorphic it does not affect any of the external momenta. We may then iterate this argument for $N^k\text{MHV}$ amplitudes, to construct the vertex expansion.

Examples

We first consider the vanishing amplitude $(- - - +)$. Here there are two diagrams:

The first gives

$$\frac{\langle 12 \rangle^3}{\langle 2\hat{P} \rangle \langle \hat{P}1 \rangle} \frac{1}{P^2} \frac{\langle \hat{P}3 \rangle^3}{\langle 34 \rangle \langle 4\hat{P} \rangle} = - \frac{[4\eta]^3}{[1\eta][2\eta][3\eta]} \frac{\langle 34 \rangle}{[21]} \quad (2.3.22)$$

and the second similarly gives

$$- \frac{[4\eta]^3}{[1\eta][2\eta][3\eta]} \frac{\langle 32 \rangle}{[41]}. \quad (2.3.23)$$

The sum of these terms then vanishes due to momentum conservation.

A less trivial example is that for the 5-point $\overline{\text{MHV}}$ amplitude

$$A(1^-, 2^-, 3^-, 4^+, 5^+) = \frac{[45]^4}{[12][23][34][45][51]}. \quad (2.3.24)$$

Here there are four diagrams:

Diagram (a) gives us:

$$\left(\frac{\langle 12 \rangle^3}{\langle 2P \rangle \langle P5 \rangle \langle 51 \rangle} \right) \frac{1}{P^2} \left(\frac{\langle P3 \rangle^3}{\langle 34 \rangle \langle 4P \rangle} \right) = \frac{\langle 12 \rangle^3 \langle 3|4|\eta \rangle^3}{\langle 15 \rangle \langle 34 \rangle^2 [34] \langle 2|3+4|\eta \rangle \langle 5|3+4|\eta \rangle \langle 4|3|\eta \rangle} \quad (2.3.25)$$

and the other diagrams contribute

$$\begin{aligned}
& + \frac{\langle 23 \rangle^3 \langle 1|2+3|\eta \rangle^3}{\langle 45 \rangle \langle 51 \rangle^2 [23] \langle 4|3+2|\eta \rangle \langle 2|3|\eta \rangle \langle 3|2|\eta \rangle} \\
& + \frac{\langle 12 \rangle^3 \langle 3|1+2|\eta \rangle^3}{\langle 34 \rangle \langle 45 \rangle^2 [12] \langle 5|1+2|\eta \rangle \langle 1|2|\eta \rangle \langle 2|1|\eta \rangle} \\
& + \frac{\langle 23 \rangle^3 \langle 1|5|\eta \rangle^3}{\langle 34 \rangle \langle 51 \rangle^2 [51] \langle 4|1+5|\eta \rangle \langle 2|1+5|\eta \rangle \langle 5|1|\eta \rangle}
\end{aligned} \tag{2.3.26}$$

This expression may be shown to give the Parke-Taylor expression after setting $|\eta] \rightarrow |4] + |5]$ with the aid of symbolic manipulation.

2.4 Computing Amplitudes at Loop Level

Schematically, an ℓ -loop amplitude can be written as a sum over loop integrals with coefficients:

$$A_n^{L\text{-loop}} = i^L \sum_j c_j \int \left(\prod_{i=1}^L \frac{d^D \ell_i}{(2\pi)^D} \right) \frac{n_j}{\prod_{a_j} P_{a_j}^2} \tag{2.4.1}$$

Where ℓ_i are the L loop momenta, a_j labels the propagators, n_j is a kinematic numerator potentially containing the loop momenta. At one loop there is a well-defined basis of integrals which in four dimensions consists of three topologies: boxes, triangles and bubbles. In theories with massive propagators, tadpoles may also appear; in massless theories, these vanish.

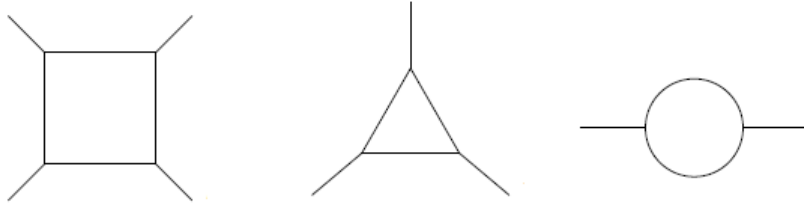


Figure 2.2: *The box, triangle and bubble topologies which can appear at one loop.*

While there have recently been developed methods for constructing the full loop amplitude directly for certain amplitudes in certain theories, we will here focus on methods by which we first deduce the loop integrand, and then evaluate the integrals.

2.4.1 The Unitarity Based Method

The S-Matrix may be written as $S = 1 + iT$ where the *forward part* T contains all scattering processes; scattering amplitudes are thus matrix elements of T with respect to asymptotic states. The unitarity of any evolution operator is clearly necessary in a consistent quantum theory, and applying this to the S-Matrix leads to the relation:

$$S^\dagger S = 1 \iff -i(T - T^\dagger) = T^\dagger T \quad (2.4.2)$$

Inserting a complete set of states $\int \sum_j |p_j\rangle\langle p_j|$ leads us to the Optical Theorem of Cutkosky

$$i\text{Disc}A(i \rightarrow f) = \sum_j \int dLIPS A^*(i \rightarrow j)A(j \rightarrow f) \quad (2.4.3)$$

where

$$dLIPS = \prod_{i=1}^n \frac{d^D q_j}{(2\pi)^D} \delta^{(+)}(q_j^2 - m_j^2) (2\pi)^D \delta^{(D)}(p_i + p_f - \sum_j q_j) \quad (2.4.4)$$

is the Lorentz invariant phase space measure. $|i\rangle, |f\rangle$ are the initial and final states, and we sum over all possible intermediate states $|j\rangle$. Note that the phase space integral sets the internal states on-shell, so order by order in perturbation theory, we can interpret this as a sum over the products of lower-loop amplitudes as illustrated in 2.4.1.

The traditional approach of the old S-Matrix formalism [23] would be to compute these dispersion integrals directly. However, we know that the amplitude must be expressed in terms of some basis of integral functions, and instead consider an ansatz

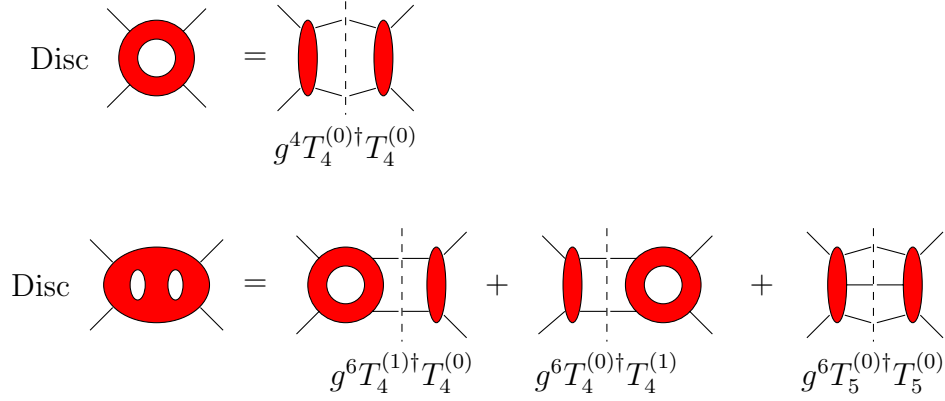


Figure 2.3: Unitarity cuts for one and two-loop four-point amplitudes.

for the amplitude of the form

$$A_n^{(\ell)} = \sum_i c_i I_i \quad (2.4.5)$$

We then systematically examine the cuts in all kinematic channels by the sewing procedure described above. By comparing the cut in each channel to the cuts of the integral functions, we may then construct and solve a linear system for the c_i and reconstruct the full amplitude from its cuts. The method is illustrated by example subsequently.

2.4.2 Examples

The simplest example of this method is the computation of the four-point one-loop amplitude $A(g^-, g^-, g^+, g^+)$ in $\mathcal{N} = 4$ Super Yang-Mills [2]. There are two kinematic channels of interest, shown in figure 2.4.2. In the s -channel cut the helicity of the internal particles is fixed across the cut, so this cut is the same as in pure Yang-Mills.

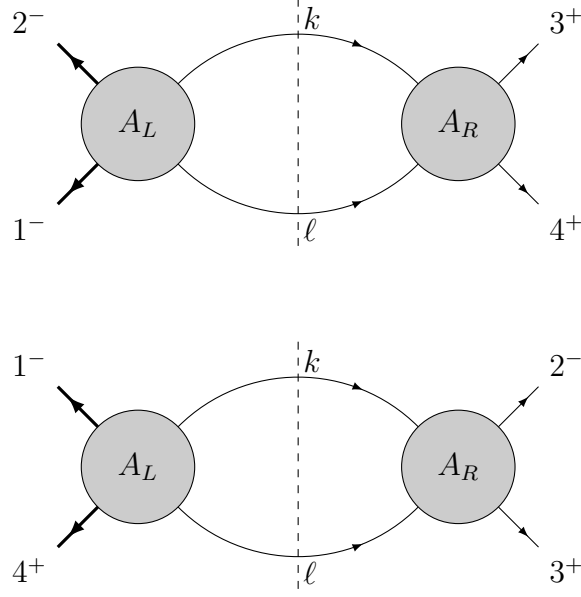


Figure 2.4: The s -channel(top) and t -channel(bottom) cuts of the four-point amplitude at one loop.

It is given

$$\begin{aligned}
A^{1\text{-loop}}(1^-, 2^-, 3^+, 4^+)|_{s\text{-cut}} &= \int A^{\text{tree}}(1^-, 3^-, \ell^+, -k^+) \times A^{\text{tree}}(k^+, -\ell^-, 3^+, 4^+) \\
&= \int \frac{\langle 12 \rangle^3}{\langle 2\ell \rangle \langle \ell k \rangle \langle k1 \rangle} \times \frac{\langle \ell k \rangle^2}{\langle \ell 3 \rangle \langle 23 \rangle \langle 4k \rangle}. \tag{2.4.6}
\end{aligned}$$

We may easily extract a factor of the tree amplitude to leave under the integrand

$$\frac{\langle 23 \rangle \langle 14 \rangle \langle \ell k \rangle^2}{\langle 2\ell \rangle \langle \ell 3 \rangle \langle 4k \rangle \langle k1 \rangle} = \left(\frac{\langle 3k \rangle}{\langle \ell 3 \rangle} + \frac{\langle 2k \rangle}{\langle 2\ell \rangle} \right) \left(\frac{\langle 1\ell \rangle}{\langle k1 \rangle} + \frac{\langle 4\ell \rangle}{\langle 4k \rangle} \right) \tag{2.4.7}$$

$$= \frac{\text{tr}(3k1\ell)}{(\ell \cdot p_3)(k \cdot p_1)} \pm \text{Permutations} \tag{2.4.8}$$

where we have used the Schouten identity to expand some spinor products. Expanding the traces in the numerator using 2.2.10 gives us terms like

$$-\frac{1}{4}su \frac{1}{(k-p_1)^2(k+p_4)^2} + \frac{(p_3 \cdot k)(p_1 \cdot \ell)}{(\ell \cdot p_3)(k \cdot p_1)} + 1 \tag{2.4.9}$$

where the first term corresponds to the cut of a scalar box integral, the second can be expanded to a mixture of boxes and triangles, and the third corresponds to a bubble. Summing over the four permutations, the latter two classes cancel and we find

$$A^{1\text{-loop}}(1^-, 2^-, 3^+, 4^+)|_{s\text{-cut}} = A^{\text{tree}} \times stI_4^{(1)}(s, t)|_{s\text{-cut}} \quad (2.4.10)$$

where

$$I_4^{(1)}(s, t) = \int \frac{d^d \ell}{(2\pi)^d} \frac{1}{\ell^2(\ell - p_1)^2(\ell - p_1 - p_2)^2(\ell + p_4)^2} \quad (2.4.11)$$

is a scalar box integral.

In the t -channel, the helicity of internal states is unconstrained. Therefore we must sum over all states in the theory.

$$\sum_h n_h \int \frac{d^D \ell_2}{(2\pi)^D} \left(\frac{\langle 1\ell \rangle \langle 2k \rangle}{\langle 1k \rangle \langle 2\ell \rangle} \right)^{2-2h} A_L(1, 4, -k, \ell) A_R(k, -\ell, 2, 3). \quad (2.4.12)$$

The matter content of $\mathcal{N} = 4$ is, in addition to the gluon, four Weyl fermions and their conjugates and six scalars. Therefore, the helicity sum is of the form $(u - 1)^4$, which after application of the Schouten identity becomes

$$\left(\frac{\langle 12 \rangle \langle \ell k \rangle}{\langle 1k \rangle \langle 2\ell \rangle} \right)^4. \quad (2.4.13)$$

Returning to the cut expression, we can easily extract a factor of the tree amplitude to find under the integral

$$A^{\text{tree}} \times \frac{\langle 12 \rangle \langle 43 \rangle \langle \ell k \rangle^2}{\langle 4\ell \rangle \langle \ell 1 \rangle \langle k2 \rangle \langle k3 \rangle} \quad (2.4.14)$$

which is identical to the s -cut expression after cyclic permutation, and identifies the t -channel cut of the same integral. Hence we have identified the single integral contributing to this amplitude, and can uplift the cut expressions to

$$A^{1\text{-loop}}(1^-, 2^-, 3^+, 4^+) = A^{\text{tree}} \times I_4^{(1)}(s, t). \quad (2.4.15)$$

For the n -point MHV amplitude, we must consider cuts in all possible kinematic channels, that is all partitions of external legs on either side of the cut. The computation proceeds similarly to the four-point t -channel cut, leading to an expression proportional to

$$A_n^{\text{tree}} \frac{\langle lk \rangle^2 \langle m_2 m_2 + 1 \rangle \langle m_1 m_1 - 1 \rangle}{\langle n_2 \ell \rangle \langle k m_1 \rangle \langle m_2 + 1 \ell \rangle \langle m_1 - 1 k \rangle} \quad (2.4.16)$$

which leads to the sum of cut boxes with numerator

$$\begin{aligned} N &= (2P \cdot m_1 P \cdot m_2 - P^2 m_1 \cdot m_2) \\ &\quad + (P + m_1) \cdot m_2 (\ell - m_1)^2 + (P + m_2) \cdot m_1 (k + m_2)^2 \\ &\quad + (\ell - m_1)^2 (k + m_2)^2. \end{aligned} \quad (2.4.17)$$

As before, the first term corresponds to the cut of a scalar box integral, the second cancels one propagator to form a triangle and third cancels two to form a bubble. Also as before on summing all terms only the first survives so we may write

$$A_n^{\text{1-loop}} = A_n^{\text{tree}} \times M_n^{(1)} \quad (2.4.18)$$

$$M_n^{(1)} = \sum_{m_1, m_2} F^{2me}(m_1, m_2, P, Q). \quad (2.4.19)$$

F^{2me} is the so-called two-mass easy box function

$$\begin{aligned} F^{2me}(p, q, P^2, Q^2) &= \int \frac{d^d \ell}{(2\pi)^d} \frac{1}{\ell^2 (\ell - P)^2 (\ell - P - q)^2 (\ell + p)^2} \\ &= \frac{1}{\epsilon^2} \left[\left(\frac{-s}{\mu^2} \right)^{-\epsilon} + \left(\frac{-t}{\mu^2} \right)^{-\epsilon} - \left(\frac{P^2}{\mu^2} \right)^{-\epsilon} - \left(\frac{Q^2}{\mu^2} \right)^{-\epsilon} \right] \\ &\quad + \text{Li}_2(1 - aP^2) + \text{Li}_2(1 - aQ^2) - \text{Li}_2(1 - as) - \text{Li}_2(1 - at) \end{aligned} \quad (2.4.20)$$

where the invariants $s = (P + p)^2$ and $t = (P + q)^2$ and a is the combination

$$a = \frac{P^2 + Q^2 - s - t}{P^2 Q^2 - st}. \quad (2.4.21)$$

2.4.3 Generalized Unitarity

In the above, we cut two propagators to find the cut of an amplitude in a particular kinematic channel. Many integrals can contribute to the same cut, and the same integral may have cuts in many channels. We may also consider cutting more propagators to reduce the number of integrals surviving in each cut. In D dimensions, there are D independent vectors; hence, one may cut up to $D\ell$ propagators simultaneously. Applying this procedure the quadruple cut isolates the coefficient of a single box integral [24].

As an example, consider the five-point one-loop MHV amplitude $A(1^-, 2^-, 3^+, 4^+, 5^+)$. Cutting four propagators completely fixes the coefficient of a box integral in a given channel. There are five possible one-mass box integrals to examine, with massive corners $P_{12} = (p_1 + p_2)$, P_{23} , P_{34} , P_{45} and P_{51} . The coefficient of the integral

$$I_{12} = \int \frac{d^d \ell}{(2\pi)^d} \frac{1}{\ell^2 (\ell + p_1 + p_2)^2 (\ell - p_5)^2 (\ell - p_5 - p_4)^2} \quad (2.4.22)$$

is determined from figure 2.4.3.

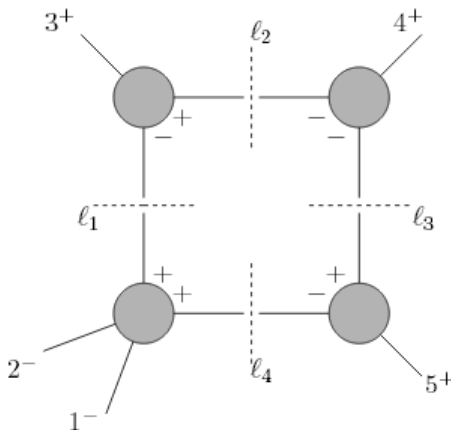


Figure 2.5: .

The helicity configuration of cut legs is fully constrained, so we find the coefficient

as a product of four tree amplitudes is given by:

$$\begin{aligned}
c_{12} &= A(-\ell_4^+, 1^-, 2^-, \ell_1^+) A(-\ell_1^-, 3^+, \ell_2^+) A(\ell_2^-, 4^+, \ell_3^-) A(\ell_3^+, 5^+, \ell_5^-) \\
&= \frac{\langle 12 \rangle^3}{\langle \ell_4 1 \rangle \langle 2 \ell_1 \rangle \langle \ell_1 \ell_4 \rangle} \frac{[3 \ell_2]^3}{[\ell_1 3][\ell_2 \ell_1]} \frac{\langle \ell_2 \ell_3 \rangle^3}{\langle \ell_2 4 \rangle \langle 4 \ell_3 \rangle} \frac{[\ell_3 5]^3}{[5 \ell_4][\ell_4 \ell_3]} \\
&= \frac{\langle 12 \rangle^3 [3 | \ell_2 \ell_3 | 5]}{\langle 2 | \ell_1 | 3 \rangle \langle 4 | \ell_2 \ell_1 \ell_4 | 5 \rangle \langle 1 | \ell_4 \ell_3 | 4 \rangle}, \tag{2.4.23}
\end{aligned}$$

which may be written as a function only of ℓ_2

$$\begin{aligned}
c_{12} &= \frac{\langle 12 \rangle^3 \langle 4 | \ell_2 | 3 \rangle^2 [45]^3}{\langle 2 | \ell_2 | 3 \rangle \langle 34 \rangle \langle 15 \rangle [45] \langle 4 | \ell_2 | 5 \rangle} \\
&= \frac{s_{34} s_{45} \langle 12 \rangle^3}{\langle 23 \rangle \langle 34 \rangle \langle 45 \rangle \langle 51 \rangle} \\
&= s_{34} s_{45} A_5^{\text{tree}}(1^-, 2^-, 3^+, 4^+, 5^+). \tag{2.4.24}
\end{aligned}$$

The coefficients of the other integrals may be obtained by cyclic permutation of external legs.

2.5 Methods for Evaluating Feynman Integrals

We are far from finished in any calculation at this point, since the Feynman integrals of the form 2.4.1 are in general highly non-trivial. Many methods have been derived for their evaluation going back to Feynman himself, on which a superb pedagogical reference is [25]. Many are based on differential equation, though here we focus on those that exploit the introduction of auxiliary parameters.

2.5.1 Reduction to Master Integrals

Although tensor integrals may be a more physically natural basis in many situations (see in particular 5.3, [26] [27]), for calculation it is generally most efficient to reduce them to a basis of scalar *master integrals*.

Passarino-Veltman Reduction

For one loop integrals, one may use purely algebraic identities to perform tensor reduction completely [28]. We accomplish this by writing for a generic linear integral

$$I_n[\ell^\mu] = \int \frac{d^d \ell}{(2\pi)^d} \frac{\ell^\mu}{\ell^2 (\ell - q_1)^2 \dots (\ell - q_n)^2} = \sum_{i=1}^{n-1} c_i q_i^\mu \quad (2.5.1)$$

where the right-hand side may be written as a linear combination over $n-1$ momenta. Note that for $n > 4$ these cannot all be linearly independent, so we may work with only some subset. We then contract with each q_i to find

$$I_n[\ell \cdot q_i] = \int \frac{d^d \ell}{(2\pi)^d} \frac{\ell \cdot q_i}{\ell^2 (\ell - q_1)^2 \dots (\ell - q_n)^2} = \sum_{i=1}^{n-1} c_i \Delta_{ij} \quad (2.5.2)$$

where $\Delta_{ij} = q_i \cdot q_j$ is called the Gram matrix. We may then write the dot product in terms of propagators through such formulae as

$$q \cdot \ell = \frac{1}{2} ((\ell + q)^2 - \ell^2 - q^2) \quad (2.5.3)$$

in order to cancel propagators and write the elements of the Gram matrix in terms of scalar integrals. We thus construct a linear system of equations which may be solved for the coefficients c_i in terms of these integrals. As an example, we consider the linear zero-mass box

$$I_4[\ell^\mu] = \int \frac{d^d \ell}{(2\pi)^d} \frac{\ell^\mu}{\ell^2 (\ell - p_1)^2 (\ell - p_1 - p_2)^2 (\ell + p_4)^2} = c_1 p_1^\mu + c_2 (p_1 + p_2)^\mu + c_4 p_4^\mu.$$

which we will write in terms of the scalar box $I_4[0]$ and the scalar triangles

$$\text{Tri}(s_{ij}) = \int \frac{d^d \ell}{(2\pi)^d} \frac{1}{\ell^2 (\ell - p_i)^2 (\ell - p_i - p_j)^2}. \quad (2.5.4)$$

Applying (2.5.3) leads to the system of equations

$$c_2 s + c_4 t = \text{Tri}(t) - \text{Tri}(s)$$

$$c_1 + 2c_2 - c_4 = I_4[0]$$

$$c_1 t - c_2 s = \text{Tri}(s) - \text{Tri}(t).$$

which is solved by

$$\begin{aligned}
c_1 &= \frac{1}{2} \frac{s}{u} I_4[0] + \text{Tri}(s) - \text{Tri}(t) \\
c_2 &= \frac{1}{2} \frac{t}{u} I_4[0] + \text{Tri}(t) - \text{Tri}(s) \\
c_4 &= -c_1.
\end{aligned} \tag{2.5.5}$$

We note that this integral in principle appears in the four-point one-loop amplitude 2.4.7 through the expansion of the trace

$$\text{Tr}(4k1\ell) = 2(p_4 \cdot \ell)(p_1 \cdot \ell) + \frac{1}{2}t(p_2 \cdot \ell) - \frac{1}{2}s(p_4 \cdot \ell) - \frac{1}{2}u(p_1 \cdot \ell) \tag{2.5.6}$$

and similar terms, where it is contained in the linear terms. We may now apply this result to the particular numerator 2.5.6, to find

$$I_4[\text{Tr}(421\ell)] = \frac{1}{4}st I_4[0] \tag{2.5.7}$$

as required.

Integration By Parts Identities

At higher loops, one must also employ integration by parts identities of the form

$$\begin{aligned}
0 &= \int d^d\ell_1 \dots d^d\ell_L \frac{\partial}{\partial \ell_i} \cdot \left(q_j \frac{1}{P_1^{\lambda_1} \dots P_n^{\lambda_n}} \right) \\
&= \int d^d\ell_1 \dots d^d\ell_L O_{ij} F(\lambda_1, \dots, \lambda_n)
\end{aligned} \tag{2.5.8}$$

where the q_j include both loop and external momenta. Note that we may write tensor integrals in terms of propagators with negative powers. The O_{ij} are the generators of a Lie algebra with commutation relations

$$[O_{ij}, O_{jk}] = \delta_{il} O_{kj} - \delta_{kj} O_{il} \tag{2.5.9}$$

and have the explicit forms

$$O_{ij} = d\delta_{ij} + \sum_{m=1}^L (1 + \delta_{mi}) s_{mj} \frac{\partial}{\partial s_{mj}} \tag{2.5.10}$$

where s_{ij} are the scalar products involving the loop momentum. These may be expressed in terms of the propagators as

$$s_{ij} = \sum_a A_{ij}^a (P_a - m_a^2) \quad (2.5.11)$$

$$\frac{\partial}{\partial s_{ij}} = \sum_{a=1}^N A_a^{ij} \frac{\partial}{\partial P_a} \quad (2.5.12)$$

for some coefficients A^{ij} . Now the operator $\frac{\partial}{\partial P_a}$ raises the power λ_a by one; and the operator P_a lowers it by one. Thus we may define the operators $\lambda_i, \mathbf{i}^+, \mathbf{i}^-$ which act to raise and lower integer powers

$$\mathbf{n}_i F(\lambda_1, \dots, \lambda_i, \dots, \ell_n) = \lambda_i F(\lambda_1, \dots, \lambda_i, \dots, \ell_n) \quad (2.5.13)$$

$$\mathbf{i}^+ F(\lambda_1, \dots, \lambda_i, \dots, \ell_n) = F(\lambda_1, \dots, \lambda_i + 1, \dots, \ell_n) \quad (2.5.14)$$

$$\mathbf{i}^- F(\lambda_1, \dots, \lambda_i, \dots, \ell_n) = F(\lambda_1, \dots, \lambda_i - 1, \dots, \ell_n). \quad (2.5.15)$$

The shift operators commute with each other, whilst

$$[\mathbf{i}^\pm, \lambda_j] = \delta_{ij} \mathbf{i}^\pm. \quad (2.5.16)$$

We may use these operators to construct IBP relations of the form

$$\sum_i \alpha_i F(\lambda_1 + b_{i,1}, \dots, b_{i,n}) = 0 \quad (2.5.17)$$

where α_i is a polynomial in λ_i and b_i are fixed integers. By making appropriate choices of λ_i one may relate a complex integral to a sum of simpler ones. In general, the goal is to reduce a given integral to a sum over scalar *Master Integrals* which may be readily evaluated.

As a simple example of this, consider the one-loop triangle with arbitrary powers in the propagators:

$$I(\lambda_1, \lambda_2, \lambda_3) = \int d^d \ell \frac{1}{P_1^{\lambda_1} P_2^{\lambda_2} P_3^{\lambda_3}} \quad (2.5.18)$$

¹It is possible, if not particularly enlightening, to write down the O_{ij} in terms of the A_{ij} and \mathbf{i}^\pm .

where

$$P_1 = \ell^2 \quad P_2 = (\ell - p_1)^2 \quad P_3 = (\ell - p_1 - p_2)^2. \quad (2.5.19)$$

We may write down IBP identities like

$$\int d^d \ell \frac{\partial}{\partial \ell_\mu} \frac{p_{1\mu}}{P_1^{\lambda_1} P_2^{\lambda_2} P_3^{\lambda_3}} = 0 \quad (2.5.20)$$

and realise them by writing out the derivatives of propagators in terms of themselves:

$$\begin{aligned} p_{1\mu} \frac{\partial}{\partial \ell_\mu} P_1 &= 2p_1 \cdot \ell = P_2 - P_1 & (2.5.21) \\ p_{1\mu} \frac{\partial}{\partial \ell_\mu} P_2 &= 2p_1 \cdot \ell + 2p_1^2 = P_2 - P_1 \\ p_{1\mu} \frac{\partial}{\partial \ell_\mu} P_3 &= 2p_1 \cdot \ell + 2p_1 \cdot p_2 = P_2 - P_1 + q^2. \end{aligned}$$

So 2.5.20 gives us

$$0 = \int d^d \ell \frac{1}{P_1^{\lambda_1} P_2^{\lambda_2} P_3^{\lambda_3}} \left(\lambda_1 - \lambda_2 - \lambda_1 \frac{P_2}{P_1} + \lambda_2 \frac{P_1}{P_2} + \lambda_3 \frac{P_1}{P_3} - \lambda_3 \frac{P_2}{P_3} - \lambda_3 \frac{q^2}{P_3} \right) \quad (2.5.22)$$

which may be interpreted as the IBP relation

$$0 = (\lambda_1 - \lambda_2 - \lambda_1 \mathbf{1}^+ \mathbf{2}^- + \lambda_2 \mathbf{1}^- \mathbf{2}^+ + \lambda_3 \mathbf{1}^- \mathbf{3}^+ - \lambda_3 \mathbf{2}^- \mathbf{3}^+ - \lambda_3 q^2 \mathbf{3}^+) I(\lambda_1, \lambda_2, \lambda_3). \quad (2.5.23)$$

The IBP identities for $q_j = p_{2\mu}, \ell_\mu$ give the relations

$$\begin{aligned} 0 &= (\lambda_2 - \lambda_3 - \lambda_1 (\mathbf{1}^+ \mathbf{2}^- - \mathbf{1}^+ \mathbf{3}^-) - \lambda_2 \mathbf{2}^+ \mathbf{3}^- + \lambda_3 \mathbf{2}^+ \mathbf{3}^- + \lambda_1 q^2 \mathbf{2}^-) I(\lambda_1, \lambda_2, \lambda_3) \\ 0 &= (d - 2\lambda_1 - \lambda_2 - \lambda_3 - \lambda_2 \mathbf{1}^- \mathbf{2}^+ - \lambda_3 \mathbf{1}^- \mathbf{3}^+ + \lambda_3 q^2 \mathbf{3}^+) I(\lambda_1, \lambda_2, \lambda_3) \end{aligned} \quad (2.5.24)$$

and we may now use these relations to reduce integrals with particular values of $\lambda_1, \lambda_2, \lambda_3$. For the simplest non-trivial case, with $\lambda_1 = \lambda_2 = \lambda_3$ we may write the integral $I(2, 1, 1)$ using the second IBP identity as

$$sI(2, 1, 1) = I(2, 1, 0) + I(1, 2, 0) - I(2, 0, 1) - I(1, 0, 2) \quad (2.5.25)$$

$$= 2I(2, 1, 0) - 2I(2, 0, 1). \quad (2.5.26)$$

One can easily see that the first term is a vanishing bubble, while the second can be passed through the third IBP relation to find

$$-sI(2, 0, 1) = (d - 3)I(1, 0, 1) - I(2, 0, 0) \quad (2.5.27)$$

where the second term is a tadpole, which vanishes. The integral is reduced to

$$I(2, 1, 1) = \frac{2(d - 3)}{q^4} I(1, 0, 1) \quad (2.5.28)$$

where $I(1, 0, 1)$ is called a Master Integral for the triangle topology. As this case was very simple we found only a single Master Integral; but in general there may be very many.

2.5.2 Feynman Parameters

An approach common to many methods is to introduce integration over auxiliary variables. We do so by use of the identity

$$\frac{1}{P_1^{\lambda_1} P_2^{\lambda_2} \dots P_n^{\lambda_n}} = \frac{\Gamma(\sum_i \lambda_i)}{\prod_i \Gamma(\lambda_i)} \int_0^1 \left(\prod_i d^n \xi_i \xi_i^{\lambda_i - 1} \right) \frac{\delta(\sum_i \xi_i - 1)}{[\xi_1 P_1 + \xi_2 P_2 + \dots \xi_n P_n]^n} \quad (2.5.29)$$

Example: The One-Loop Triangle

$$\text{Tri}^{(1)}(q^2) = \int \frac{d^d \ell}{(2\pi)^d} \frac{1}{\ell^2 (\ell - p_1)^2 (\ell + p_2)^2} \quad (2.5.30)$$

Applying 2.5.29 twice casts the integrand in the form

$$\begin{aligned} & \int_0^1 \frac{dx}{(\ell^2 - 2x\ell \cdot p_1)^2 (\ell - p_2)^2} \\ &= \int dx dy \frac{y}{\ell^2 - 2xy\ell \cdot p_1 + 2(1-y)\ell \cdot p_2} \\ &= \int dx dy \frac{y}{(\ell'^2 - xy(1-y)q^2)^3}. \end{aligned} \quad (2.5.31)$$

We may perform the integration over ℓ' yielding

$$\int \frac{d^d \ell}{(2\pi)^d} \frac{1}{(\ell^2 - \Delta)^n} = \frac{(-1)^n}{(4\pi)^{d/2}} \frac{\Gamma(n - d/2)}{\Gamma(n)} \left(\frac{1}{\Delta} \right)^{n - \frac{d}{2}} \quad (2.5.32)$$

leaving us with the auxiliary integral

$$\int_0^1 \frac{dx}{x^{1-\epsilon}} \int_0^1 dy y^\epsilon (1-y)^{\epsilon-1} = \frac{1}{\epsilon} B(1+\epsilon, \epsilon). \quad (2.5.33)$$

Putting the two together and applying elementary identities for the Γ and B functions gives us the result

$$\text{Tri}(q^2, \epsilon) = -(-q^2)^{-\epsilon} \frac{\Gamma(1+\epsilon)\Gamma^2(\epsilon)}{\Gamma(1+2\epsilon)}. \quad (2.5.34)$$

Example: The Zero-Mass Box Function

In general, applying Feynman paramaterization to a one-loop n -gon scalar integral with masless propagators in $4 + \epsilon$ dimensions gives

$$I_n = \Gamma(n-2+\epsilon) \int_0^1 d^n x_i \delta(1 - \sum_i x_i) \frac{1}{\left[\sum_{i,j=1}^n Y_{ij} x_i x_j \right]^{n-2+\epsilon}} \quad (2.5.35)$$

after performing the loop integration, where

$$Y_{ij} = -\frac{1}{2}(k_i + k_{j-1})^2, \quad Y_{ii} = 0. \quad (2.5.36)$$

For a box integral with massive corners m_1, m_2, m_3, m_4 the denominator is

$$\sum_{i,j=1}^n Y_{ij} = -s x_1 x_3 - t x_2 x_4 - m_1^2 x_1 x_2 - m_2^2 x_2 x_3 - m_3^2 x_3 x_4 - m_4^2 x_4 x_1. \quad (2.5.37)$$

In the simplest case, the massless box 2.4.11, this takes the form

$$I_4^{(1)} = \Gamma(2+\epsilon) \int_0^1 d^4 x_i \delta(1 - \sum_{i=1}^4 x_i) \frac{1}{[-s x_1 x_3 - t x_2 x_4]^{2+\epsilon}} \quad (2.5.38)$$

which may be directly integrated after the substitution

$$x_1 = y(1-x), \quad x_2 = z(1-y), \quad x_3 = (1-y)(1-z), \quad x_4 = xy \quad (2.5.39)$$

which factorises the integrand in the form

$$I_4 = \Gamma(2+\epsilon) \int_0^1 dy [y(1-y)]^{-2-\epsilon} \int_0^1 \frac{dx dy}{[-s(1-x)(1-z) - txz]^{2+\epsilon}} \quad (2.5.40)$$

$$= \frac{\Gamma(2+\epsilon)\Gamma(-\epsilon)^2}{\Gamma(-2\epsilon)} \int_0^1 \frac{dx dy}{[-s(1-x)(1-z) - txz]^{2+\epsilon}} \quad (2.5.41)$$

where we have performed the integral over y . Performing the integral over x leaves us with

$$I_4(s, t) = \frac{\Gamma(2 + \epsilon)\Gamma(-\epsilon)^2}{\Gamma(-2\epsilon)} \int_0^1 \frac{dz}{s - (s+t)z} [(-t)^{-1-\epsilon} z^{-1-\epsilon} + (-s)^{-1-\epsilon} (1-z)^{-1-\epsilon}] \quad (2.5.42)$$

$$= \frac{\Gamma(2 + \epsilon)\Gamma(-\epsilon)^2}{\Gamma(-2\epsilon)} [f(s, t; \epsilon) + f(t, s; \epsilon)] \quad (2.5.43)$$

where we have defined

$$f(s, t; \epsilon) = (-t)^{-1-\epsilon} \int_0^1 \frac{dz}{s - (s+t)z} \left[z^{-1-\epsilon} + \left(\frac{s}{s+t} \right)^{-1-\epsilon} \right]. \quad (2.5.44)$$

The result, to all orders in ϵ , is given in terms of hypergeometric functions

$$I_4(s, t) = \frac{\Gamma(2 + \epsilon)\Gamma(-\epsilon)^2}{st\Gamma(-2\epsilon)} \left[(-s)_2^{-\epsilon} F_1 \left(1, -\epsilon; 1 - \epsilon; 1 + \frac{s}{t} \right) + (-t)_2^{-\epsilon} F_1 \left(1, -\epsilon; 1 - \epsilon; 1 + \frac{t}{s} \right) \right]. \quad (2.5.45)$$

2.5.3 Mellin-Barnes

This method is based upon the identity

$$\frac{1}{(X + Y)^\lambda} = \frac{1}{\Gamma(\lambda)} \frac{1}{2\pi i} \int_{-i\infty}^{+i\infty} dz \Gamma(\lambda + z) \Gamma(-z) \frac{X^z}{Y^{\lambda+z}} \quad (2.5.46)$$

where contour is chosen to separate poles with a $\Gamma(\dots + z)$ dependence (called left poles) from those with a $\Gamma(\dots - z)$ dependence.

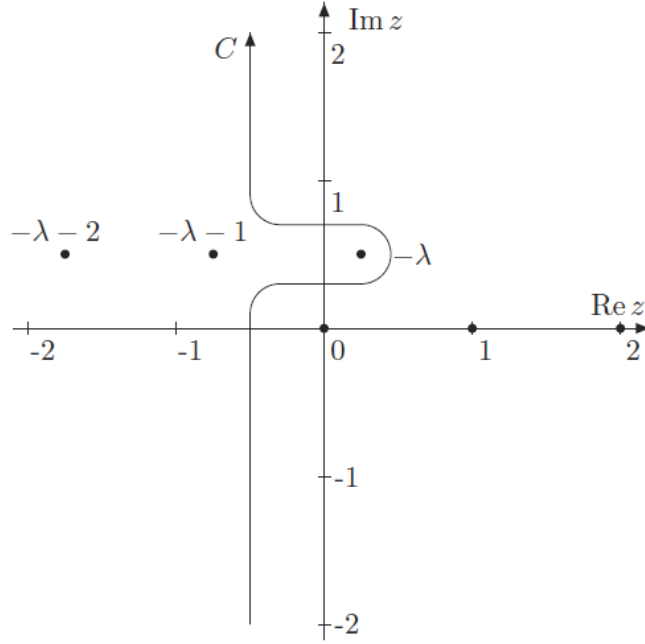


Figure 2.6: An example of a Mellin-Barnes integration contour.

The most basic application is to convert massive propagators into massless ones and integrate over a massless integral, but it may also be applied to Feynman parametric representations, which as we have seen are generically of the form 2.5.46, in order to break up terms in the denominator. After doing so, the integral is cast in the form of an n -fold Mellin-Barnes Representation

$$\mathcal{R} = \frac{1}{2\pi i} \int_{-i\infty}^{+i\infty} \dots \int_{-i\infty}^{+i\infty} \prod_i dz_i f(z_1, \dots, z_n; s_1, \dots, s_p; \lambda_1, \dots, \lambda_q; \epsilon) \frac{\prod_j \Gamma(A_j + V_j + c_j \epsilon)}{\prod_k \Gamma(B_k + W_k + d_k \epsilon)} \quad (2.5.47)$$

where s_i are the kinematic invariants and λ_i are the powers of the propagators. A_j and B_k are linear combinations of $\lambda_i s$; V_j and W_k are linear combinations of $z_i s$; and c_j , d_k are constants. The function f is in general a product of powers of s_i . The construction of such representations has been automatized in the Mathematica package `AMBRE` [29], which we shall utilize extensively. As a simple example which may be done by hand, consider the massless box integral with Feynman parametrization

2.5.40. We may apply 2.5.46 with $Y = -sx_1x_3$ and $X = -tx_2x_4$ to find

$$\int_0^1 \frac{dx dy}{[-s(1-x)(1-y) - txy]^{2+\epsilon}} = \frac{1}{\Gamma(2+\epsilon)} \frac{1}{2\pi i} \int_{-i\infty}^{+i\infty} dz \Gamma(2+\epsilon+z) \Gamma(-z) \int_0^1 \frac{dz dy (xy)^z}{[(1-x)(1-y)]^{2+\epsilon+z}} \quad (2.5.48)$$

and we may immediately evaluate the Feynman parameter integral in terms of Γ functions. The result gives the MB representation for the massless box

$$I_4(s, t) = \frac{i\pi^{d/2}}{\Gamma(-2\epsilon)(-s)^{2+\epsilon}} \frac{1}{2\pi i} \int_{-i\infty}^{+i\infty} dz \left(\frac{t}{s}\right)^z \Gamma(2+\epsilon+z) \Gamma(1+z)^2 \Gamma(-1-\epsilon-z)^2 \Gamma(-z). \quad (2.5.49)$$

Once acquired, these representations may often be simplified by the application of Barnes's lemmas

$$\int_{-i\infty}^{+i\infty} dz \Gamma(a+z) \Gamma(b+z) \Gamma(c-z) \Gamma(d-z) = \frac{\Gamma(a+c) \Gamma(a+d) \Gamma(b+c) \Gamma(b+d)}{\Gamma(a+b+c+d)} \quad (2.5.50)$$

$$\begin{aligned} & \int_{-i\infty}^{+i\infty} dz \frac{\Gamma(a+z) \Gamma(b+z) \Gamma(c+z) \Gamma(d-z) \Gamma(e-z)}{\Gamma(a+b+c+d+e+z)} \\ &= \frac{\Gamma(a+d) \Gamma(a+e) \Gamma(b+d) \Gamma(b+e) \Gamma(c+d) \Gamma(c+e)}{\Gamma(a+b+d+e) \Gamma(a+c+d+e) \Gamma(b+c+d+e)}. \end{aligned} \quad (2.5.51)$$

In some cases, this procedure saturates all the z integrations and one finds an exact expression in terms of Γ functions.

When no exact solution can be derived, there are two common approaches to extract the ϵ expansion of the MB representation. We proceed by following what is called in the literature Strategy B, following the work of [30] [31].

We note that in general although the condition that the integration contour separate right and left poles is necessary to guarantee the equivalence of the MB representation and the original loop integral it cannot in general be satisfied for physically meaningful values of the dimension and the powers of the propagators, ie. those where ϵ is close to zero. We proceed therefore by beginning with a contour where the separation condition is satisfied and then analytically continue to the $\epsilon \rightarrow 0$ regime.

- We chose our integration contours to be straight lines parallel to the Im axis, such that the real parts of the arguments of all Γ functions are positive.
- This condition determines allowed values of ϵ , including some starting value ϵ_0 and a boundary value ϵ_1 where the contour first intersects a pole. Here we will work with $\epsilon < 0$ so that ϵ_1 is a maximum, but the argument applies analogously for $\epsilon > 0$. If ϵ can be taken to zero without intersecting a pole, we may safely expand about $\epsilon = 0$.
- For $\epsilon_1 < 0$, we must determine the residue where the pole crosses the contour. Then we may write

$$\mathcal{R}(\epsilon_0) = \mathcal{R}(\epsilon_1) \pm \text{Res}[\mathcal{R}]|_{z_i=z_*} \quad (2.5.52)$$

The residue term is now an $(n - 1)$ -fold MB representation, which is added for a left pole and subtracted for a right pole.

- We have thus analytically continued from $\epsilon = \epsilon_0$ to $\epsilon = \epsilon_1$. We now iterate the process starting from ϵ_1 until we may expand about $\epsilon = 0$.

Since this process is algorithmic, it may be implemented computationally, notably by the Mathematica package MB. One obtains a sum of analytic Γ functions and remaining contour integrals which in general must be attacked numerically.

2.5.4 Infrared Divergences

A general feature of the S -Matrix in theories with massless particles is the presence of infrared divergences. Unlike UV divergences, these are not renormalized away but instead cancel in the computation of physical quantities such as the cross sections of colour singlet states. There are two types of integration region which give rise to such divergences; the low-energy region of some virtual particle and the region where

a vertical particle is collinear with some external state. Both lead to integrals of the form

$$\int \frac{dk}{k^{1+\epsilon}} \propto \frac{1}{\epsilon} \quad (2.5.53)$$

and since they may occur simultaneously the leading singularity at ℓ loops is at most $1/\epsilon^{2\ell}$. As an illustration, consider one mass triangle at one-loop in $4 + \epsilon$ -dimensions

$$\begin{aligned} \text{Tri}^{(1)}(q^2) &= \int \frac{d^d \ell}{(2\pi)^d} \frac{1}{\ell^2(\ell - p_1)^2(\ell + p_2)^2} \\ &= (-q^2)^{-\epsilon} \left[-\frac{1}{\epsilon^2} + \frac{\zeta_2}{2} + \mathcal{O}(\epsilon) \right] \end{aligned} \quad (2.5.54)$$

where in the limit $\ell \rightarrow 0$ we also have $\ell_1 \rightarrow p_1$ and $\ell_2 \rightarrow p_2$. In general, this behaviour will be observed for any integral with adjacent massless legs².

The IR divergences of QED and of Gravity analysed by Weinberg [32] in the 1960s are much simpler than those of non-abelian gauge theories, since the self coupling is for photons absent and for soft gravitons very weak. In fact, it was speculated at the time that the problem of IR divergences in Yang-Mills theory may rule it out as a description of nature! A general n -point amplitude in non-Abelian Yang-Mills Theory may be factorised in the following way [33]

$$A_n = J \left(\frac{Q^2}{\mu^2}, \alpha(\mu), \epsilon \right) \times S \left(p_i, \frac{Q^2}{\mu^2}, \alpha(\mu), \epsilon \right) \times h_n \left(p_i, \frac{Q^2}{\mu^2}, \alpha(\mu), \epsilon \right). \quad (2.5.55)$$

Here Q^2 is some characteristic scale for particles of momentum p_i , $\alpha(\mu)$ is the running coupling and μ is a renormalization scale. J is a jet function describing collinear behaviour, the soft function S and the hard function h_n is an IR finite piece which contains the short-distance dynamics. A_n and the finite hard function h_n are vectors in the space of colour structure, while S is a matrix; however, if we restrict ourselves to planar theories (or leading colour), it is proportional to the identity and may be absorbed into the definition of J .

²We do not always chose to make this manifest. For instance, in the case of the two-mass easy box function, we write the divergent part as $\frac{1}{\epsilon^2} \left[\left(\frac{-s}{\mu^2} \right)^{-\epsilon} + \left(\frac{-t}{\mu^2} \right)^{-\epsilon} - \left(\frac{-P^2}{\mu^2} \right)^{-\epsilon} - \left(\frac{-Q^2}{\mu^2} \right)^{-\epsilon} \right]$, which yields only a $1/\epsilon$ pole after expanding the terms of the form $s^{-\epsilon}$.

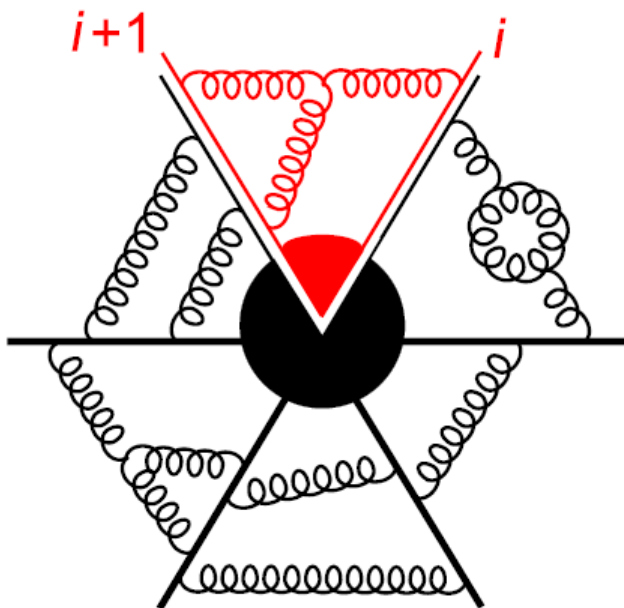


Figure 2.7: *IR structure of planar scattering amplitudes. The straight lines represent hard external states, the curly lines carry soft or collinear momenta. Exchange occurs only between adjacent “slices”. Taken from [34]*

As shown in figure 2.7, in the planar limit soft exchanges are restricted to wedges between adjacent external lines [34]. Then the divergence is proportional to the amplitude for the decay of some colour singlet into two external states.

In $\mathcal{N} = 4$ Super Yang-Mills, an excellent candidate is the form factor of the shortest BPS operator

$$F(q^2, \lambda; \epsilon) = \langle \phi_{12}(p_1) \phi_{12}(p_2) | \text{Tr}(\phi_{12} \phi_{12} | 0 \rangle \quad (2.5.56)$$

since it is protected from UV divergences by supersymmetry. Then the amplitude may be written as

$$A_n = \left[\prod_{i=1}^n F(s_{i,i+1}, \lambda; \epsilon) \right]^{1/2} \times h_n(p_i, \lambda; \epsilon). \quad (2.5.57)$$

This form factor obeys renormalization group equations [35] [36] [37] owing to the

necessity of independence on the factorization scale Q^2 . These are solved for $\mathcal{N} = 4$ by [34]

$$A_n = \exp \left[-\frac{1}{8} \sum_{\ell=1}^{\infty} a^\ell \left(\frac{\gamma_K^{(\ell)}}{(\ell\epsilon)^2} + \frac{2G_0^{(\ell)}}{\ell\epsilon} \right) \sum_{i=1}^n \left(\frac{\mu^2}{s_{i,i+1}} \right)^{\ell\epsilon} \right] \times h_n \quad (2.5.58)$$

where γ_K is the cusp anomalous dimension and G_0 is the collinear anomalous dimension. This may be further refined to

$$A_n = \exp \left[\sum_{\ell=1}^{\infty} a^\ell f^{(\ell)}(\epsilon) \hat{I}_n(\ell\epsilon) \right] \tilde{h}_n \quad (2.5.59)$$

where $\hat{I}(\ell\epsilon)$ is the divergent part of the one-loop amplitude with the substitution $\epsilon \rightarrow \ell\epsilon$ and

$$f^{(\ell)}(\epsilon) = f_0^{(\ell)} + \epsilon f_1^{(\ell)} + \epsilon^2 f_2^{(\ell)}. \quad (2.5.60)$$

Although the description above is given for $\mathcal{N} = 4$, the argument is applicable to a broad range of gauge theories.

2.6 Wilson Loops

A natural class of observables in any gauge theory are the Wilson Loops

$$W(C) = \frac{1}{N} \langle 0 | \text{Tr} P \exp \left(ig \oint_C dx^\mu A_\mu \right) | 0 \rangle \quad (2.6.1)$$

corresponding naturally to the path integral contribution of a particle in a background field. Gauge invariance is guaranteed by the closure of the contour. These objects in principle form a complete set of observables just as local operators do. It can easily be seen by expanding the exponential that the Wilson Loop has a perturbative expansion of the form

$$W(C) \propto 1 + ig \oint dx^\mu \langle A_\mu(x) \rangle + (ig)^2 \oint dx^\mu dy^\nu \langle A_\mu(x) A_\nu(y) \rangle + \dots \quad (2.6.2)$$

The (*ig*) coefficient vanishes for any theory with unbroken Poincare symmetry, so the first order term has the interpretation of integrating a propagator over the possible endpoints on the contour.

2.6.1 Divergences and Renormalization

UV divergences of Wilson Loops occur in the integration region where propagators are pinched to a point. The first case to consider is a smooth contour, where in general the divergence is linear in the cut-off and proportional to the length of the contour, and often disappears in dimensional regularization [38]. It can be absorbed into an overall factor:

$$W(C) = e^{-KL(C)} \times \text{finite} \quad (2.6.3)$$

which has an interpretation as the mass renormalization of a test particle.

This linear divergence is the only one present for a smooth contour [39] [40]. The interesting behaviour occurs when the contour possesses cusps. For instance, it was shown by Polyakov [38] that for cusp angle α at one loop

$$W(C) = 1 - 2g^2 C_F [\alpha \cot \alpha - 1] \log \left(\frac{L}{a} \right) \quad (2.6.4)$$

where C_F is the fundamental quadratic Casimir and a is the short-distance cut-off. More generally, the cusp divergence can be removed by multiplicative renormalization

$$W_R(C) = Z(\alpha)W(C). \quad (2.6.5)$$

The divergence depends on the contour only via the cusps, which are locally independent, so the renormalization associated with multiple cusps factorise:

$$Z(\alpha_1, \alpha_2, \dots, \alpha_n) = Z(\alpha_1)Z(\alpha_2) \dots Z(\alpha_n). \quad (2.6.6)$$

One may derive [41] a renormalization group equation for the Wilson loop. leading

the to the general result

$$Z^{-1}(\alpha, g, \epsilon) = \exp \left[\int_0^g dg' \gamma_K(\alpha, g', \epsilon) / \beta(g', \epsilon) \right] \quad (2.6.7)$$

where γ_K is the same cusp anomalous dimension as in 2.5.59. In $\mathcal{N} = 4$ sYM this is solved by

$$Z(\alpha, g, \epsilon) = \exp \left[\sum_{\ell=1}^{\infty} \frac{g^{2\ell}}{2\ell} \frac{\gamma_K^{(\ell)}(\alpha, g)}{\epsilon} \right] \quad (2.6.8)$$

and we see that like the IR divergences of scattering amplitudes the UV divergences of Wilson Loops exponentiate.

2.6.2 Lightlike Contours

A particularly important class of Wilson Loops are those defined by polygonal contours where each segment is lightlike. The contribution from a propagator starting and ending on the same segment vanishes in dimensional regularization, so the lowest order contribution is then given by the following two diagrams:

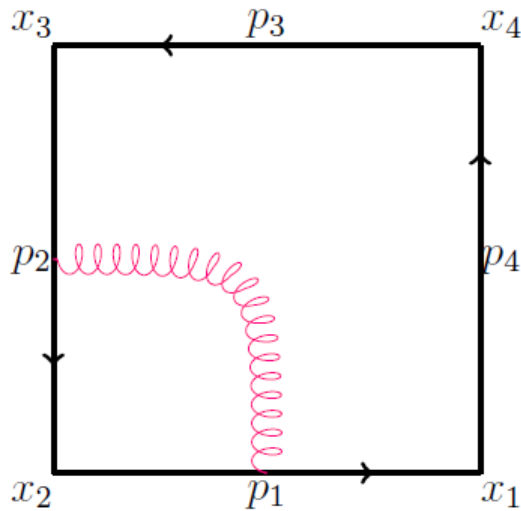


Figure 2.8: *Case (a), the lightlike cusp diagram.*

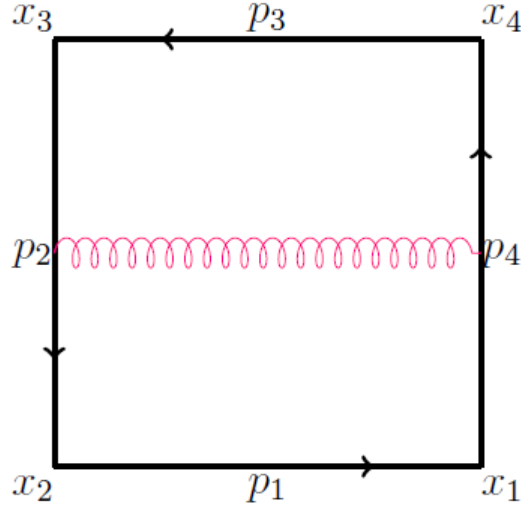


Figure 2.9: *Case (b), the finite contribution where the propagator stretches between two non-adjacent segments.*

Case (a) is a special case of the cusp diagram discussed above. Here we work in dimensional regularization using the propagator in Feynman gauge:

$$\Delta_{\mu\nu}(z) = -\frac{\Gamma(1-\epsilon)}{4\pi^{2-\epsilon}} \frac{\eta_{\mu\nu}}{(-z^2 + i\epsilon_F)^{1-\epsilon}} \quad (2.6.9)$$

so the cusp diagram is given by

$$\begin{aligned} & - (ig)^2 \frac{\Gamma(1-\epsilon)}{4\pi^{2-\epsilon}} \int d\sigma d\tau \frac{(p_i \cdot p_j)}{[(p_i \sigma - p_j \tau)^2]^{1-\epsilon}} \\ & = - (ig)^2 \frac{\Gamma(1-\epsilon)}{4\pi^{2-\epsilon}} \left[\frac{1}{2} \frac{(-s_{ij})^{-\epsilon}}{\epsilon^2} \right]. \end{aligned} \quad (2.6.10)$$

Diagram (b) is finite, so we may evaluate it in four dimensions. For simplicity we consider the case of the tetragon, where we have:

$$- (ig)^2 \frac{1}{2} \frac{\Gamma(1-\epsilon)}{4\pi^{2-\epsilon}} \mathcal{F}_\epsilon \quad (2.6.11)$$

and

$$\begin{aligned}
\mathcal{F}_0 &= \int d\sigma d\tau \frac{-s_{12} - s_{14}}{-s_{12}\sigma + s_{14}\tau - s_{12} + s_{14}\sigma\tau} \\
&= -\text{Li}_2\left(\frac{s_{12}}{s_{14}}\right) - \text{Li}_2\left(\frac{s_{14}}{s_{12}}\right) \\
&= \frac{1}{2}\log^2\left(\frac{s_{12}}{s_{14}}\right) + \frac{\pi^2}{2}
\end{aligned} \tag{2.6.12}$$

where between the second and third lines we have used the identity

$$\text{Li}_2(z) + \text{Li}_2(1/z) + \frac{1}{2}\log^2(-z) + \frac{\pi^2}{6} = 0. \tag{2.6.13}$$

Note the functional dependence is on polylogarithms of weight two, which is a natural consequence of the perturbative structure of this Wilson Loop as an iterated integral.

2.7 Form Factors

The first step in investigating off-shell quantities is to consider form factors. These are the matrix elements of Gauge Invariant Operators,

$$F(1 \dots n) = \delta^{(4)}(q - \sum_i^n p_i) \langle 1 \dots n | \mathcal{O}(0) | 0 \rangle = \int d^4x e^{-iqx} \langle 1 \dots n | \mathcal{O}(x) | 0 \rangle, \tag{2.7.1}$$

and as such interpolate between scattering amplitudes and correlation functions. In particular, using the methods of generalized unitarity, we may construct loop-level correlation functions by sewing tree level form-factors [15].

We have already seen the important connection of one form factor to infrared divergences. Form factors also have physical application in their own right, in particular when considering effective couplings to off-shell currents. For instance, in the Standard Model the Higgs does not couple to the gluons directly but to the quarks via Yukawa couplings

$$\mathcal{L}_Y = -\frac{H}{v} \left(\sum_l m_l q_l \bar{q}_l + M_t t \bar{t} \right) \tag{2.7.2}$$

where v is the Higgs VEV and l labels the light quarks. Since the coupling to the Higgs is proportional to the mass we separate the top quark contribution as this is dominant.

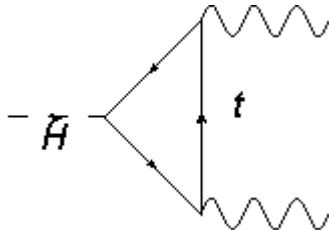


Figure 2.10: *The dominant contribution to the process $H \rightarrow gg$. Note that the coupling to the Higgs is proportional to m_t .*

In the heavy top limit $m_t \rightarrow \infty$ the coupling has been shown to be independent of m_t so it may be integrated out, leaving an effective term in the Lagrangian [42]

$$\mathcal{L}_{eff} \propto \frac{\alpha_S}{12\pi v} H \text{tr} F^2. \quad (2.7.3)$$

It may then be seen that the amplitudes $H \rightarrow n$ gluons is given to first order by the form factor of this operator, which bears many similarities to objects we will consider in this thesis. Another famous case is that of $e^+e^- \rightarrow \text{Hadrons}$, where \mathcal{O} is the hadronic electromagnetic current.

Having on-shell external states, the methods described above for scattering amplitudes are amenable to the study of form factors as well. Consider, for instance, the simplest form factor in $\mathcal{N} = 4$ sYM, the Sudakov form factor described above, at one loop. The operator under consideration is the scalar bilinear $\mathcal{O} = \text{Tr}(\phi_{12}\phi_{12})$. The form factor is then $F = \langle \phi(p_1)\phi(p_2) | \mathcal{O}(0) | 0 \rangle$, with $q := p_1 + p_2$. At tree level, this object is trivially unity. It has just the one kinematic channel, captured by 2.7(a) and doubled by the contribution of the case $\ell_1 \leftrightarrow \ell_2$. The four-scalar amplitude is given:

$$A(\phi_{12}(p_1), \phi_{12}(p_2), \bar{\phi}_{12}(\ell_1), \bar{\phi}_{12}(\ell_2)) = \frac{\langle 12 \rangle \langle \ell_1 \ell_2 \rangle}{\langle 2 \ell_1 \rangle \langle \ell_2 1 \rangle} \quad (2.7.4)$$

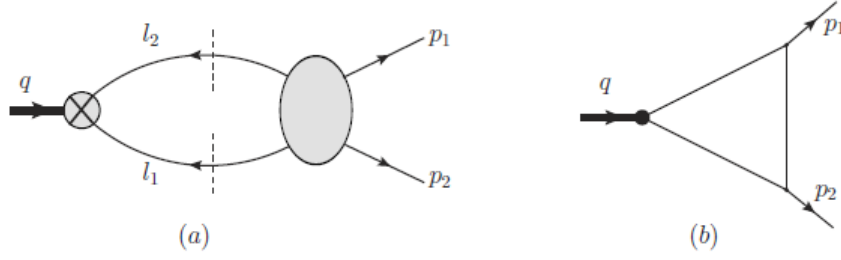


Figure 2.11: (a) Shows the q^2 channel cut of the Sudakov form factor. The cut identifies the one-mass triangle integral (b).

Now we see that to cut leads to

$$\begin{aligned}
 F^{(1)}(q^2)|_{q^2\text{-cut}} &= 2 \int dLIPS \frac{\langle 12 \rangle \langle \ell_1 \ell_2 \rangle}{\langle 2 \ell_1 \rangle \langle \ell_2 1 \rangle} \\
 &= -2q^2 \int dLIPS \frac{1}{(\ell_2 + p_2)^2}
 \end{aligned} \tag{2.7.5}$$

which can immediately be lifted to a loop integral since there is but one kinematic channel.

We may also use BCFW recursion to construct form factors with additional gluonic external states, since all the factorization theorems apply to form factors. We use the three-point amplitude

$$A(1_\phi, 2_\phi, 3^+) = \frac{[23][31]}{[12]} \tag{2.7.6}$$

together with the Sudakov form factor to seed the recursion relations. For the simplest case, that of the three-point form factor $F(1_\phi, 2_\phi, 3^+)$ we have

$$\begin{aligned}
 F(1_\phi, P_\phi; q) \frac{1}{P^2} A(P_\phi, 2_\phi, 3^+) &= 1 \cdot \frac{1}{\langle 23 \rangle [32]} \frac{[23][3\hat{P}]}{[\hat{P}2]} \\
 &= \frac{1}{\langle 23 \rangle} \frac{\langle 1|2+3|3 \rangle}{\langle 1|2+3|2 \rangle} \\
 &= \frac{\langle 12 \rangle}{\langle 23 \rangle \langle 31 \rangle}
 \end{aligned} \tag{2.7.7}$$

so we may write:

$$F_3^{\text{MHV}}(i_\phi, j_\phi, k^+) = \frac{\langle ij \rangle}{\langle jk \rangle \langle ki \rangle}, \quad F_3(i_\phi, j_\phi, k^-) = \frac{[ij]}{[jk][ki]}. \quad (2.7.8)$$

We may now iterate the above process to derive an infinite sequence of form factors

$$F^{\text{MHV}}(1^+, \dots, i_\phi, \dots, j_\phi, \dots, n^+; q) = \frac{\langle ij \rangle^2}{\langle 12 \rangle \langle 23 \rangle \dots \langle n1 \rangle}. \quad (2.7.9)$$

More complex solutions to the form factor recursion relations will be discussed in depth in later chapters.

Chapter 3

Computable Models

Having appraised the armaments, we now survey the battlefield. In science as in war it is important to chose battles one can win; and though the techniques outlined in the previous chapter are generally applicable, there are certain theories in which their application is elegantly simple and we may progress far further than in the tangled forest of reality. These theories possess enhanced symmetry which places strict constraints on observable quantities. Both supersymmetry and conformal symmetry are by now old and well-understood; but the theories in which this phenomenon is most emphatic also possess additional hidden symmetries which in principle render them integrable.

3.1 Superconformal Symmetry

Supersymmetry and conformal symmetry place very strong constraints on field theories.

It should be noted that in principle we may not define asymptotic states in a conformal field theory, and consequently the scattering cross-section is not an IR-

safe observable. We must regard the amplitudes we compute as existing only in the presence of an IR regulator. Working in dimensional regularization this carries little physical meaning; if we wish we may regard the CFT as the UV fixed point of an RG flow, and an IR cut-off must be applied at some scale. We may also see a more physical picture in the case of $\mathcal{N} = 4$ sYM by using the massive Coulomb branch regulator of [43] [44] [45]. Alternatively, we may regard amplitudes in conformal theories as building blocks of amplitudes in other theories where scattering is completely well-defined. In particular, we may write the one-loop amplitude for gluon scattering in QCD as

$$A_{QCD} = A_{\mathcal{N}=4} - 4A_{\mathcal{N}=1} + A_{\mathcal{N}=0} \quad (3.1.1)$$

where $A_{\mathcal{N}=1}$ is the amplitude with a chiral $\mathcal{N} = 1$ multiplet running in the loop and $A_{\mathcal{N}=0}$ is that with a complex scalar.

3.1.1 Conformal Transformations

In a conformal theory, the metric is invariant up to a local rescaling

$$x \rightarrow x' \quad g_{\mu\nu} \rightarrow g'_{\mu\nu} = \rho(x)g_{\mu\nu} \quad (3.1.2)$$

which also preserves angles. Starting from an infinitesimal transform

$$x'_\mu = x_\mu + k_\mu \quad (3.1.3)$$

one may show that the most general form of the killing vector k_μ in $d > 2$ is given by

$$k^\mu = a^\mu + \omega_{\mu\nu}x^\nu + \lambda x^\mu + 2(x \cdot b)x^\mu - b^\mu x^2. \quad (3.1.4)$$

Here a^μ and $\omega_{\mu\nu}$ parametrises the translations and rotations of the familiar Poicare group. λ parametrizes dilatations, while b^μ is the parameter for the so-called special conformal transformations or conformal boosts. The generators for these are given

by

$$D = -ix^\mu \partial_\mu \quad (3.1.5)$$

$$K^\mu = -i(x^\mu x^\nu \partial_\nu - x^2 \partial^\mu) \quad (3.1.6)$$

respectively. In addition to the familiar commutation relations of the Poincare algebra, we also have

$$[D, P_\mu] = iP_\mu \quad [K_\rho, M_{\mu\nu}] = i(\eta_{\rho\mu} K_\nu - \eta_{\rho\nu} K_\mu) \quad (3.1.7)$$

$$[D, K_\mu] = -iK_\mu \quad [K_\mu P_\nu] = 2i(\eta_{\mu\nu} D - M_{\mu\nu}) \quad (3.1.8)$$

which defines the conformal algebra. We note that if we define the anti-symmetric operators J_{ab} with $a = 0, 1, \dots, d+1$ by

$$J_{\mu\nu} = M_{\mu\nu} \quad J_{d,d+1} = D, \quad J_{\mu d} = \frac{1}{2}(P_\mu - K_\mu) \quad J_{\mu, d+1} = \frac{1}{2}(P_\mu + K_\mu) \quad (3.1.9)$$

these follow the commutation relations of the rotation group

$$[J_{ab}, J_{cd}] = i(\eta_{ad} J_{bc} - \eta_{ac} J_{bd} + \eta_{bc} J_{ad} - \eta_{bd} J_{ac}) \quad (3.1.10)$$

with signature $(+ \dots - +)$. Hence, we see that the conformal group in d dimensions is $SO(2, d)$ and has $(d+1)(d+2)/2$ generators. In $d = 4$ these fifteen comprise four translations, six Lorentz transformations, one dilatation and four special conformal transformations.

We now turn our attention to finite transformations. For translations, Lorentz transformations and rotations these clearly take the form

$$x'_\mu = x_\mu + a_\mu \quad x'_\mu = \Lambda_\mu^\nu x^\nu \quad x'_\mu = \lambda x_\mu. \quad (3.1.11)$$

For the special conformal transformation one finds

$$x'^\mu = \frac{x^\mu - b^\mu x^2}{1 - 2b \cdot x + x^2 b^2}. \quad (3.1.12)$$

This may be readily obtained by introducing the finite transformation of conformal inversion

$$I : x^\mu \rightarrow \frac{x^\mu}{x^2} \quad (3.1.13)$$

which clearly satisfies and then applying

$$I \circ P \circ I : x^\mu \rightarrow \frac{x^\mu}{x^2} \rightarrow \frac{x^\mu}{x^2} - b^\mu \rightarrow \frac{x^\mu - b^\mu x^2}{1 - 2b \cdot x + x^2 b^2}. \quad (3.1.14)$$

Hence, we may also say that conformal symmetry is built from Poincare symmetry plus dilatations and inversions, although the latter lack an infinitesimal form and do not form part of the algebra. It is in general much easier to consider to the scaling of quantities under inversions than under special transformations.

3.1.2 Conformal Primaries

The transformation of a scalar field under a finite conformal transformation takes the form

$$\phi'(x') = \left| \frac{\partial x'}{\partial x} \right|^{\Delta/d} \phi(x). \quad (3.1.15)$$

Under dilations this reduces to $\phi(x) \rightarrow \lambda^{-\Delta} \phi(x)$, where Δ is the scaling dimension.

In general this receives quantum corrections, so we may write

$$\Delta = \Delta_0 + \gamma \quad (3.1.16)$$

where γ is called the anomalous dimension. For a general field with Lorentz indices α we have

$$\Phi'_\alpha(x') = \left| \frac{\partial x'}{\partial x} \right|^{\Delta/d} R_\alpha^\beta \Phi_\beta(x) \quad (3.1.17)$$

where R_α^β is the appropriate representation of the Lorentz transformation.

We can build representations of the conformal group in the following way. The action of the dilatation operator on a general local operator takes the form

$$[D, \mathcal{O}(x)] = i(-\Delta + x \partial_x) \mathcal{O}(x). \quad (3.1.18)$$

We may now let D act of $[K_\mu, \mathcal{O}(0)]$ which leads via the Jacobi identity to

$$\begin{aligned} [D, [K_\mu, \mathcal{O}(0)]] &= [[D, K_\mu], \mathcal{O}(0)] + [K_\mu, [D, \mathcal{O}(0)]] \\ &= -i(\Delta - 1)[K_\mu, \mathcal{O}(0)] \end{aligned} \tag{3.1.19}$$

Thus we see that acting with K_μ lowers the dimension of an operator by 1. In a unitary theory the dimensions of all operators must be positive (excluding the identity), so if we iterate this process we must at some point terminate; ie, there must exist some $\tilde{\mathcal{O}}$ such that

$$[K_\mu, \tilde{\mathcal{O}}] = 0. \tag{3.1.20}$$

Such operators are called *primary*. Given a primary operator we may build operators with higher dimension by acting on it with the generators of the conformal algebra; these are called the conformal descendants of $\tilde{\mathcal{O}}$. Note that since the conformal boosts always shift the dimension by an integer, the anomalous dimension of all operators in such a representation is the same.

3.1.3 Correlation Functions

Conformal symmetry strongly restricts the form observables. Consider for example the two-point correlator of the scalar operators $\mathcal{O}_1, \mathcal{O}_2$ with dimensions Δ_1, Δ_2 respectively. From Poincare invariance we know it can only depend on the Lorentz invariant $x_{12} = (x_1^\mu - x_2^\mu)^2$ so we may write

$$\langle \mathcal{O}_1(x_1) \mathcal{O}_2(x_2) \rangle = f(x_{12}). \tag{3.1.21}$$

Now we also demand covariance under dilatations, which requires

$$\langle \mathcal{O}_1(x_1) \mathcal{O}_2(x_2) \rangle = c(x_{12})^{(-\Delta_1 + \Delta_2)/2} \tag{3.1.22}$$

where c is some constant. Finally we note that covariance under conformal boosts requires

$$\langle \mathcal{O}_1(x_1)\mathcal{O}_2(x_2) \rangle = c(x_{12})^{-\Delta} \quad \text{for } \Delta_1 = \Delta_2, \text{ otherwise } 0 \quad (3.1.23)$$

and the two-point function is totally constrained by symmetry. Similar reasoning applies at three points, where we find

$$\langle \mathcal{O}_1(x_1)\mathcal{O}_2(x_2)\mathcal{O}_3(x_3) \rangle = c(x_{12})^{-(\Delta_1+\Delta_2-\Delta_3)/2}(x_{23})^{-(\Delta_2+\Delta_3-\Delta_1)/2}(x_{31})^{-(\Delta_3+\Delta_1-\Delta_2)/2} \quad (3.1.24)$$

and operators with spin are similarly constrained.

Something new happens at four points, where we may begin to write down new conformal invariants called *conformal cross ratios* of the form

$$\frac{x_{ij}^2 x_{kl}^2}{x_{ik}^2 x_{jl}^2}. \quad (3.1.25)$$

At four points, there are two such:

$$u = \frac{x_{12}^2 x_{34}^2}{x_{13}^2 x_{24}^2} \quad v = \frac{x_{14}^2 x_{23}^2}{x_{13}^2 x_{24}^2}, \quad (3.1.26)$$

so the four-point function contains a theory-dependent function of u, v with a prefactor carrying the conformal weights at the external points. For instance for four scalar operators of dimension 2:

$$\langle \mathcal{O}_1(x_1)\mathcal{O}_2(x_2)\mathcal{O}_3(x_3)\mathcal{O}_4(x_4) \rangle = \frac{1}{x_{12}^2 x_{24}^2 x_{43}^2 x_{31}^2} f(u, v). \quad (3.1.27)$$

We note here the important point that for massless on-shell kinematics such as found in scattering amplitudes, the arrival of cross ratios is delayed until six points.

3.1.4 Superconformal Symmetry

In a conformal theory with supersymmetry, we enhance the symmetry by commuting the supercharges with the special conformal generators:

$$[K^\mu, Q_{\alpha A}] = 2\sigma_{\alpha\dot{\alpha}}^\mu \epsilon^{\dot{\alpha}\beta} \tilde{S}_{\beta A} \quad [K^\mu, \tilde{Q}_{\dot{\alpha}}^A] = 2\sigma_{\alpha\dot{\alpha}}^\mu \epsilon^{\alpha\beta} S_{\beta}^A \quad (3.1.28)$$

S, \tilde{S} are called the superconformal generators, since they bear the same relation to the conformal boosts as the supercharges bear to momentum:

$$\{S_\alpha^A, S_{\dot{\alpha}}^B\} = 2\sigma_{\alpha\dot{\alpha}}^\mu K_\mu \delta^{AB} \quad (3.1.29)$$

and they analogously act to lower the dimension of a local operator by 1/2. Therefore one may define a superconformal primary operator by

$$[S, \mathcal{O}]_\pm = 0 \quad (3.1.30)$$

and its superconformal descendants by acting thereon with Q . As for conformal primaries, all descendants have the same anomalous dimension. Note that all superconformal primaries are primary with respect to K^μ , but the converse is not true. With the addition of the superconformal primaries, the algebra is enhanced to include

$$\{Q_{\alpha A}, S_\beta^B\} = -i\epsilon_{\alpha\beta}\gamma^{IJ}{}_A{}^B R_{IJ} + 2\sigma_{\alpha\beta}^{\mu\nu}\delta_A^B M_{\mu\nu} - \frac{1}{2}\delta_A^B D. \quad (3.1.31)$$

A particularly important class of superconformal primary operators are those that commute with some of the supercharges

$$[Q_\alpha^A, \mathcal{O}] = 0 \quad \text{for some } A, \alpha. \quad (3.1.32)$$

It then follows that

$$[\{Q_{\alpha A}, S_\beta^B\}, \mathcal{O}] = [-i\epsilon_{\alpha\beta}\gamma^{IJ}{}_A{}^B R_{IJ} + 2\sigma_{\alpha\beta}^{\mu\nu}\delta_A^B M_{\mu\nu} - \frac{1}{2}\delta_A^B D, \mathcal{O}]. \quad (3.1.33)$$

If \mathcal{O} is a scalar, this reduces to a relation between the action of the R -symmetry and the dimension:

$$\gamma^{IJ}{}_A{}^B [R_{IJ}, \mathcal{O}] = \Delta \delta_A^B \mathcal{O} \quad (3.1.34)$$

which is satisfied for at most half the supersymmetries when the R -charge equals the dimension. In extended supersymmetries where the R -charge is a vector, we need only consider operators with R -charge $(J, 0, \dots, 0)$ and $\Delta = J$ since any rotations

thereof will sit in the same representation of the R -symmetry. These operators are called BPS operators, or Chiral Primaries.

In general, the dimension of an operator depends on the coupling g . As we have seen, descendants of a given primary have the same anomalous dimension, and we have shown that BPS operators commute with some of the supercharges for all values of the coupling. Since the dimension is proportional to the R -charge, which is a discrete quantity, it cannot change with the variation of a continuous parameter like the coupling; therefore, the anomalous dimension of BPS operators vanishes and their correlation functions are free of UV divergences.

3.1.5 Classical and Quantum CFTs

Which theories can possess conformal symmetry? The mass operator $m^2 = p^2$ does not commute with dilatations

$$e^{i\alpha D} p^2 e^{-i\alpha D} = e^{2\alpha} p^2. \quad (3.1.35)$$

Consequently, conformal symmetry requires either a massless theory or one with a continuous mass spectrum. More generally, it is clear that theories with dimensionful couplings will never be conformally invariant.

At the classical level it can be shown [46] that all theories with dimensionless non-derivative and Yang-Mills couplings are conformal. It is then possible [47] to redefine the canonical energy-momentum tensor $T_{\mu\nu}$ by the addition of total derivatives such that

$$J^\mu = k_\nu \theta^{\mu\nu}, \quad \theta^{\mu\nu} = \theta^{\nu\mu}, \quad \partial_\mu \theta^{\mu\nu} = 0, \quad (3.1.36)$$

where J_μ is the Noether current associated to a conformal transformation and k_μ is the Killing vector defined in 3.1.4. Hence, we may write the conservation of the

current as

$$\partial_\mu J^\mu = \frac{1}{2}(\partial_\mu k_\nu + \partial_\nu k_\mu)\theta^{\mu\nu} = \frac{1}{2}(\partial \cdot k)\theta^\mu{}_\mu \quad (3.1.37)$$

and conformal symmetry is equivalent to the vanishing of the trace of the energy momentum tensor. This tracelessness may be violated by an anomaly in the quantum theory, which is in general proportional to the β functions. For instance, in massless QCD the conformal anomaly is given by $\beta(g)/(2g)F^2$ [48]. This matches our classical intuition that for conformal invariance to hold the couplings must be dimensionless. We can then say that a quantum theory has conformal symmetry iff

- The classical couplings are dimensionless.
- $\beta(g) = 0$ for all g .

3.2 $\mathcal{N} = 4$ Super Yang-Mills

Lagrangian and Field Content

$\mathcal{N} = 4$ Super Yang-Mills is the maximally supersymmetric renormalizable field theory in four dimensions, consisting of a single $\mathcal{N} = 4$ Vector multiplet with the associated R-symmetry $SU(4)$. The Lagrangian may be obtained from $\mathcal{N} = 1$ sYM in ten dimensions [49].

$$\mathcal{L}_{10} = \text{Tr} \left(-\frac{1}{4} F_{MN} F^{MN} + \frac{ig}{2} \bar{\Psi} \Gamma^N D_N \Psi \right). \quad (3.2.1)$$

The dimensional reduction is made by requiring that the fields do not depend on six of the spacetime dimensions, i.e.

$$\partial^{4+m} A^N = 0, \quad \partial^{4+m} \Psi = 0, \quad \partial^{4+m} \bar{\Psi} = 0, \quad m = 1, \dots, 6. \quad (3.2.2)$$

One must then make a choice of representation of the ten-dimensional Γ matrices in terms of the four and six dimensional γ matrices. One such is

$$\Gamma_\mu = \gamma_\mu \otimes 1 \quad \text{for } \mu = 1, \dots, 4, \Gamma_{4+m} = \gamma_5 \otimes \tilde{\Gamma}_m \quad \text{for } m = 1, \dots, 6 \quad (3.2.3)$$

where γ_μ and γ_5 are the standard four dimensional Dirac matrices and $\tilde{\Gamma}_m$ are the six dimensional euclidean Dirac matrices given by

$$\tilde{\Gamma}_m = \begin{pmatrix} 0 & \tilde{\sigma}_m \\ \tilde{\sigma}_m^{-1} & 0 \end{pmatrix}. \quad (3.2.4)$$

We also get six scalars from the remaining components of the gauge field A_N

$$\phi_m = A_{4+m}. \quad (3.2.5)$$

Using the six dimensional $\tilde{\sigma}_m$ we can write

$$\phi_{AB} = -\frac{1}{2}(\tilde{\sigma}_m)_{AB}\phi_m. \quad (3.2.6)$$

This leads to the following Lagrangian in four dimensions.

$$\begin{aligned} \mathcal{L}_4 = \text{Tr} \left(-\frac{1}{4}F_{\mu\nu}F^{\mu\nu} + i\lambda_A\sigma^\mu D_\mu\bar{\lambda}^A + \frac{1}{2}D_\mu\phi_{AB}D^\mu\phi^{AB} \right. \\ \left. + ig\lambda_A[\lambda_B, \phi^{AB}] + ig\bar{\lambda}^A[\lambda^B, \phi_{AB}] + g^2[\phi_{AB}, \phi_{CD}][\phi^{AB}, \phi^{CD}] \right). \end{aligned} \quad (3.2.7)$$

The matter content is a gauge field A^μ , four complex fermions $\lambda^{\alpha A}$ and six real scalars ϕ_{AB} , all in the adjoint representation of the gauge group. Note that this formulation makes the R -symmetry manifest as $SU(4)$; it is also common in the literature not to implement 3.2.6 and consider the $SO(6)$ R -symmetry of the six scalars ϕ_m , which are often combined into the complex scalars $Z = \phi_1 + i\phi_2$, $W = \phi_3 + i\phi_4$, $X = \phi_5 + i\phi_6$.

Conformal Symmetry and UV Finiteness

The form and relative factors of 3.2.7 are fixed by supersymmetry; there is a single coupling constant g . It's β function has been shown to vanish up to three loops by

direct calculation [50] [51] [52] and there exist numerous arguments that this holds to all loops [53], [54], [55], [56]. Therefore, superconformal symmetry is preserved in the quantum theory and SUSY-invariant quantities are UV-finite.

Dynamical Phases

The scalar potential term is

$$-g^2[\phi_{AB}, \phi_{CD}]^2. \quad (3.2.8)$$

This potential is flat, so there are two classes of ground states:

- The superconformal phase, where $\langle \phi_{AB} \rangle = 0$ for all A, B . The gauge group and superconformal symmetry are unbroken.
- The Coulomb phase, where $\langle (\phi_{AB})^I_J \rangle \neq 0$ for some choice of R-indices A, B and gauge indices I, J . The detailed dynamics will depend on the particular choice of residual symmetry, but in general the gauge group will be broken to a product $U(N_1) \times U(N_2) \times \dots$ and the R -symmetry will break to some subgroup. Some of the scalars and their superpartners will acquire a mass so conformal symmetry is also spontaneously broken.

3.2.1 Superamplitudes

Now we turn to the S-Matrix in $\mathcal{N} = 4$. Supersymmetry imposes many relations between amplitudes in the form of super Ward identities arising from the expansion of

$$0 = \langle 0 | [\bar{Q}_{\dot{\alpha}}^A, \varphi(1), \dots, \varphi(n)] | 0 \rangle = \sum_{i=1}^n \langle 0 | \varphi(1) \dots [\bar{Q}_{\dot{\alpha}}^A, \varphi(i)] \dots \varphi(n) | 0 \rangle. \quad (3.2.9)$$

On shell, the supersymmetry algebra is

$$\{q_{\alpha}^I, \bar{q}_{J\dot{\alpha}}\} = \delta_J^I \lambda_{\alpha} \tilde{\lambda}_{\dot{\alpha}} \quad (3.2.10)$$

and we can decompose the spinor q_α^I into

$$q_\alpha^I = \lambda_\alpha q_1^I + \mu_\alpha q_2^I \quad (3.2.11)$$

with $\langle \lambda \mu \rangle \neq 0$. By contracting with λ^α we see that q_2 and \bar{q}_2 anticommute with all generators, and can be set to zero. Then we see that the superalgebra can be represented by Grassmann variables

$$\{q_1^I, \bar{q}_{1J}\} = \delta_J^I \quad q^I = \eta^I \quad \bar{q}_I = \frac{\partial}{\partial \eta^I}. \quad (3.2.12)$$

Therefore, we can define the Nair superwavefunction [57]

$$\Phi(p, \eta) := g^+(p) + \eta_A \lambda^A(p) + \frac{\eta_A \eta_B}{2!} \phi^{AB}(p) + \epsilon^{ABCD} \frac{\eta_A \eta_B \eta_C}{3!} \bar{\lambda}_D(p) + \eta_1 \eta_2 \eta_3 \eta_4 g^-(p) \quad (3.2.13)$$

We can now write a superamplitude, as a function of both p and η , that contains all external states of the theory

$$\mathcal{A}_n(\lambda_i, \tilde{\lambda}_i, \eta_i) = \mathcal{A}(\Phi_i) \quad (3.2.14)$$

and the component amplitudes are extracted by expanding to appropriate powers in η . For instance, the fully gluonic MHV amplitude will be the coefficient of $(\eta_i)^2 (\eta_j)^2$.

In this formalism the super Ward identities are fully equivalent to the annihilation of the superamplitude by the supermomenta Q, \bar{Q} . In spinor helicity notation these take the form

$$Q_\alpha^A = \sum_i \lambda_{i\alpha} \eta_i^A, \quad \bar{Q}_{\dot{\alpha}A} = \sum_i \tilde{\lambda}_{i\dot{\alpha}} \frac{\partial}{\partial \eta^A}. \quad (3.2.15)$$

We note that the fermionic delta function encoding supermomentum conservation has the form

$$\delta^{(8)}(Q_\alpha^A) = \prod_A \prod_\alpha Q_\alpha^A = \prod_A \langle ij \rangle \eta_i^A \eta_j^A. \quad (3.2.16)$$

which is annihilated by $\bar{Q}_{\dot{\alpha}A}$ on account of momentum conservation. Therefore half of the supersymmetry constraints are imposed automatically if the amplitude is of

the form

$$\mathcal{A}_n = \delta^{(4)} \left(\sum_i \lambda_{i\alpha} \tilde{\lambda}_{i\dot{\alpha}} \right) \delta^{(8)} \left(\sum_i \lambda_{i\alpha} \eta_i^A \right) \mathcal{F}_n \quad (3.2.17)$$

with the other half placing constraints on the degree $4n$ grassmann polynomial \mathcal{F}_n .

We then note that expanding the fermionic delta function to the order $(\eta_i)^4(\eta_j)^4$ produces the numerator of the Parke-Taylor formula, so we may succinctly write the tree-level superamplitude as [8]

$$\mathcal{A}_n = \frac{\delta^{(4)}(\sum_i \lambda_i \tilde{\lambda}_i) \delta^{(8)}(\sum_i \lambda_i \eta_i)}{\langle 12 \rangle \langle 23 \rangle \dots \langle n1 \rangle} \mathcal{P}_n \quad (3.2.18)$$

$$\mathcal{P}_n = 1 + \mathcal{P}_n^{\text{MHV}} + \mathcal{P}_n^{\text{NMHV}} + \dots + \mathcal{P}_n^{\overline{\text{MHV}}} \quad (3.2.19)$$

where the $SU(4)$ R-symmetry constrains each term $\mathcal{P}_n^{\text{N}^k\text{MHV}}$ to be of degree $4k$.

As well as allowing us to efficiently describe relations between amplitudes, this description is also highly efficient for loop-level calculations where we must sum over particles in cuts. If we consider the one loop superamplitude in a generic cut as in section 2.4, we may now write

$$\mathcal{A}_n|_{\text{P,Q-cut}} = \int d^4\eta_\ell d^4\eta_k \mathcal{A}_L \mathcal{A}_R. \quad (3.2.20)$$

Now we consider the product of fermionic delta-functions which will appear in the above. We note that the support of the second delta-function allows us to write the important identity

$$\int d^4\eta_\ell d^4\eta_k \delta^{(8)}(Q_L) \delta^{(8)}(Q_R) = \delta^{(8)}(Q) \int d^4\eta_\ell d^4\eta_k \delta^{(8)}(Q_R). \quad (3.2.21)$$

We then expand the delta function under the integral using equation 3.2.16 and perform the fermionic integration, which picks out the term proportional to $\eta_\ell^4 \eta_k^4$ giving us a factor of $\langle \ell k \rangle^4$. The cut expression now takes the form

$$\mathcal{A}_n^{(0)} \frac{\langle \ell k \rangle^2 \langle m_2 m_2 + 1 \rangle \langle m_1 m_1 - 1 \rangle}{\langle n_2 \ell \rangle \langle k m_1 \rangle \langle m_2 + 1 \ell \rangle \langle m_1 - 1 k \rangle} \quad (3.2.22)$$

whence we can proceed as described above, where the fermionic integration has replaced the sum over states.

We can also use superamplitudes in computations at tree level. The BCFW shifts earlier introduced do not respect supermomentum conservation; and $[i, j]$ shift also shifts q_α^A by $-z\eta_j\lambda_i$. They must be modified by shifting fermionic variables by

$$\eta_i \rightarrow \eta_i(z) = \eta_i + z\eta_j \quad (3.2.23)$$

which induces the following on the supermomentum

$$q_i \rightarrow q_i(z) = q_i + z\eta_j\lambda_i. \quad (3.2.24)$$

The sum over all internal helicity configurations can be carried out, like at loop level, by a Grassmann integral, so we may write the supersymmetric BCFW relation as

$$\mathcal{A}_n = \sum_{i,j} \int d^4\eta_P \hat{\mathcal{A}}_L \frac{1}{P_{ij}^2} \hat{\mathcal{A}}_R. \quad (3.2.25)$$

3.2.2 Amplitudes on The Coulomb Branch

Here we describe amplitudes on a particular point on the Coulomb branch, which have been studied at tree level by [58]. We move to a particular point on the Coulomb Branch by considering a stack of $(N + M)$ D3-Branes. We separate M Branes from the rest, choosing non-zero scalar VEVs

$$\begin{aligned} \langle (\phi^{12})_J^I \rangle &= \langle (\phi^{34})_I^J \rangle = v\delta_J^I \text{ for } I, J \in U(M) \\ \langle \phi^{ab} \rangle &= 0 \text{ otherwise.} \end{aligned} \quad (3.2.26)$$

This preserves $\mathcal{N} = 4$ supersymmetry, but breaks the R -symmetry to $\text{Sp}(4) \supset \text{SU}(2) \times \text{SU}(2)$ and the gauge group to $U(N) \times U(M)$. We now have massive $\mathcal{N} = 4$ multiplets arising from strings stretched between branes, in the bifundamental of

$U(N) \times U(M)$ with mass $m^2 = g^2 v^2$ containing massive W-bosons, their fermionic partners and five scalars w .

To write massive amplitudes we will use the massive spinor helicity formalism of [59]. We introduce a null reference vector q and write

$$p_i = p_i^\perp + \frac{m_i^2}{p_i \cdot q} q \quad \text{with } p_i^{\perp 2} = 0 \quad (3.2.27)$$

where m_i is the mass of the i th particle. One then writes amplitudes in terms of the spinors $\langle i^\perp |$, $\langle q |$ and their conjugates associated with the null vectors p_i^\perp and q . For transversely polarised vector bosons the three-point amplitudes are then:

$$\begin{aligned} \langle W_1^- \bar{W}_2^+ g_3^+ \rangle &= \frac{[2^\perp 3]^\perp{}^3}{[1^\perp 2^\perp][2^\perp 3]} \\ \langle W_1^+ \bar{W}_2^+ g_3^- \rangle &= \frac{[1^\perp 2^\perp]^\perp{}^3}{[2^\perp 3][31^\perp]} \end{aligned} \quad (3.2.28)$$

exactly as in the conformal phase with appropriately perped momenta. Since mass can be considered momenta transverse to the branes, we have the important condition

$$\sum_i m_i = 0 \quad (3.2.29)$$

in any amplitude. Crucially this means that for uniform VEVs there must be an even number of massive particles in each amplitude. Also, the broken R -symmetry admits helicity configurations forbidden in the conformal phase; of particular importance is the Ultra Helicity Violating (UHV) amplitude

$$\langle W^- \bar{W}^+ g^+ g^+ \rangle = \frac{m^2 \langle q 1^\perp \rangle^2 [34]}{\langle q 2^\perp \rangle^2 \langle 34 \rangle (t + m^2)} \quad (3.2.30)$$

which is the first in an infinite sequence of such amplitudes (here t is the standard Mandelstam variable). Note that it smoothly disappears as $m^2 \rightarrow 0$. The four-point MHV amplitude is given:

$$\langle W^- \bar{W}^- g^+ g^+ \rangle = \frac{\langle 1^\perp 2^\perp \rangle^2 [34]}{\langle 34 \rangle (t + m^2)} \quad (3.2.31)$$

To write superamplitudes on the Coulomb Branch, the SUSY invariants are split between the two SU(2) subsectors. For some solvable functions K_n and with $\mu_i = m_i/[qi^\perp]$:

$$\begin{aligned}\delta_{12} = & \delta^{(4)}(|i^\perp\rangle) + K_4 \delta^{(2)}(\langle qi^\perp \rangle \eta_{ia}) \delta^{(2)}(\mu_i \eta_{ia}) \\ & + K'_4 [\delta^{(2)}(|i^\perp\rangle) \eta_{i1}] \delta(\langle qi^\perp \rangle \eta_{i2}) \delta(\mu_i \eta_{i2}) + \delta^{(2)}(|i^\perp\rangle) \eta_{i1}] \delta(\langle qi^\perp \rangle \eta_{i2}) \delta(\mu_i \eta_{i1}) \\ & + K_2 \delta^{(2)}(\langle qi^\perp \rangle \eta_{ia}) + K_6 \delta^{(4)}(|i^\perp\rangle \eta_{ia}) \delta^{(2)}(\mu_i \eta_{ia})\end{aligned}\tag{3.2.32}$$

and similarly for $R = 3, 4$. The complete four-point superamplitude is given:

$$\mathcal{A}_4 = \frac{[1^\perp 2^\perp][34]}{\langle 34 \rangle x_{13}(x_{23} + m^2)} \delta_{12} \times \delta_{34}.\tag{3.2.33}$$

Note that this is an η -polynomial of mixed degree, from η^6 to η^{12} which mixes MHV and UHV amplitudes.

The structure of the superamplitude simplifies significantly if we introduce the a linear orthogonality condition on q such that the perped momenta satisfy momentum conservation among themselves:

$$\sum_i p_i^\perp = 0.\tag{3.2.34}$$

For two massive lines, this implies that $q \cdot (p_1 + p_2) = 0$ and the K-functions simplify dramatically, leading to the following factorised form of δ_{12} :

$$\delta_{12} = \left[\delta^{(4)}(|i^\perp\rangle \eta_{ia}) + \frac{m \langle 1^\perp 2^\perp \rangle}{\langle q1^\perp \rangle \langle q2^\perp \rangle} \delta^{(2)}(\langle qi^\perp \rangle \eta_{ia}) \right] \times \left[1 - \frac{[q1^\perp][q2^\perp]}{m[1^\perp 2^\perp]} \delta^{(2)}(\mu_i \eta_{ia}) \right].\tag{3.2.35}$$

A similar factorisation condition holds for four or more massive lines, but in such cases the remaining K -functions do not simplify quite so dramatically.

3.2.3 BPS Operators

Since all fields transform in the adjoint, it is clear that the simplest gauge invariant operators take the form of traces of products

$$\mathcal{O} = \text{Tr}(\chi_1 \chi_2 \dots \chi_n). \quad (3.2.36)$$

where χ_I can be any of the covariantly transforming fields, possibly including covariant derivatives. We can build more operators by taking products of traces; in the planar limit the dimension of a product of operators becomes equal to the sum of their dimensions, so all information about the spectrum of local operators is contained in the single trace operators.

The chiral primary, or half-BPS operators satisfying the condition 3.1.34 carry R -charge $(J, 0, 0)$. This is clearly satisfied at zero coupling by operators of the form

$$\mathcal{O}_J = \text{Tr}(\phi_{AB}^J) \quad (3.2.37)$$

or any other product of scalars that does not contain both ϕ_{AB} and $\bar{\phi}^{AB}$ for any A, B . Since the dimension of this operator is protected, this holds for all coupling. Our paradigmatic example shall be the operator

$$\mathcal{O}_{ABCD} = \text{Tr}(\phi_{AB}\phi_{CD}) - \frac{1}{12}\epsilon_{ABCD}\text{Tr}(\bar{\phi}^{LM}\phi_{LM}) \quad (3.2.38)$$

transforming in the $\mathbf{20}'$ of $SU(4)$. This operator forms the lowest weight state of the stress-tensor multiplet also containing the on-shell Lagrangian \mathcal{L} and the stress-energy tensor $T_{\mu\nu}$.

3.2.4 Form Factors

We discuss here the bosonic form factors of BPS operators. Without loss of generality we consider the operator

$$\mathcal{O} = \text{Tr}(\phi_{12}\phi_{12}) \quad (3.2.39)$$

which is a component of the 1/2-BPS operator 3.2.38. We have already shown in section 2.7 that at one loop the Sudakov form factor is given by

$$F^{(1)} = 2q^2 \text{Tri}(q^2, \epsilon). \quad (3.2.40)$$

Two-Loop Sudakov

As at one loop there is a single kinematic channel so we may perform two particle cuts and lift to an integral. There are two distinct configurations to consider: in the first a tree-level form factor and a one-loop amplitude enter the cut, in the second the cut divides a one-loop form factor from a tree level amplitude. We will focus on former case, where we must for the first time consider non-planar contributions even at leading N [60].

Including colour indices, the tree-level form factor is given $F^{(0)}(q^2) = \delta^{a_{\ell_1} a_{\ell_2}}$. At one loop the full amplitude may be written

$$\begin{aligned} \mathcal{A}^{(1)}(1, \dots, n) &= \mathcal{A}_P^{(1)} + \mathcal{A}_{NP}^{(1)} \\ &= N \sum_{\sigma \in S_n/Z_n} \text{Tr}(T^{a_{\sigma 1}} \dots T^{a_{\sigma n}}) A_{n;1}^{(1)}(1, \dots, n) \\ &\quad + \sum_{\sigma \in S_n/S_{n;c}} \sum_{c=2}^{n/2+1} \text{Tr}(T^{a_{\sigma 1}} \dots T^{a_{\sigma c-1}}) \text{Tr}(T^{a_{\sigma c} a_{\sigma n}}) A_{n;c}(1, \dots, n) \end{aligned} \quad (3.2.41)$$

where $S_{n;c}$ is the subset of permutations leaving the double-trace structure invariant. Considering first the planar part there are six possible structures

$$\begin{aligned} &\text{Tr}(1, 2, \ell_1, \ell_2), \quad \text{Tr}(1, 2, \ell_2, \ell_1), \quad \text{Tr}(1, \ell_1, \ell_2, 2), \quad \text{Tr}(1, \ell_2, \ell_1, 2) \\ &\text{Tr}(1, \ell_1, 2, \ell_2), \quad \text{Tr}(1, \ell_2, 2, \ell_1). \end{aligned} \quad (3.2.42)$$

Using the identity 2.1.2 we see that those with adjacent loop momenta are leading in colour when contracted with the form factor. All four traces give $N \text{Tr}(a_1 a_2) =$

$N^2\delta^{a_1a_2}$. The contribution to the cut from the planar integrand is then

$$N^2\delta^{a_1a_2} \left(A_{4;1}^{(1)}(1, 2, \ell_1, \ell_2) + A_{4;1}^{(1)}(1, 2, \ell_2, \ell_1) + A_{4;1}^{(1)}(2, 1, \ell_1, \ell_2) + A_{4;1}^{(1)}(2, 1, \ell_2, \ell_1) \right). \quad (3.2.43)$$

The non-planar amplitude at four points is given by

$$\mathcal{A}_{NP}^{(1)} = \text{Tr}(12)\text{Tr}(\ell_1\ell_2)A_{4;3}^{(1)}(1, 2, \ell_1, \ell_2) + \text{Tr}(1\ell_1)\text{Tr}(2\ell_2)A_{4;3}^{(1)}(1, \ell_1, 2, \ell_2) + \dots \quad (3.2.44)$$

where the leading colour structure contracted with the form factor is $\text{Tr}(12)\text{Tr}(\ell_1\ell_2)$

which carries $N^2\delta^{a_1a_2}$. The combination $A_{4;3}^{(1)}$ is given

$$\begin{aligned} A_{4;3}^{(1)} = & A_{4;1}^{(1)}(2, 1, \ell_1, \ell_2) + A_{4;1}^{(1)}(2, \ell_1, 1, \ell_2) + A_{4;1}^{(1)}(\ell_1, 2, 1, \ell_2) \\ & + A_{4;1}^{(1)}(1, 2, \ell_1, \ell_2) + A_{4;1}^{(1)}(1, \ell_1, 2, \ell_2) + A_{4;1}^{(1)}(\ell_1, 1, 2, \ell_2). \end{aligned} \quad (3.2.45)$$

Thus the two-loop cut integrand is given by

$$F^{(2)}(q^2)|_{q^2\text{-cut}} = 2N^2\delta^{a_1a_2} \int d\text{LIPS} [4A^{(1)}(1, 2, \ell_1, \ell_2) + 2A^{(1)}(1, \ell_1, 2, \ell_2)]. \quad (3.2.46)$$

The one-loop amplitude is proportional to the tree amplitude

$$A^{(1)}(1, 2, 3, 4) = A^{(0)}(1, 2, 3, 4)F^{0m}(1, 2, 3, 4) \quad (3.2.47)$$

so by the same calculation as 2.7 we find

$$F^{(2)a_1a_2}(q^2) = N^2\delta^{a_1a_2} F^{(2)}(q^2) \quad (3.2.48)$$

where

$$F^{(2)}(q^2) = 2 [4LT(q^2) + CT(q^2)]. \quad (3.2.49)$$

Here $LT(q^2)$ and $CT(q^2)$ are the scalar ladder and crossed triangles given by A.2.1 and A.2.3 respectively. One can compare with the exponentiation formula 2.5.59 finding

$$F^{(2)}(q^2, \epsilon) - \frac{1}{2} [F^{(1)}(q^2, \epsilon)]^2 = (-q^2)^{-2\epsilon} \left[\frac{\zeta_2}{\epsilon^2} + \frac{\zeta_3}{\epsilon} + O(\epsilon) \right] \quad (3.2.50)$$

which is of the correct form with

$$f_0^{(1)} = -2\zeta_2, \quad f_1^{(1)} = -2\zeta_3. \quad (3.2.51)$$

MHV Form Factors at One Loop

We will now consider the one-loop MHV form factors first computed in [61]. In a general kinematic channel we have

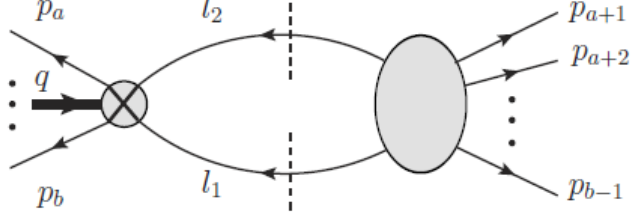


Figure 3.1: The cut of the MHV form factor in a generic kinematic channel.

$$\begin{aligned}
 F^{(1)}|_{s_{a+1,b-1}\text{-cut}} &= \int d\text{LIPS}(\ell_1, \ell_2, P_{a+1,b-1}) \\
 &\quad F^{(0)}(-\ell_2^\phi, -\ell_1^\phi, b^+, \dots, a^+) \\
 &\quad \times A(\ell_1, \ell_2, (a+1)^+, \dots, i^\phi, \dots, j^\phi, \dots, (b-1)^+). \quad (3.2.52)
 \end{aligned}$$

This leads to the following cut integrand:

$$F^{(0)} \times \frac{\langle a \ a+1 \rangle \langle \ell_1 \ell_2 \rangle^2 \langle b-1 \ b \rangle}{\langle a \ell_2 \rangle \langle \ell_2 \ a+1 \rangle \langle b-1 \ \ell_1 \rangle \langle \ell_1 b \rangle} \quad (3.2.53)$$

which we recognise as being in the same form as 2.4.16, and we can apply the same analysis. This leads us to a sum of four terms

$$R(b, a+1) + R(b-1, a) - R(b, a) - R(b-1, a+1) \quad (3.2.54)$$

with

$$\begin{aligned}
 R(b, a) &= \frac{\langle a \ell_1 \rangle \langle b \ell_2 \rangle}{\langle a \ell_2 \rangle \langle b \ell_1 \rangle} \\
 &= 1 + \frac{(p_b P)}{2(p_b \ell_1)} + \frac{(p_a P)}{2(p_a \ell_2)} + \frac{(p_a P)(p_b P) - P^2(p_a p_b)}{2(p_b \ell_1)(p_a \ell_2)} \quad (3.2.55)
 \end{aligned}$$

where $P = p_a + \dots + p_b$. Thus each $R(i, j)$ gives rise to the cut of a box, two triangles and a two-mass easy box function with massive corners P^2 and $(P - q)^2$. As in the case of the scattering amplitude, the bubbles cancel when all the terms are included. The same is true of the triangles, except in the case $a = b$, when there survives one contribution

$$2 \frac{(p_a P)}{2(p_a \ell_1)} \quad (3.2.56)$$

corresponding to a two-mass triangle with massless leg p_a and massive legs $P_{a-1, a+1}^2$ and q^2 . Otherwise permuting the legs on either side of the cut merely runs through the partitions of masses assigned to the corners as for the scattering amplitude.

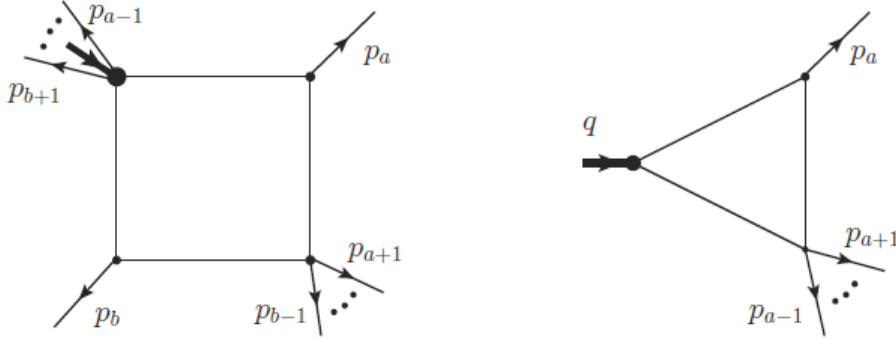


Figure 3.2: The box and triangle integrals contributing to the one-loop MHV form factor

3.2.5 Hidden Symmetries and Dualities

Dual Superconformal Symmetry

The S-Matrix of $\mathcal{N} = 4$ has several remarkable symmetry properties that are completely invisible at the level of the Lagrangian. The first of these is the so-called dual

superconformal symmetry, which may be seen by writing the amplitude as a function of dual variables x_i such that

$$p_i^\mu = x_i^\mu - x_{i+1}^\mu = x_{i,i+1}^\mu, \quad x_{i+n}^\mu = x_i^\mu \quad (3.2.57)$$

$$x_i^{\alpha\dot{\alpha}} - x_{i+1}^{\alpha\dot{\alpha}} = \lambda_i^\alpha \tilde{\lambda}_i^{\dot{\alpha}}. \quad (3.2.58)$$

Then, for example, the box integral that appears in the one-loop amplitude takes the form

$$\begin{aligned} stI_4^{(1)} &= \int \frac{d^d \ell}{(2\pi)^d} \frac{1}{\ell^2 (\ell - p_1)^2 (\ell - p_1 - p_2)^2 (\ell + p_4)^2} \\ &= \int \frac{d^d x_1}{(2\pi)^d} \frac{x_{13}^2 x_{24}^2}{x_{1l}^2 x_{2l}^2 x_{3l}^2 x_{4l}^2}. \end{aligned} \quad (3.2.59)$$

Poincare symmetry is trivially preserved in x -space, as are dilatations, while inversions act as

$$x_{ij}^2 \rightarrow \frac{x_{ij}^2}{x_i^2 x_j^2} \quad d^d x_l \rightarrow \frac{d^d x_l}{(x_l^2)^d}. \quad (3.2.60)$$

Hence we see that the integrand is covariant under conformal transformations for $d = 4$. Introducing dimensional regularization explicitly breaks this covariance, so the symmetry is anomalous. Dual supermomentum variables can then be defined through

$$\theta_i^{\alpha A} - \theta_{i+1}^{\alpha A} = \lambda_i^\alpha \eta_i^A = Q_i^{\alpha A} \quad (3.2.61)$$

leading to a separate dual superconformal symmetry which acts canonically on the chiral superspace x_i, θ_i . The action of inversions on the original on-shell superspace is

$$I[\lambda_i^\alpha] = \frac{x_i^{\dot{\alpha}\beta} \lambda_{i\beta}}{x_i^2} \quad I[\tilde{\lambda}_i^{\dot{\alpha}}] = \frac{x_i^{\alpha\beta} \tilde{\lambda}_{i\dot{\beta}}}{x_i^2} \quad (3.2.62)$$

$$I[\langle ii+1 \rangle] = \frac{\langle ii+1 \rangle}{x_i^2} \quad I[[ii+1]] = \frac{[ii+1]}{x_{i+2}^2}. \quad (3.2.63)$$

Hence, we can see that the tree-level superamplitude is dual conformal covariant.

Amplitude/Wilson Loop Duality

In terms of the embeddings of $\mathcal{N} = 4$ in String Theory, dual conformal symmetry is a consequence of a T-duality that relates the D-Brane description to the Holographic description. This leads to the remarkable equivalence of various observables [9].

At strong coupling, a natural way to approach gluon scattering in String Theory is by considering the scattering of open strings ending on a stack of $D3$ -Branes. If we place this stack in AdS_5 far from the boundary at radial coordinate z^1 , then the proper momentum of the strings is kz/R . Hence, for a given amplitude, this set up corresponds to the scattering of strings with large momentum at fixed angle, a regime that is well described by classical String Theory [62].

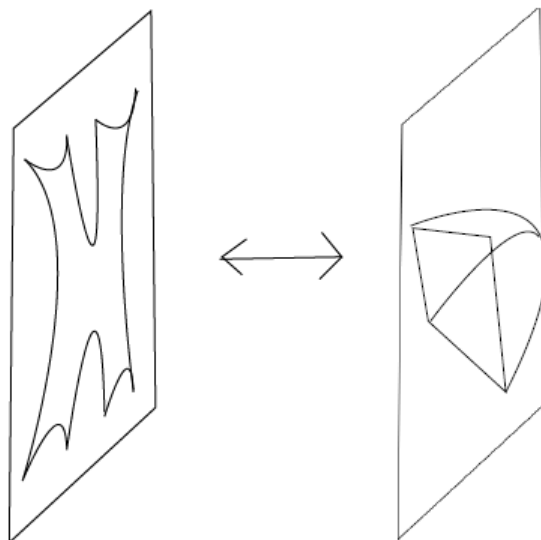


Figure 3.3: *T-duality exchanges Dirichlet for Neumann boundary conditions, sending string scattering states on a stack of D-Branes to a polygonal contour near the boundary.*

¹ z can be regarded as an IR regulator. After T -duality, it becomes a UV regulator.

Applying T -duality preserves the AdS_5 metric while acting on our system in the following way:

- The stack is sent close to the boundary by the action in the radial direction $z \rightarrow R^2/z$.
- The Neumann boundary conditions governing string scattering are exchanged for Dirichlet conditions, which constrain the worldsheet to end on the concatenated lines $\Delta y^\mu = 2\pi k^\mu$.

Note that the second is exactly the transformation to dual variables 3.2.57. Momentum conservation and the on-shell conditions ensure that these segments form a closed light-like polygon.

We have now mapped the scattering of gluons at strong coupling to the calculation of a minimal surface on the boundary of AdS_5 ending on a polygon defined by the duality transformation of the external momenta. This is exactly the criterion for computing a Wilson Loop in the AdS/CFT correspondence; hence, we have identified an equivalence at strong coupling between scattering amplitudes and polygonal lightlike Wilson Loops. The dual conformal symmetry of the amplitudes corresponds to the conformal symmetry on the Wilson Loop side, and vice versa, with the IR divergences of the amplitudes corresponding to the UV divergences of the Wilson Loop.

At weak coupling, this equivalence holds order by order in perturbation theory. Note in particular the equivalence between equations 2.4.11 and 2.6.12; the lightlike n -gon was also shown to reproduce the one-loop two-mass easy box functions in [10]. At strong coupling, powerful integrability techniques may be used to construct a solution to the minimal surface problem in terms of a Y -system, and it was subsequently shown by Maldacena and Zhiboidev [63] that an *open* Wilson Line computes the form factor

of any operator with a dimension small compared with λ .

The Dual Conformal Anomaly, The BDS Ansatz and the Remainder Function

As we have seen, the MHV amplitudes take the form

$$A_n = A_n^{\text{tree}} \times M_n(a) \quad (3.2.64)$$

where the helicity blind function $M_n(a)$ contains all dependence on the coupling constant. We have also seen that the IR divergences exponentiate in a controlled way. Analysis of the particular integral functions appearing for four and five-point amplitudes led Bern, Dixon and Smirnov [34] to conjecture that this extends also to the finite part of the amplitude, and the full amplitude is given iteratively by

$$M_n(a) = 1 + \sum_{\ell} a^{\ell} M_n^{(\ell)} = \exp \left[\sum_{\ell} a^{\ell} f^{(\ell)} M_n^{(1)}(\ell\epsilon) + C^{(\ell)} + E^{(\ell)}(\epsilon) \right]. \quad (3.2.65)$$

Although this conjecture breaks down at higher points, it is a useful starting point to see how the hidden symmetries we have described constrain the amplitude. The Wilson Loop description allows us to treat the violation of dual conformal symmetry directly in terms of anomalous Ward identities. We recall that the integration measure in $d = 4 - 2\epsilon$ does not match the weight of the Lagrangian, leading to a non-vanishing variation of the action:

$$\delta S = \frac{2\epsilon}{g^2 \mu^{2\epsilon}} \int d^d x \mathcal{L}(x). \quad (3.2.66)$$

For the Wilson Loop this adds an operator insertion $\langle \delta S W_n \rangle$ leading to anomalous terms for the action of the dual conformal generators [64]:

$$D \log \langle W_n \rangle = -\frac{2i\epsilon}{g^2 \mu^{2\epsilon}} \int d^d x \frac{\langle \mathcal{L}(x) W_n \rangle}{\langle W_n \rangle} \quad (3.2.67)$$

$$K^{\nu} \log \langle W_n \rangle = -\frac{4i\epsilon}{g^2 \mu^{2\epsilon}} \int d^d x x^{\nu} \frac{\langle \mathcal{L}(x) W_n \rangle}{\langle W_n \rangle} \quad (3.2.68)$$

which due to the factor of ϵ depends only on the divergent part of the correlator on the right hand side. Writing $\log\langle W_n \rangle = Z_n + F_n$, where Z_n is the divergent and F_n the finite part, it may be shown that

$$K^\mu F_n = \frac{1}{2} \gamma_K \sum_{i=1}^n \log \left(\frac{x_{i,i+2}^2}{x_{i-1,i+1}^2} \right) x_{i,i+1}^\mu \quad (3.2.69)$$

which leads to a differential equation for the F_n . For $n = 4, 5$ it has the unique solutions:

$$F_4 = \frac{1}{4} \gamma_K \log^2 \left(\frac{x_{13}^2}{x_{24}^2} \right) + \text{const.} \quad (3.2.70)$$

$$F_5 = -\frac{1}{8} \gamma_K \sum_{n=1}^5 \log \left(\frac{x_{i,i+2}^2}{x_{i,i+3}^2} \right) \log \left(\frac{x_{i+1,i+3}^2}{x_{i+2,i+4}^2} \right) + \text{const.} \quad (3.2.71)$$

which match precisely the BDS form for the finite part of the amplitude. However, starting at six points we may begin to build conformal cross ratios

$$u_1 = \frac{x_{13}^2 x_{46}^2}{x_{14}^2 x_{36}^2} \quad u_2 = \frac{x_{24}^2 x_{15}^2}{x_{21}^2 x_{45}^2} \quad u_3 = \frac{x_{35}^2 x_{26}^2}{x_{36}^2 x_{25}^2} \quad (3.2.72)$$

which are annihilated by K^μ . Hence, F_n also depends on some arbitrary function $R_n(u_i)$ which is unconstrained by dual conformal symmetry. In general the amplitude can be written

$$M_n = M_n^{BDS} \times R_n \quad (3.2.73)$$

and computing the n-point amplitude is reduced to the problem of computing the remainder function.

3.3 ABJM Theory

ABJM Theory describes the world-volume dynamics of multiple M2-Branes at a Z_k Orbifold singularity [65]. It is an $\mathcal{N} = 6$ superconformal Chern-Simons-Matter Theory described by the $\mathcal{N} = 2$ quiver figure 3.3

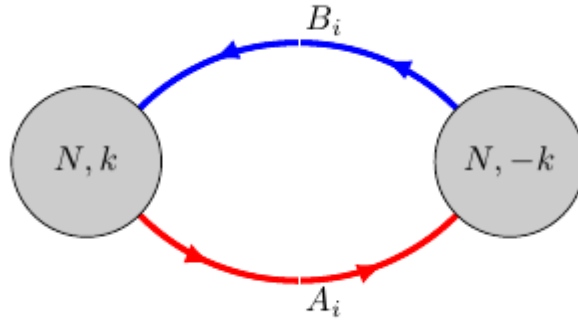


Figure 3.4: The quiver representation of ABJM Theory. The Nodes represent Chern-Simons Gauge Groups, the arrows bifundamental chiral multiplets transforming in the fundamental of the head and the antifundamental of the tail.

with the product gauge group $U(N)_k \times U(N)_{-k}$ and four bifundamental chiral multiplets A_1, A_2, B_1, B_2 , endowed with the superpotential

$$\mathcal{W} = \frac{2\pi}{k} \epsilon^{ij} \epsilon^{kl} \text{Tr}(A_i B_j A_k B_l). \quad (3.3.1)$$

The superpotential clearly possesses $SU(2)_A \times SU(2)_B$ R-symmetry, but this is enhanced by further $SU(2)$ s acting on the doublet (A_i, B_i^\dagger) . These combine to form the full $SU(4)_R$ R-symmetry, with the scalars $\phi_I = (A_1, A_2, B_1^\dagger, B_2^\dagger)$ transforming in the fundamental representation. Due to the topological nature of the Chern-Simons action

$$\mathcal{L}_{CS} = \frac{k}{4\pi} \int d^3x \epsilon^{\mu\nu\lambda} \text{tr} \left(\frac{1}{2} A_\mu \partial_\nu A_\lambda + \frac{i}{3} A_\mu A_\nu A_\lambda \right) \quad (3.3.2)$$

the gauge fields and their superpartners are non-dynamical and may be regarded as auxiliary fields.

Like $\mathcal{N} = 4$ ABJM Theory has a well understood holographic dual in Type IIA String Theory on $AdS_4 \times \mathbb{CP}^3$. As well as being a window into M2-Brane physics, in this context at finite temperature with a chemical potential it has provided a popular

toy model for condensed matter systems at strong coupling, particularly superconductors [66]. Our interest lies in taking our exploration of on-shell methods into what prima-facie is a very different theory to $\mathcal{N} = 4$ sYM. Surprisingly, the amplitudes of both theories share many important qualities; most pertinently, ABJM has been found to be integrable [67] [68] and its amplitudes possess dual superconformal symmetry [69]. Although issues with fermionic T-duality preclude the existence of Wilson Loop duality beyond four points [70] [71] the amplitudes display uniform transcendentality.

3.3.1 The Spinor Helicity Formalism in Three Dimensions

We are considering a theory in $(2 + 1)$ dimensions, where the spinors are in $SL(2, \mathbb{R})$ and the little group is \mathbb{Z}_2 . A null momentum is then given by

$$p^{\alpha\beta} = \lambda^\alpha \lambda^\beta \tag{3.3.3}$$

and therefore all Lorentz invariants are built from one kind of bracket

$$\langle ij \rangle = \epsilon_{\alpha\beta} \lambda_i^\alpha \lambda_j^\beta, \quad s_{ij} = \langle ij \rangle^2. \tag{3.3.4}$$

We note that the reality of these spinors requires the vanishing of three-point amplitudes, so recursion must proceed from four points. A crucial feature of the BCFW recursion relations was that the momentum shift q must keep all legs on-shell, ie. it must satisfy

$$q \cdot p_i = q \cdot p_j = q^2 = 0. \tag{3.3.5}$$

In three dimensions, uniquely, this condition cannot be satisfied unless $q = 0$. Indeed, it cannot be satisfied for any *linear* transformation. We must rather use [69]

$$\begin{pmatrix} \lambda_i \\ \lambda_j \end{pmatrix} = R(z) \begin{pmatrix} \lambda_i \\ \lambda_j \end{pmatrix}, \quad R(z) = \frac{1}{2} \begin{pmatrix} z + z^{-1} & i(z - z^{-1}) \\ -i(z - z^{-1}) & z + z^{-1} \end{pmatrix}. \tag{3.3.6}$$

With this shift on arbitrary legs i, j , we can extract the physical amplitude as a sum of residues via a contour integral,

$$A(z=1) = -\frac{1}{2\pi i} \sum_{\chi, k} \oint_{z=z_{k, \chi}} \frac{dz}{z-1} \frac{\hat{A}_L(z) \hat{A}_R(z)}{\hat{P}_\chi^2(z)} \quad (3.3.7)$$

where χ labels the factorization channels and $z_{k, \chi}$ are the two poles of the propagator $\hat{P}_\chi^2(z)$. The quadratic equation for the poles can be solved, and after further algebra, leads to

$$A(z=1) = \sum_{\chi} \frac{1}{P_\chi^2} (H(z_{1, \chi}, z_{2, \chi}) A_L(z_{1, \chi}) A_R(z_{1, \chi}) + (z_{1, \chi} \leftrightarrow z_{2, \chi})) \quad (3.3.8)$$

where

$$H(z, w) = \begin{cases} \frac{z^2(w^2-1)}{z^2-w^2}, & (i-j) \text{ even} \\ \frac{z(w^2-1)}{z^2-w^2}, & (i-j) \text{ odd.} \end{cases} \quad (3.3.9)$$

At loop level, the basis of integrals can be reduced to triangles and bubbles.

Of particular interest, the one-loop triangles with massless corners vanish; while the fully massive triangle is a rational function of the masses

$$\begin{aligned} I_3 &= \int \frac{d^3 \ell}{2\pi^3} \frac{1}{\ell^2 (\ell - p_1)^2 (\ell + p_3)^2} \\ &= -\frac{i\pi}{2} \frac{1}{\sqrt{-p_1^2 - i\epsilon} \sqrt{-p_2^2 - i\epsilon} \sqrt{-p_3^2 - i\epsilon}}. \end{aligned} \quad (3.3.10)$$

So new analytic structures enter only at two loops and higher. If we require dual conformal symmetry we observe that the integral

$$I_3 = \int \frac{d^d x_\ell}{x_{1\ell}^2 x_{2\ell}^2 x_{3\ell}^2} \quad (3.3.11)$$

is not invariant under inversions, which must be compensated for by the factor

$$\sqrt{-x_{12}^2} \sqrt{-x_{23}^2} \sqrt{-x_{31}^2} = \sqrt{-p_1^2 - i\epsilon} \sqrt{-p_2^2 - i\epsilon} \sqrt{-p_3^2 - i\epsilon} \quad (3.3.12)$$

and we see that the three-mass triangle is constant [72]. This is consistent with the fact that one cannot construct a conformal cross-ratio from three momenta.

3.3.2 Superamplitudes

Since the Chern-Simons gauge field is non-dynamical, scattering amplitudes can contain only the scalars and fermions. We can capture the states of ABJM Theory as functions on $\mathcal{N} = 3$ superspace using two superfields [73]:

$$\Phi(\lambda, \eta) = \phi^4(\lambda) + \eta^A \psi_A(\lambda) + \frac{1}{2} \epsilon_{ABC} \eta^A \eta^B \phi^C(\lambda) + \frac{1}{3!} \epsilon_{ABC} \eta^A \eta^B \eta^C \psi_4(\lambda) \quad (3.3.13)$$

$$\bar{\Phi}(\lambda, \eta) = \bar{\psi}^4(\lambda) + \eta^A \bar{\phi}_A(\lambda) + \frac{1}{2} \epsilon_{ABC} \eta^A \eta^B \bar{\psi}^C(\lambda) + \frac{1}{3!} \epsilon_{ABC} \eta^A \eta^B \eta^C \bar{\phi}_4(\lambda). \quad (3.3.14)$$

Note that only $SU(3)$ R-symmetry is manifest. The Supersymmetry generators have the form

$$Q^{\alpha A} = \lambda^\alpha \eta^A \quad Q_A^\alpha = \lambda^\alpha \frac{\partial}{\partial \eta^A}, \quad (3.3.15)$$

and the R-symmetry generators have the form

$$R^{AB} = \eta^A \eta^B \quad R_B^A = \eta^A \frac{\partial}{\partial \eta^B} - \frac{1}{2} \delta_B^A \quad R_{AB} = \frac{\partial}{\partial \eta^A} \frac{\partial}{\partial \eta^B}. \quad (3.3.16)$$

From the second of these, we see that the fermionic degree of an n -point scattering amplitude is $3n/2$. This is in stark contrast to the case of $\mathcal{N} = 4$ sYM where the fermionic degree depends on the MHV level. The only amplitude that resembles its four-dimensional counterpart is that for $n = 4$

$$\mathcal{A} = \frac{\delta^{(3)}(\sum_{i=1}^4 \lambda_i \lambda_i) \delta^{(6)}(\sum_{i=1}^4 \lambda_i \eta_i)}{\langle 12 \rangle \langle 23 \rangle}. \quad (3.3.17)$$

which is fixed by little group scaling.

Note also that for a colour-ordered amplitude

$$\mathcal{A}(\Phi_1, \bar{\Phi}_2, \dots, \bar{\Phi}_{n-1}, \Phi_n) \quad (3.3.18)$$

gauge invariance with respect to the product gauge group requires that n is even and that Φ and $\bar{\Phi}$ alternate.

3.3.3 The Four-Point Amplitude at One and Two Loops

The four-point amplitude at two loops was first computed by [74]. As a superconformal theory, we expect the one-loop amplitudes can be expanded in terms of one-loop triangle functions. Since one and two-mass triangles vanish in three dimensions, we expect the one-loop amplitude to also vanish below six points. However, the one loop *integrand* will be important for form factor calculations, so we will describe it here.

To obtain a non-zero integrand we must consider two-particle cuts, so we will be computing numerated boxes. It will also behove us to work with a basis of dual conformal integrals. This achieved by selecting

$$\begin{aligned} I_4^{(1)} &= \int \frac{d^3 x_\ell}{(2\pi)^3} \frac{2x_{5\ell}^2 \epsilon_{\mu\nu\rho} x_{21}^\mu x_{31}^\nu x_{41}^\rho + 2x_{31}^2 \epsilon_{\mu\nu\rho} x_{\ell 1}^\mu x_{21}^\nu x_{41}^\rho}{x_{1\ell}^2 x_{2\ell}^2 x_{3\ell}^2 x_{4\ell}^2} \\ &= \int \frac{d^3 \ell}{(2\pi)^3} \frac{2\ell^2 \epsilon_{\mu\nu\rho} p_1^\mu p_2^\nu p_4^\rho + 2s \epsilon_{\mu\nu\rho} \ell^\mu p_1^\nu p_4^\rho}{\ell^2 (\ell - p_1)^2 (\ell - p_1 - p_2)^2 (\ell + p_4)^2} \end{aligned} \quad (3.3.19)$$

which is best seen by regarding three dimensional conformal symmetry as five-dimensional Lorentz symmetry.

The cut in the s -channel gives us

$$c_s = \delta^{(3)}(P) \int d^3 \eta_\ell d^3 \eta_k \frac{\delta^{(6)}(Q_L) \delta^{(6)}(Q_R)}{\langle 21 \rangle \langle 1\ell \rangle \langle \ell k \rangle \langle \ell 4 \rangle}. \quad (3.3.20)$$

Combining the delta functions and performing the η integrations leads to

$$\int d^3 \eta_\ell d^3 \eta_k \delta^{(6)}(Q_L) \delta^{(6)}(Q_R) = \delta^{(6)}(Q) \langle \ell k \rangle^3 \quad (3.3.21)$$

so we may write

$$c_s = \delta^{(6)}(P) \delta^{(6)}(Q) \frac{\langle \ell k \rangle^3}{\langle 21 \rangle \langle 1\ell \rangle \langle \ell k \rangle \langle \ell 4 \rangle} = \mathcal{A}^{(0)} \frac{\langle 12 \rangle^2 \langle \ell 1 \rangle \langle 41 \rangle \langle 4\ell \rangle}{(\ell + p_4)^2 (\ell - p_1)^2} \quad (3.3.22)$$

which corresponds to the s -cut of the box integral 3.3.19. A similar calculation conforms that

$$\mathcal{A}_4^{(1)} = \mathcal{A}_4^{(0)} I_4^{(1)} \quad (3.3.23)$$

which vanishes since after PV reduction $I_4^{(1)}$ reduces to a sum of one-mass triangles.

At two loops, we begin by constructing a basis of linearly independent dual conformally invariant integrals:

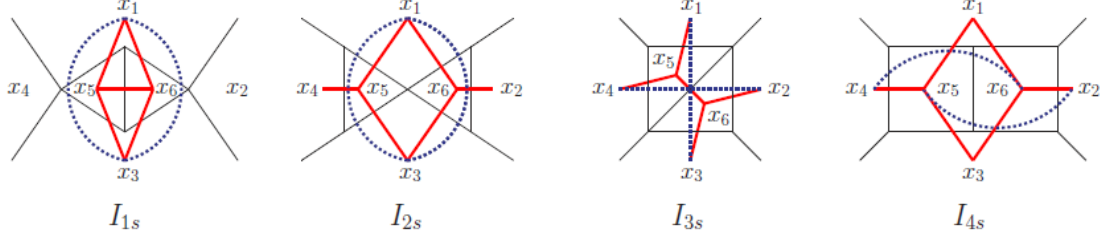


Figure 3.5: *The basis of dual conformal integrals; the dotted blue lines represent numerators. Taken from [74]*

$$I_{1s} = \int \frac{d^3x_5 d^3x_6}{(2\pi)^6} \frac{x_{13}^4}{x_{51}^2 x_{53}^2 x_{56}^2 x_{61}^2 x_{63}^2}, \quad (3.3.24)$$

$$I_{2s} = \int \frac{d^3x_5 d^3x_6}{(2\pi)^6} \frac{x_{13}^4 x_{42}^2}{x_{51}^2 x_{53}^2 x_{54}^2 x_{61}^2 x_{62}^2 x_{63}^2} \quad (3.3.25)$$

$$I_{3s} = \int \frac{d^3x_5 d^3x_6}{(2\pi)^6} \frac{x_{13}^2 x_{42}^2}{x_{51}^2 x_{54}^2 x_{56}^2 x_{62}^2 x_{63}^2} \quad (3.3.26)$$

$$I_{4s} = \int \frac{d^3x_5 d^3x_6}{(2\pi)^6} \frac{x_{13}^4 x_{52}^2 x_{64}^2}{x_{51}^2 x_{53}^2 x_{54}^2 x_{56}^2 x_{61}^2 x_{62}^2 x_{63}^2} \quad (3.3.27)$$

and the corresponding cyclic rotations with $s \leftrightarrow t$. It will also be helpful to include the combination

$$I_{0s} = \frac{1}{2}(I_{1s} - I_{2s} + I_{3s} + I_{3t} + I_{4s}) \quad (3.3.28)$$

which plays the analogous role to $I_4^{(1)}$ as a natural $5d$ invariant. We may now write an ansatz for the amplitude of the form

$$\mathcal{A}_4^{(2)} = A_4^{(0)} \sum_{i=0}^3 [c_{is} I_{is} + (s \rightarrow t)] \quad (3.3.29)$$

which we stress can only be written at this stage due to the presence of a dual conformal basis. There are now two distinct classes of cut unrelated by cyclic permutations:

In the double s-channel cut one finds by sewing tree amplitudes:

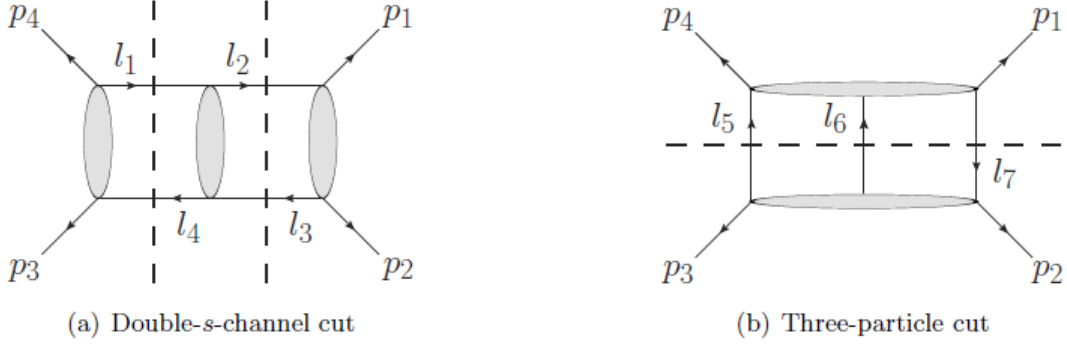


Figure 3.6: *The double s-channel cut (a) is obtained by sewing three four-point tree amplitudes. The triple cut (b) must vanish as it contains tree amplitudes with an odd number of legs. Taken from [74]*

$$C_s = \mathcal{A}_4^{(0)} \rho_1 s^2 \langle 14 \rangle \langle 4\ell_1 \rangle \langle \ell_1 \ell_2 \rangle \langle \ell_2 1 \rangle \quad (3.3.30)$$

with

$$\rho_1^{-1} = \langle 4\ell_1 \rangle^2 \langle \ell_1 \ell_2 \rangle^2 \langle \ell_2 1 \rangle^2. \quad (3.3.31)$$

Only the integrals I_{0s}, I_{1s}, I_{2s} contribute in this channel. Their cut integrands are:

$$I_{0s}|_{s-s\text{-cut}} = s^2 \rho_1 (\langle \ell_1 4 \rangle \langle \ell_2 1 \rangle - \langle 14 \rangle \langle 4\ell_1 \rangle \langle \ell_1 \ell_2 \rangle \langle \ell_2 1 \rangle), \quad (3.3.32)$$

$$I_{1s}|_{s-s\text{-cut}} = s^2 \rho_1 \langle \ell_1 4 \rangle^2 \langle \ell_2 1 \rangle^2, \quad (3.3.33)$$

$$I_{2s}|_{s-s\text{-cut}} = s^2 \rho_1 \langle 14 \rangle^2 \langle \ell_1 \ell_2 \rangle^2 \quad (3.3.34)$$

where we have employed the Schouten identities to express each expression in terms of linearly independent spinor products. We must now solve

$$(c_{0s} I_{0s} + c_{1s} I_{1s} + c_{2s} I_{2s})|_{s-s\text{-cut}} = \rho_1 s^2 \langle 14 \rangle \langle 4\ell_1 \rangle \langle \ell_1 \ell_2 \rangle \langle \ell_2 1 \rangle \quad (3.3.35)$$

which leads to

$$c_{0s} = -1, \quad c_{1s} = 1, \quad c_{2s} = 0. \quad (3.3.36)$$

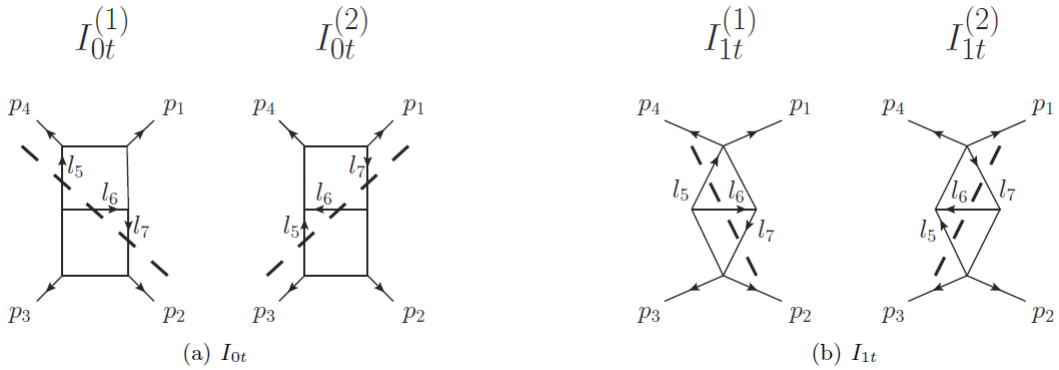


Figure 3.7: *The two possible triples cuts of the integrals appearing in*

The triple cut (b) necessarily vanishes, since it sews tree amplitudes with an odd number of legs. It receives contributions from the integrals $I_{0s}, I_{3s}, I_{0t}, I_{1t}, I_{3t}$; it should be noted that some of the integrals 3.7 have two possible cuts, which must be summed over. We will not dwell on the details here, but the cut conditions lead to a system of equations solved by:

$$c_{0s} = c_{0t} = -c_{1s} = -c_{1t} = -1, \quad c_{2s} = c_{2t} = c_{3s} = c_{3t} = 0. \quad (3.3.37)$$

Combining the result of the two cuts we find:

$$\mathcal{A}_4^{(2)} = \left(\frac{N}{k}\right) \mathcal{A}_4^{(0)} [-I_{0s} + I_{1s} + (s \rightarrow t)]. \quad (3.3.38)$$

The integrals can be evaluated using Feynman parameters and Mellin-Barnes representations. The final result is:

$$\mathcal{A}_4^{(2)} = -\frac{1}{16\pi^2} \mathcal{A}_4^{(0)} \left[\frac{(-s/\mu^2)}{\epsilon^2} + \frac{(-t/\mu^2)}{\epsilon^2} - \frac{1}{2} \log^2 \left(\frac{s}{t}\right) - 4\zeta_2 - 3\log^2 2 \right]. \quad (3.3.39)$$

3.3.4 Colour Ordering

Colour ordering in ABJM differs somewhat from the cases we have discussed thus far on account of the product gauge group. Complete tree amplitudes, which we call $\tilde{\mathcal{A}}$,

are given by [67, 75]

$$\tilde{\mathcal{A}}(\bar{1}, 2, \dots, n) = \sum_{\mathcal{P}_n} \text{sgn}(\sigma) \mathcal{A}^{(0)}(\sigma(\bar{1}), \sigma(2), \sigma(\bar{3}), \dots, \sigma(n)) [\sigma(\bar{1}), \sigma(2), \sigma(\bar{3}), \dots, \sigma(n)], \quad (3.3.40)$$

where $\mathcal{P}_n := (S_{n/2} \times S_{n/2})/C_{n/2}$ are permutations of n sites that only mix even (bosonic) and odd (fermionic) particles among themselves, modulo cyclic permutations by two sites, and the function $\text{sgn}(\sigma)$ is equal to -1 if σ involves an odd permutation of the odd (fermionic) sites, and $+1$ otherwise. $\mathcal{A}^{(0)}(\bar{1}, 2, \bar{3}, \dots, n)$ are colour-ordered tree amplitudes, and we have also defined

$$[\bar{1}, 2, \bar{3}, \dots, n] := \delta_{i_2}^{\bar{i}_1} \delta_{i_3}^{i_2} \delta_{i_4}^{\bar{i}_3} \cdots \delta_{i_1}^{i_n}, \quad (3.3.41)$$

and in the following we will just write $[1, 2, \dots, n]$ without specifying if a particle is barred (i.e. fermionic) or non-barred (bosonic), with the understanding that the first entry in the bracket always represents a fermionic field.

As an example, we consider the complete four-point amplitude at tree level. It includes the two colour structures $[1, 2, 3, 4]$ and $[1, 4, 3, 2]$ (see Figure 3.8) and is given by the following expression:

$$\tilde{\mathcal{A}}^{(0)}(\bar{1}, 2, \bar{3}, 4) = \mathcal{A}^{(0)}(\bar{1}, 2, \bar{3}, 4) \left([1, 2, 3, 4] - [1, 4, 3, 2] \right). \quad (3.3.42)$$

We have also used that

$$\mathcal{A}^{(0)}(\bar{1}, 2, \bar{3}, 4) = \mathcal{A}^{(0)}(\bar{3}, 2, \bar{1}, 4), \quad (3.3.43)$$

a fact that follows from (3.3.17).

3.3.5 Half-BPS operators

The quivers of ABJM theory and the conifold theory encode the same data. Hence, one would expect the BPS operators to be of the form $\mathcal{O}_{2n} = \text{Tr}(\phi^{I_1} \bar{\phi}_{J_1} \dots \phi^{I_n} \bar{\phi}_{J_n})$.

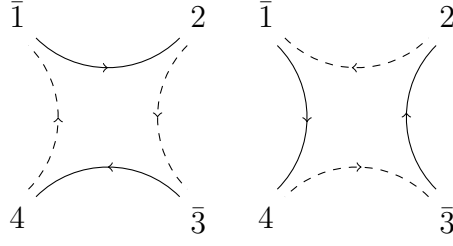


Figure 3.8: *The two possible colour orderings $[1, 2, 3, 4]$ and $[1, 4, 3, 2]$ appearing in the four-point tree-level amplitude (3.3.42).*

For the shortest case, consider the variation of operators of the form $\text{Tr}(\phi^I \bar{\phi}_J)$ with $I \neq J$. Setting for example $I = 1$ and $J = 4$, this expands to

$$\delta \text{Tr}(\phi^1 \bar{\phi}_4) = \text{Tr}(\delta \phi^1 \bar{\phi}_4 + \phi^1 \delta \bar{\phi}_4). \quad (3.3.44)$$

Following [76], we use the transformations:

$$\delta \phi^I = i \omega^{IJ} \psi_J, \quad (3.3.45)$$

$$\delta \bar{\phi}_I = i \bar{\psi}^J \omega_{IJ}. \quad (3.3.46)$$

The ω_{IJ} 's are given in terms of the $(2+1)$ -dimensional Majorana spinors, ϵ_i ($i = 1, \dots, 6$) which are the supersymmetry generators:

$$\omega_{IJ} = \epsilon_i (\Gamma^i)_{IJ}, \quad (3.3.47)$$

$$\omega^{IJ} = \epsilon_i ((\Gamma^i)^*)^{IJ}, \quad (3.3.48)$$

that are antisymmetric in I, J . The 4×4 matrices Γ^i are given by:

$$\Gamma^1 = \sigma_2 \otimes 1_2, \quad \Gamma^4 = -\sigma_1 \otimes \sigma_2, \quad (3.3.49)$$

$$\Gamma^2 = -i\sigma_2 \otimes \sigma_3, \quad \Gamma^5 = \sigma_3 \otimes \sigma_2, \quad (3.3.50)$$

$$\Gamma^3 = i\sigma_2 \otimes \sigma_1, \quad \Gamma^6 = -i1_2 \otimes \sigma_2, \quad (3.3.51)$$

and satisfy the following relations,

$$\{\Gamma^i, \Gamma^{j\dagger}\} = 2\delta_{ij}, \quad (\Gamma^i)_{IJ} = -(\Gamma^i)_{JI}, \quad (3.3.52)$$

$$\frac{1}{2} \epsilon^{IJKL} \Gamma_{KL}^i = -(\Gamma^{j\dagger})^{IJ} = ((\Gamma^i)^*)^{IJ}, \quad (3.3.53)$$

leading to

$$(\omega^{IJ})_\alpha = ((\omega_{IJ})^*)_\alpha, \quad \omega^{IJ} = \frac{1}{2}\epsilon^{IJKL}\omega_{KL}. \quad (3.3.54)$$

Explicitly, ω_{IJ} is given by the following matrix:

$$\omega_{IJ} = \begin{pmatrix} 0 & -i\epsilon_5 - \epsilon_6 & -i\epsilon_1 - \epsilon_2 & \epsilon_3 + i\epsilon_4 \\ i\epsilon_5 + \epsilon_6 & 0 & \epsilon_3 - i\epsilon_4 & -i\epsilon_1 + \epsilon_2 \\ i\epsilon_1 + \epsilon_2 & -\epsilon_3 + i\epsilon_4 & 0 & i\epsilon_5 - \epsilon_6 \\ -\epsilon_3 - i\epsilon_4 & i\epsilon_1 - \epsilon_2 & -i\epsilon_5 + \epsilon_6 & 0 \end{pmatrix}. \quad (3.3.55)$$

The term $\phi^1\delta\bar{\phi}_4$ yields

$$\phi^1\delta\bar{\phi}_4 = \phi^1 \left[-\bar{\psi}^1(\epsilon_3 + i\epsilon_4) + i\bar{\psi}^2(\epsilon_1 + i\epsilon_2) - i\bar{\psi}^3(\epsilon_5 + i\epsilon_6) + 0 \right]. \quad (3.3.56)$$

Therefore, requiring $\phi^1\delta\bar{\phi}_4 = 0$ the conditions are:

$$\begin{aligned} \epsilon_1 + i\epsilon_2 &= 0, \\ \epsilon_3 + i\epsilon_4 &= 0, \\ \epsilon_5 + i\epsilon_6 &= 0, \end{aligned} \quad (3.3.57)$$

which relate half of the generators with the other half by constraining the components $\omega_{4J} = 0$.

Note that because of the relations (3.3.54) which set components of the form ω_{4L} to zero, the entries ω^{IJ} with $I, J \in (1, 2, 3)$ automatically vanish implying that $\delta\phi^I = 0 \iff I \in (1, 2, 3)$. This procedure may be iterated to show that generally the operators $\text{Tr}(\bar{\phi}_I\phi^J)$ for $I \neq J$ are indeed half-BPS. In the present work the operators under consideration are of the type

$$\mathcal{O} = \text{Tr}(\phi^A\bar{\phi}_4), \quad (3.3.58)$$

where $A \neq 4$.

Chapter 4

Super Form Factors in $\mathcal{N} = 4$ Super Yang-Mills

In this chapter we present the results of [16]. We expand the analysis of form factors of half-BPS operators in $\mathcal{N} = 4$ super Yang-Mills. In particular, we extend various on-shell techniques known for amplitudes to the case of form factors, including MHV rules, recursion relations, unitarity and dual MHV rules. As an application, we present the solution of the recursion relation for split-helicity form factors. We then consider form factors of the stress-tensor multiplet operator and of its chiral truncation, and write down supersymmetric Ward identities using chiral as well as non-chiral superspace formalisms. This allows us to obtain compact formulae for families of form factors, such as the maximally non-MHV case. Finally we generalise dual MHV rules in dual momentum space to form factors.

4.1 Tree-level methods

In this section we will develop and extend tree-level methods for form factors by generalising the corresponding methods for amplitudes, namely MHV diagrams [4] and on-shell recursions relations [5, 21].

We then proceed to obtain several new results including the NMHV and all split-helicity cases. We will not present the calculations with both methods for all examples but wish to stress here that we have made extensive checks to confirm that the results obtained with either method always agree. The supersymmetrisation of these methods will be considered in Section 4.

4.1.1 MHV diagrams

We start with a simple extension of the MHV diagram method [4] to form factors. We will test this here only in tree-level calculations, but the extension to loop level, following [77], is straightforward.

Specifically, we will be interested in calculating NMHV form factors of the simplest class of operators in $\mathcal{N} = 4$ SYM, namely the half-BPS operators $\text{Tr}(\phi_{12}\phi_{12})$. They take the form

$$\langle g^+(p_1) \cdots \phi_{12}(p_i) \cdots \phi_{12}(p_j) \cdots g^+(p_{n-1}) g^-(p_n) | \text{Tr}(\phi_{12}\phi_{12})(x) | 0 \rangle, \quad (4.1.1)$$

where all but one of the gluons have positive helicity. The strategy of the calculation is very simple – we need to augment the set of usual MHV vertices for amplitudes by including a new family of MHV vertices, obtained by continuing off shell the tree-level MHV form factors of the half-BPS operators. The expressions for these quantities

were derived in [60], and are given by

$$\begin{aligned} & \int d^4x e^{-iqx} \langle g^+(p_1) \cdots \phi_{12}(p_i) \cdots \phi_{12}(p_j) \cdots g^+(p_n) | \text{Tr}(\phi_{12}\phi_{12})(x) | 0 \rangle \\ &= g^{n-2} (2\pi)^4 \delta^{(4)} \left(\sum_{k=1}^n \lambda_k \tilde{\lambda}_k - q \right) F_{\text{MHV}} , \end{aligned} \quad (4.1.2)$$

where

$$F_{\text{MHV}} = \frac{\langle ij \rangle^2}{\langle 12 \rangle \cdots \langle n1 \rangle} . \quad (4.1.3)$$

Here $p_m := \lambda_m \tilde{\lambda}_m$ are on-shell momenta of the external particles, and $q := \sum_{m=1}^n p_m$ is the momentum carried by the operator insertion. It was observed in [60] that, since (4.1.3) is a holomorphic function of the spinor variables, the MHV form factors are localised on a complex line in twistor space, similarly to the MHV amplitudes [3].

Using localisation as an inspiration, we propose to use an appropriate off-shell continuation of 4.1.3 as a new vertex to construct the perturbative expansion of non-MHV form factors of the operator $\text{Tr}(\phi_{12}\phi_{12})$. The off-shell continuation is the standard one introduced in [4]. The momentum L of an internal, off-shell particle is decomposed as $L = l + z\xi$, where $l = \lambda_L \tilde{\lambda}_L$ is an on-shell momentum and ξ an arbitrary reference null momentum. The off-shell continuation of [4] consists then in using the spinor λ_L as the spinor variable associated with the internal leg of momentum L , where

$$\lambda_{L,\alpha} = \frac{L_{\alpha\dot{\alpha}} \tilde{\xi}^{\dot{\alpha}}}{[\tilde{\lambda}_L, \tilde{\xi}]} . \quad (4.1.4)$$

The denominator in the right-hand side of (4.1.4) will be irrelevant for our applications since each MHV diagram is invariant under rescalings of the internal spinor variables. Hence, we will discard it and simply replace $\lambda_{L,\alpha} \rightarrow L_{\alpha\dot{\alpha}} \tilde{\xi}^{\dot{\alpha}}$.

NMHV form factors

Using the MHV rules outlined in the previous section, we now present an example of derivation of an NMHV form factor. Specifically, the form factor we consider is

$$F_{\text{NMHV}}(1_{\phi_{12}}, 2_{\phi_{12}}, 3_{g^-}, 4_{g^+}) := \langle \phi_{12}(p_1)\phi_{12}(p_2)g^-(p_3)g^+(p_4) | \text{Tr}(\phi_{12}\phi_{12})(0) | 0 \rangle. \quad (4.1.5)$$

There are four MHV diagrams contributing to (4.1.5), depicted in Figure 4.1. A

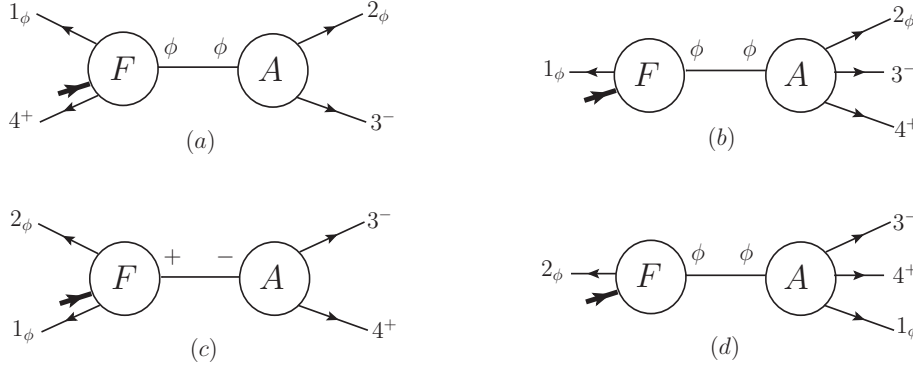


Figure 4.1: *The four MHV diagrams contributing to the NMHV form factor (4.1.5).*

short calculation shows that these are given by the following expressions:

$$\begin{aligned} \text{Diagram (a)} &= \frac{[2\xi]}{[\xi 3]} \frac{1}{[32]\langle 41 \rangle} \frac{\langle 1|q - p_4|\xi \rangle}{|\langle 4|q - p_1|\xi \rangle|}, \\ \text{Diagram (b)} &= \frac{\langle 23 \rangle}{\langle 34 \rangle s_{234}} \frac{\langle 3|p_2 + p_4|\xi \rangle^2}{\langle 2|p_3 + p_4|\xi \rangle \langle 4|p_2 + p_3|\xi \rangle}, \\ \text{Diagram (c)} &= \frac{\langle 12 \rangle [\xi 4]^3}{[43] [3\xi]} \frac{1}{\langle 2|p_3 + p_4|\xi \rangle \langle 1|p_3 + p_4|\xi \rangle}, \\ \text{Diagram (d)} &= \frac{1}{s_{341}} \frac{\langle 13 \rangle^2}{\langle 34 \rangle \langle 41 \rangle} \frac{\langle 3|p_4 + p_1|\xi \rangle}{\langle 1|p_3 + p_4|\xi \rangle}. \end{aligned} \quad (4.1.6)$$

We have checked that the sum of all MHV diagrams is independent of the choice of the reference spinor $\tilde{\xi}$. A particularly convenient choice of $\tilde{\xi}$ is $\tilde{\xi} = \tilde{\lambda}_4$, in which case we get

$$\begin{aligned} F_{\text{NMHV}}(1_{\phi_{12}}, 2_{\phi_{12}}, 3_{g^-}, 4_{g^+}) &= \frac{[24]}{[34]} \frac{1}{\langle 4|p_2 + p_3|4 \rangle} \left[\frac{\langle 1|q|4 \rangle}{[23]\langle 41 \rangle} + \frac{[24]\langle 23 \rangle^2}{\langle 34 \rangle} \frac{1}{s_{234}} \right] \\ &+ \frac{\langle 13 \rangle^2 [14]}{\langle 41 \rangle \langle 34 \rangle [43]} \frac{1}{s_{341}}. \end{aligned} \quad (4.1.7)$$

It is straightforward to apply this procedure to more general form factors but for brevity we will not present them here. However, we mention that all results derived in the next subsection using recursion relations have been compared with formulae obtained from MHV diagrams finding a perfect match in all cases.

4.1.2 Recursion relations

In this subsection we study the application of recursion relations to the derivation of tree-level form factors. As a warm-up we will re-derive the NMHV form factor in (4.1.5) finding agreement with (4.1.7), and then move on to consider more general cases including split-helicity configurations. Since form factors contain a single operator insertion, it is clear that every recursive diagram will contain one amplitude and one form factor as the factorisation properties used in the case of tree-level recursions for amplitudes also apply to tree-level form factors. This is the only modification to the on-shell recursion relations of [21]. In Appendix A we discuss the behaviour of form factors under large complex deformations, and confirm the validity of the calculations below, i.e. we show that under the shifts used the form factors vanish as $z \rightarrow \infty$.

Let us begin by re-deriving the NMHV form factor (4.1.5). We will use a $[34\rangle$ shift, namely

$$\hat{\lambda}_3 := \tilde{\lambda}_3 + z\tilde{\lambda}_4, \quad \hat{\lambda}_4 := \lambda_4 - z\lambda_3. \quad (4.1.8)$$

There are two recursive diagrams, depicted in Figure 4.2 below. A short calculation shows that

$$\begin{aligned} \text{Diagram (a)} &= \frac{[24]^2}{[23][34]} \frac{1}{s_{234}} \frac{\langle 1|q|4\rangle}{\langle 1|q|2\rangle}, \\ \text{Diagram (b)} &= \frac{\langle 13\rangle^2}{\langle 34\rangle\langle 41\rangle} \frac{1}{s_{341}} \frac{\langle 3|q|2\rangle}{\langle 1|q|2\rangle}, \end{aligned} \quad (4.1.9)$$

so that

$$F_{\text{NMHV}}(1_{\phi_{12}}, 2_{\phi_{12}}, 3_{g^-}, 4_{g^+}) = \frac{1}{\langle 1|q|2\rangle} \left[\frac{[24]^2}{[23][34]} \frac{1}{s_{234}} \langle 1|q|4\rangle + \frac{\langle 13\rangle^2}{\langle 34\rangle\langle 41\rangle} \frac{1}{s_{341}} \langle 3|q|2\rangle \right]. \quad (4.1.10)$$

It is interesting to note that the $1/\langle 1|q|2\rangle$ pole is in fact spurious. This can be shown by using the identities

$$\begin{aligned} \langle 1|q p_4|3\rangle + \langle 1|q p_2|3\rangle &= \langle 13\rangle s_{234}, \\ [4|p_3 q|2] + [4|p_1 q|2] &= [42] s_{341}, \end{aligned} \quad (4.1.11)$$

which allow to recast the form factor in the alternative form

$$F_{\text{NMHV}}(1_{\phi_{12}}, 2_{\phi_{12}}, 3_{g^-}, 4_{g^+}) = \frac{1}{s_{34} [23] \langle 41\rangle} \left[\frac{\langle 14\rangle \langle 23\rangle [24]^2}{s_{234}} + \frac{[41][32] \langle 13\rangle^2}{s_{341}} + [24] \langle 13\rangle \right]. \quad (4.1.12)$$

We have checked that our result (4.1.7) for the form factor derived using MHV diagrams, and (4.1.12), obtained using recursion relations, are in agreement.

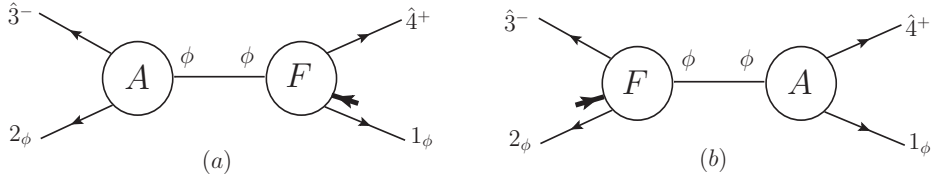


Figure 4.2: *The two recursive diagrams contributing to the NMHV form factor (4.1.5).*

Recursion relations for the split-helicity form factor

In the previous section we found that the BCF recursion relation for the NMHV form factor with a $[3, 4]$ shift has just two diagrams. This property in fact holds for all form factors of the form $F_{\phi^2; q-2, n-q}(1_\phi, 2_\phi, 3^-, \dots, q^-, (q+1)^+, \dots, n^+)$, which we call henceforth *split-helicity*. As we will show shortly, performing a $[q, q+1]$ shift leads to a general, closed-form solution of the BCFW recursion relations for this special

class of form factors. Note that all split-helicity gluon scattering amplitudes were computed in [78] – we construct here a similar solution for form factors.

Each recursive diagram with a $[q, q+1]$ shift contains a three-point amplitude and an $(n-1)$ -point form factor. We can neatly combine the three-point amplitude and the propagator in a prefactor to write¹

$$\begin{aligned}
F_{q-2, n-q} &= \frac{[q-1q+1]}{[q-1q][qq+1]} F_{q-3, n-q}(1_\phi, 2_\phi, 3^-, \dots, \widehat{q-1}^-, \widehat{q+1}^+, \dots, n^+) \\
&+ \frac{\langle qq+2 \rangle}{\langle qq+1 \rangle \langle q+1q+2 \rangle} F_{q-2, n-q-1}(1_\phi, 2_\phi, 3^-, \dots, \widehat{q}^-, \widehat{q+2}^+, \dots, n^+),
\end{aligned} \tag{4.1.13}$$

where the shifted spinors of the external momenta that appear in the lower-point form factors are

$$\lambda_{\widehat{q+1}} = \frac{[q-1|P_{q,q+1}}{[q-1q+1]}, \tag{4.1.14a}$$

$$\tilde{\lambda}_{\widehat{q}} = \frac{P_{q,q+2}|q+2 \rangle}{\langle qq+2 \rangle}, \tag{4.1.14b}$$

with $P_{a,b} = p_a + \dots + p_b$. Furthermore, the shifted spinors associated with internal legs are relabelled as

$$\lambda_{\widehat{p}_{q-1q}}(z = z_{q-1q}) \rightarrow \lambda_{\widehat{q-1}} = \frac{P_{q,q+1}|q+1 \rangle}{[q-1q+1]}, \tag{4.1.15a}$$

$$\tilde{\lambda}_{\widehat{p}_{q+1q+2}}(z = z_{q+1q+2}) \rightarrow \tilde{\lambda}_{\widehat{q+2}} = \frac{\langle q|P_{q,q+2}}{\langle qq+2 \rangle}, \tag{4.1.15b}$$

so that the notation remains compatible with subsequent recursions. Crucially, all lower-point form factors appearing in (4.1.16) are of split-helicity form, so that the split helicity form factors are closed under recursions. Once we have reduced the form factor to expressions that involve only MHV and $\overline{\text{MHV}}$ terms, we can insert the shifted momenta.

¹For the rest of this section we will always assume that the operator $\mathcal{O} = \text{Tr}(\phi_{12}\phi_{12})$ is inserted and will not mention it explicitly. Although the solution is presented for this particular insertion, the construction can be generalised to form factors involving other operators.

It is useful to illustrate the structure of the recursion relations for split-helicity form factors using a square lattice as in Figure 4.3. Consider for example the form factor $F_{2,2}$. In this case, the first iteration using equation (4.1.16) relates $F_{2,2}$ to the form factors $F_{2,1}$ and $F_{1,2}$, which however are neither MHV nor $\overline{\text{MHV}}$. The next iteration leads to an expression involving one $F_{2,0}$, two $F_{1,1}$'s and one $F_{0,2}$ evaluated at some shifted momenta. A final iteration would then allow us to express the answer in terms of MHV and $\overline{\text{MHV}}$ form factors alone, or even to reduce everything down to $F_{0,0}$. It is also easy to see that this pattern generalises to arbitrary split-helicity form factors and that each term generated by subsequent recursions corresponds to a unique path between the form factor and the MHV or $\overline{\text{MHV}}$ edges of the lattice, as illustrated in Figure 4.3.

Recursion relations for the split-helicity form factor

In the previous section we found that the BCF recursion relation for the NMHV form factor with a $[3, 4\rangle$ shift has just two diagrams. This property in fact holds for all form factors of the form $F_{\phi^2; q-2, n-q}(1_\phi, 2_\phi, 3^-, \dots, q^-, (q+1)^+, \dots, n^+)$, which we call henceforth *split-helicity*. As we will show shortly, performing a $[q, q+1\rangle$ shift leads to a general, closed-form solution of the BCFW recursion relations for this special class of form factors. Note that all split-helicity gluon scattering amplitudes were computed in [78] – we construct here a similar solution for form factors.

Each recursive diagram with a $[q, q+1\rangle$ shift contains a three-point amplitude and an $(n-1)$ -point form factor. We can neatly combine the three-point amplitude and

the propagator in a prefactor to write²

$$\begin{aligned}
F_{q-2,n-q} &= \frac{[q-1q+1]}{[q-1q][qq+1]} F_{q-3,n-q}(1_\phi, 2_\phi, 3^-, \dots, \widehat{q-1}^-, \widehat{q+1}^+, \dots, n^+) \\
&+ \frac{\langle qq+2 \rangle}{\langle qq+1 \rangle \langle q+1q+2 \rangle} F_{q-2,n-q-1}(1_\phi, 2_\phi, 3^-, \dots, \widehat{q}^-, \widehat{q+2}^+, \dots, n^+),
\end{aligned} \tag{4.1.16}$$

where the shifted spinors of the external momenta that appear in the lower-point form factors are

$$\lambda_{\widehat{q+1}} = \frac{[q-1|P_{q,q+1}}{[q-1q+1]}, \tag{4.1.17a}$$

$$\tilde{\lambda}_{\widehat{q}} = \frac{P_{q,q+2}|q+2\rangle}{\langle qq+2\rangle}, \tag{4.1.17b}$$

with $P_{a,b} = p_a + \dots + p_b$. Furthermore, the shifted spinors associated with internal legs are relabelled as

$$\lambda_{\widehat{p}_{q-1q}}(z = z_{q-1q}) \rightarrow \lambda_{\widehat{q-1}} = \frac{P_{q,q+1}|q+1\rangle}{[q-1q+1]}, \tag{4.1.18a}$$

$$\tilde{\lambda}_{\widehat{p}_{q+1q+2}}(z = z_{q+1q+2}) \rightarrow \tilde{\lambda}_{\widehat{q+2}} = \frac{\langle q|P_{q,q+2}}{\langle qq+2\rangle}, \tag{4.1.18b}$$

so that the notation remains compatible with subsequent recursions. Crucially, all lower-point form factors appearing in (4.1.16) are of split-helicity form, so that the split helicity form factors are closed under recursions. Once we have reduced the form factor to expressions that involve only MHV and $\overline{\text{MHV}}$ terms, we can insert the shifted momenta.

It is useful to illustrate the structure of the recursion relations for split-helicity form factors using a square lattice as in Figure 4.3. Consider for example the form factor $F_{2,2}$. In this case, the first iteration using equation (4.1.16) relates $F_{2,2}$ to the form factors $F_{2,1}$ and $F_{1,2}$, which however are neither MHV nor $\overline{\text{MHV}}$. The next

²For the rest of this section we will always assume that the operator $\mathcal{O} = \text{Tr}(\phi_{12}\phi_{12})$ is inserted and will not mention it explicitly. Although the solution is presented for this particular insertion, the construction can be generalised to form factors involving other operators.

iteration leads to an expression involving one $F_{2,0}$, two $F_{1,1}$'s and one $F_{0,2}$ evaluated at some shifted momenta. A final iteration would then allow us to express the answer in terms of MHV and $\overline{\text{MHV}}$ form factors alone, or even to reduce everything down to $F_{0,0}$. It is also easy to see that this pattern generalises to arbitrary split-helicity form factors and that each term generated by subsequent recursions corresponds to a unique path between the form factor and the MHV or $\overline{\text{MHV}}$ edges of the lattice, as illustrated in Figure 4.3.

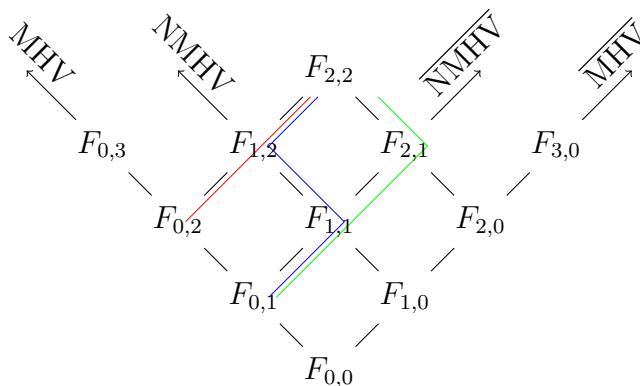


Figure 4.3: *The iterative structure of split-helicity form factors illustrated by a square lattice. The three coloured paths ending on the MHV line are in one-to-one correspondence with terms that appear in the iterated recursion of $F_{2,2}$. Similarly there will be three paths (terms) that end on the $\overline{\text{MHV}}$ line.*

In principle, all we need to do to compute a split-helicity form factor is to collect all prefactors picked up at each step of the recursion process and follow the iterated momentum shifts along a particular path on the lattice.

Solution for the split-helicity form factor

A very efficient way to organise the recursion is in terms of *zig-zag diagrams*, like those introduced in [78] for split-helicity gluon amplitudes. It is natural to split the

terms of the solution into those corresponding to paths ending on the MHV or $\overline{\text{MHV}}$ lines, respectively.

Zig-zag diagrams that correspond to recursion terms with an MHV form factor will be denoted as MHV zig-zags and the ones with an $\overline{\text{MHV}}$ form factor as $\overline{\text{MHV}}$ zig-zags. Note that we have therefore two types of diagrams, in contrast to the case of amplitudes in [78]. One can make this separation also for amplitudes as it only means that we terminate the iterated recursion once we reach an $\overline{\text{MHV}}$ term, instead of recursing it further down to $F_{0,0}$ (or $A_{2,2}$ for the case of amplitudes). In the path picture of the previous section, this separation corresponds to the fact that there is a unique path between any $\overline{\text{MHV}}$ form factor and $F_{0,0}$, hence one can replace that part of the recursion directly with an $\overline{\text{MHV}}$ form factor. Because the MHV zig-zags defined below are not compatible with two point objects such as $F_{0,0}$ we chose to use this formalism with two types of diagrams. This has the added advantage that it makes the parity symmetry of $F_{q-2,q-2}$ form factors manifest.

The MHV zig-zags are parameterised with $2k + 1$ labels

$$2 \leq a_1 < \dots < a_k < q - 1 \quad \text{and} \quad n \geq b_1 > \dots > b_{k+1} > q, \quad k \geq 0,$$

representing expressions in the following manner

$$= \frac{N_1 N_2 N_3}{D_1 D_2 D_3} \quad (4.1.19)$$

while the $\overline{\text{MHV}}$ zig-zags are parametrised with $2k + 1$ labels

$$2 \leq \bar{b}_1 < \dots < \bar{b}_{k+1} < q \quad \text{and} \quad n \geq \bar{a}_1 > \dots > \bar{a}_k > q + 1, \quad k \geq 0,$$

representing expressions, similarly shown below

$$= \frac{\bar{N}_1 \bar{N}_2 \bar{N}_3}{\bar{D}_1 \bar{D}_2 \bar{D}_3} \quad (4.1.20)$$

where $N_{1,2,3}$ and $D_{1,2,3}$ are defined as

$$\begin{aligned} N_1 &= \langle 1 | P_{2,b_1} P_{a_1+1,b_1} P_{a_1+1,b_2} P_{a_2+1,b_2} \cdots P_{q,b_{k+1}} | q \rangle \\ &\quad \times [2 | P_{a_1+1,b_1} P_{a_1+1,b_2} P_{a_2+1,b_2} \cdots P_{q,b_{k+1}} | q \rangle^2 \\ N_2 &= \langle b_1 + 1 | b_1 \rangle \langle b_2 + 1 | b_2 \rangle \cdots \langle b_{k+1} + 1 | b_{k+1} \rangle \\ N_3 &= [a_1 a_1 + 1] \cdots [a_k a_k + 1] \\ D_1 &= P_{2,b_1}^2 P_{a_1+1,b_1}^2 P_{a_1+1,b_2}^2 P_{a_2+1,b_2}^2 \cdots P_{q,b_{k+1}}^2 \\ D_2 &= Z_{q,1} \bar{Z}_{2,q-1} \\ D_3 &= [2 | P_{2,b_1} | b_1 + 1 \rangle \langle b_1 | P_{a_1+1,b_1} | a_1 \rangle [a_1 + 1 | P_{a_1+1,b_2} | b_2 + 1 \rangle \cdots \langle b_{k+1} | P_{q,b_{k+1}} | q - 1 \rangle \end{aligned} \quad (4.1.21a)$$

$$\begin{aligned} \bar{N}_1 &= [q + 1 | P_{\bar{b}_{k+1}+1,q+1}, \dots, P_{\bar{b}_2+1,\bar{a}_2}, P_{\bar{b}_2+1,\bar{a}_1}, P_{\bar{b}_1+1,\bar{a}_1} | 1 \rangle^2 \\ &\quad \times [q + 1 | P_{\bar{b}_{k+1}+1,q+1}, \dots, P_{\bar{b}_2+1,\bar{a}_2}, P_{\bar{b}_2+1,\bar{a}_1}, P_{\bar{b}_1+1,\bar{a}_1} P_{\bar{b}_1+1,1} | 2 \rangle \\ \bar{N}_2 &= [\bar{b}_1 \bar{b}_1 + 1] \cdots [\bar{b}_{k+1} \bar{b}_{k+1} + 1] \\ \bar{N}_3 &= \langle \bar{a}_1 + 1 | \bar{a}_1 \rangle \cdots \langle \bar{a}_k + 1 | \bar{a}_k \rangle \\ \bar{D}_1 &= P_{\bar{b}_1+1,1}^2 P_{\bar{b}_1+1,\bar{a}_1}^2 P_{\bar{b}_2+1,\bar{a}_1}^2 \cdots P_{\bar{b}_k+1,q+1}^2 \\ \bar{D}_2 &= \bar{Z}_{2,q+1} Z_{q+2,1} \\ \bar{D}_3 &= \langle 1 | P_{\bar{b}_1+1,1} | \bar{b}_1 \rangle [\bar{b}_1 + 1 | P_{\bar{b}_1+1,\bar{a}_1} | \bar{a}_1 + 1 \rangle \langle \bar{a}_1 | P_{\bar{b}_2+1,\bar{a}_1} | \bar{b}_2 \rangle \cdots [\bar{b}_k + 1 | P_{\bar{b}_k+1,q+1} | q + 2 \rangle, \end{aligned} \quad (4.1.21b)$$

with

$$Z_{i,j} = \langle i | i + 1 \rangle \cdots \langle j - 1 | j \rangle, \quad \bar{Z}_{i,j} = [i | i + 1] \cdots [j - 1 | j]. \quad (4.1.21c)$$

The split-helicity form factor is then the sum of all recursion terms, or equivalently the sum of all possible MHV and $\overline{\text{MHV}}$ zig-zags, which is equal to

$$F_{q-2, n-q-2} = \sum_{\{a_i, b_i\}} \frac{N_1 N_2 N_3}{D_1 D_2 D_3} + \sum_{\{\bar{a}_i, \bar{b}_i\}} \frac{\bar{N}_1 \bar{N}_2 \bar{N}_3}{\bar{D}_1 \bar{D}_2 \bar{D}_3}. \quad (4.1.22)$$

Notice that for the form factors with equal number of negative and positive helicity gluons, the $\overline{\text{MHV}}$ zig-zags can be obtained from the MHV ones by changing $(2, 3, \dots, q) \rightarrow (1, n, \dots, q+1)$ and $\langle ij \rangle \rightarrow [ji]$.

Let us now explain the precise relation between the zig-zag diagrams and the paths on the split-helicity form factor lattice. Let a path with r_1 steps to the right, l_1 steps to the left followed by r_2 steps to the right etc. be represented by

$$R^{r_k} \dots R^{r_2} L^{l_1} R^{r_1}. \quad (4.1.23)$$

Then an MHV zig-zag labelled by $\{a_i, b_i\}$ corresponds to the path:

$$L^{a_1-1} R^{b_1-b_2} \dots L^{a_k-a_{k-1}} R^{b_k-b_{k+1}} L^{q-1-a_k} R^{b_k-(q+1)},$$

while an $\overline{\text{MHV}}$ zig-zag labelled by $\{\bar{a}_i, \bar{b}_i\}$ corresponds to the path:

$$R^{\bar{a}_1+1} L^{\bar{b}_2-\bar{b}_1} \dots R^{\bar{a}_k-\bar{a}_{k-1}} L^{\bar{b}_{k+1}-\bar{b}_k} R^{\bar{a}_k-q-1} L^{q-\bar{b}_{k+1}-1}.$$

Note that if there are no a_i indices in the MHV zig-zag diagram we set $a_1 = 1$; and if there are no \bar{a}_i in the $\overline{\text{MHV}}$ zig-zag diagram we set $\bar{a}_1 = n$. All powers in the above formulae are modulo n .

Examples

Here we present some examples to show that the solution (4.1.22) reproduces the correct expressions.

MHV case

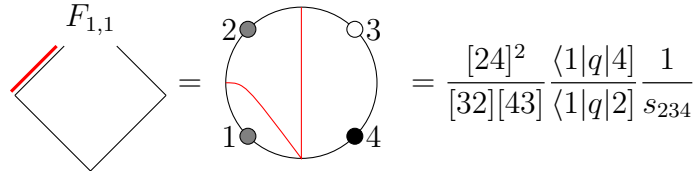
The zig-zag diagrams collapse onto a point between 1 and 2 as there are neither b_i nor \bar{a}_i . Hence, the only contributions are $N_1 = \langle 12 \rangle$ and $D_2 = F_{2,1}$ and

$$F_{1,n-3}(1_\phi, 2_\phi, 3^+, \dots, n^+) = \frac{\langle 12 \rangle}{\langle 23 \rangle \langle 34 \rangle \dots \langle n1 \rangle}, \quad (4.1.24)$$

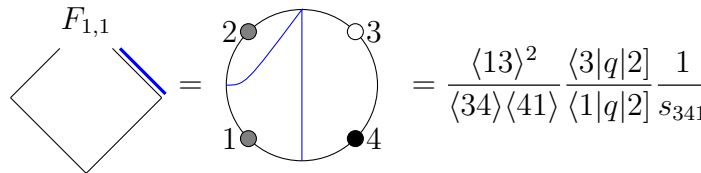
as required. The situation for MHV amplitudes is similar [78]. An equivalent calculation for the $\overline{\text{MHV}}$ zig-zag gives the $\overline{\text{MHV}}$ form factor.

NMHV case

At four points, there is exactly one MHV and one $\overline{\text{MHV}}$ zig-zag, representing one move to the left and one move to the right. Comparing with equations (4.1.19) and (4.1.20) one can read off $b_1 = 4$ for the MHV zig-zag and $\bar{b}_1 = 2$ for the $\overline{\text{MHV}}$ zig-zag.



$$F_{1,1} = \text{diamond with red double line on left} = \text{circle with red path and legs 1, 2, 3, 4} = \frac{[24]^2}{[32][43]} \frac{\langle 1|q|4 \rangle}{\langle 1|q|2 \rangle} \frac{1}{s_{234}} \quad (4.1.25)$$



$$F_{1,1} = \text{diamond with blue double line on right} = \text{circle with blue path and legs 1, 2, 3, 4} = \frac{\langle 13 \rangle^2}{\langle 34 \rangle \langle 41 \rangle} \frac{\langle 3|q|2 \rangle}{\langle 1|q|2 \rangle} \frac{1}{s_{341}} \quad (4.1.26)$$

This result is in agreement with the previous section.

In general, for the NMHV form factors, there is one $\overline{\text{MHV}}$ zig-zag corresponding to the path which proceeds along the NMHV line until it reaches the $\overline{\text{MHV}}$ edge of the lattice, and $n - 3$ MHV zig-zags where the path shifts onto the MHV edge before it arrives at the $\overline{\text{MHV}}$ edge. The MHV paths and the corresponding zig-zags are shown in Figure 4.4.

An $N^2\text{MHV}$ example

As it can be seen from the lattice in Figure 4.3, there are three MHV and three $\overline{\text{MHV}}$ terms in the recursion of the six-point split-helicity form factor. These are listed below, where the subscripts encode the shape of the path as described earlier.

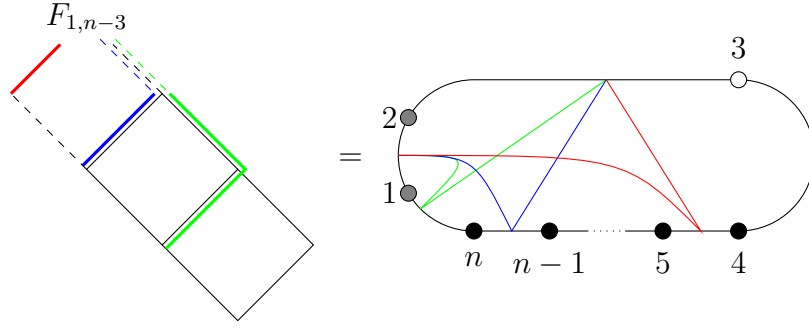


Figure 4.4: *Correspondence of lattice paths and MHV zig-zags for NMHV form factors.*

For example, F_{RLL} is the term which corresponds to the path that starts with a step to right and terminates at the MHV edge with two steps to the left. The MHV terms are:

- $b_1 = 5$, no a :

$$F_{LL} = \text{Diagram} = -\frac{[25]^2}{[23][34][45]\langle 61 \rangle} \frac{1}{P_{2,5}^2} \frac{[5|P_{2,4}|1\rangle}{[2|P_{2,5}|6\rangle} \quad (4.1.27a)$$

- $b_1 = 6$, no a :

$$F_{RLL} = \text{Diagram} = \frac{1}{\langle 45 \rangle \langle 56 \rangle [23]} \frac{1}{P_{2,6}^2 P_{4,6}^2} \frac{\langle 1|P_{2,6}P_{4,6}|4\rangle [2|P_{4,6}|4\rangle^2}{[2|P_{2,6}|1\rangle \langle 6|P_{4,6}|3\rangle} \quad (4.1.27b)$$

- $b_1 = 6$, $b_2 = 5$, $a_1 = 2$:

$$F_{LRL} = \text{Diagram} = \frac{1}{[34][45]} \frac{1}{P_{2,6}^2 P_{3,6}^2 P_{3,5}^2} \frac{\langle 1|P_{2,6}P_{3,6}P_{3,5}|5\rangle [2|P_{3,6}P_{3,5}|5]^2}{[2|P_{2,6}|1]\langle 6|P_{3,6}|2\rangle [3|P_{3,5}|6]} \quad (4.1.27c)$$

The $\overline{\text{MHV}}$ terms are:

- $\bar{b}_1 = 3$, no \bar{a}

$$F_{RR} = \text{Diagram} = \frac{\langle 14\rangle^2}{\langle 45\rangle\langle 56\rangle\langle 61\rangle[23]} \frac{1}{P_{4,1}^2} \frac{\langle 4|P_{4,1}|2\rangle}{\langle 1|P_{4,1}|3\rangle} \quad (4.1.28a)$$

- $\bar{b}_1 = 2$, no \bar{a}

$$F_{LRR} = \text{Diagram} = \frac{1}{[34][45]\langle 61\rangle} \frac{1}{P_{3,5}^2 P_{3,1}^2} \frac{\langle 1|P_{3,5}|5\rangle^2 [5|P_{3,5}P_{3,1}|2]}{\langle 1|P_{3,1}|2\rangle [3|P_{3,5}|6]} \quad (4.1.28b)$$

- $\bar{b}_1 = 2$, $b_2 = 3$, $\bar{a}_1 = 6$

$$F_{RLR} = \text{Diagram} = \frac{1}{\langle 45\rangle\langle 56\rangle} \frac{1}{P_{3,1}^2 P_{3,6}^2 P_{4,6}^2} \frac{\langle 4|P_{4,6}P_{3,1}|1\rangle^2 \langle 5|P_{4,6}P_{3,6}P_{3,1}|2\rangle}{\langle 1|P_{3,1}|2\rangle [3|P_{3,6}|1]\langle 6|P_{4,6}|3\rangle [4|P_{4,6}|6]} \quad (4.1.28c)$$

We have checked this result against an MHV diagram calculation and both methods yield the same result.

4.2 Supersymmetric form factors and Ward identities

The purpose of this section is to write down supersymmetric Ward identities for certain appropriately defined form factors of supersymmetric operators. By solving these Ward identities, we will learn about the structure of these form factors.

To begin, we recall the familiar fact that in $\mathcal{N} = 4$ SYM one can efficiently package all scattering amplitudes with fixed total helicity and fixed number of particles n into a superamplitude [57], thereby making manifest some of the supersymmetries of the theory. This object depends on auxiliary fermionic variables $\eta_{i,A}$, one for each particle $i = 1, \dots, n$, with A an anti-fundamental $SU(4)$ index. The superamplitude can be Taylor-expanded in the η variables, with a specific correspondence between powers of η and particular external states. This correspondence can be read off from the Nair super-wavefunction [57], which encodes all the annihilation operators of the physical states,

$$\Phi(p, \eta) := g^+(p) + \eta_A \lambda^A(p) + \frac{\eta^A \eta^B}{2!} \phi^{AB}(p) + \epsilon^{ABCD} \frac{\eta^A \eta^B \eta^C}{3!} \bar{\lambda}_D(p) + \eta_1 \eta_2 \eta_3 \eta_4 g^-(p), \quad (4.2.1)$$

where $(g^+(p), \dots, g^-(p))$ are the annihilation operators of the corresponding states. In order to select a state with a particular helicity h_i , we need to expand the superamplitude and pick the term with $2 - 2h_i$ powers of η_i .

This familiar framework becomes richer for form factors. Indeed, one can consider form factors of bosonic operators – such as $\text{Tr}(\phi_{AB}\phi_{AB})$ – with an external supersymmetric state described using the Nair approach, but one can also supersymmetrise the operator itself, as we shall see in the next section.

A comment on notation – we denote a form factor as $\langle 0 | \Phi(1) \cdots \Phi(n) \mathcal{O} | 0 \rangle$ or

equivalently $\langle 1 \cdots n | \mathcal{O} | 0 \rangle$, where $|i\rangle := \Phi^\dagger(i)|0\rangle$ is a Nair superstate, which satisfies

$$\langle i | P = \langle i | p_i, \quad \langle i | Q = \langle i | \lambda_i \eta_i, \quad \langle i | \bar{Q} = \langle i | \frac{\partial}{\partial \eta_i} \tilde{\lambda}_i, \quad (4.2.2)$$

where the derivative in the last equation acts on the state on its left. We also adopt the notation $\langle 1 \cdots n | := \langle 0 | \Phi(1) \cdots \Phi(n)$.

4.2.1 Form factor of the chiral stress-tensor multiplet operator

We now consider the form factor of the chiral supersymmetric operator³ $\mathcal{T}(x, \theta^+)$ considered recently in [11, 81]. This operator is the chiral part of the stress-tensor multiplet operator, $\mathcal{T}(x, \theta^+) := \mathcal{T}(x, \theta^+, \bar{\theta}_- = 0, u)$ and we report here its expression from [11] for convenience,

$$\begin{aligned} \mathcal{T}(x, \theta^+) &= \text{Tr}(\phi^{++} \phi^{++}) + i2\sqrt{2}\theta_\alpha^{+a} \text{Tr}(\lambda_a^{+\alpha} \phi^{++}) \\ &+ \theta_\alpha^{+a} \epsilon_{ab} \theta_\beta^{+b} \text{Tr}\left(\lambda^{+c(\alpha} \lambda_c^{+\beta)} - i\sqrt{2}F^{\alpha\beta} \phi^{++}\right) \\ &- \theta_\alpha^{+a} \epsilon^{\alpha\beta} \theta_\beta^{+b} \text{Tr}\left(\lambda_{(a}^{+\gamma} \lambda_{b)}^+_{\gamma} - g\sqrt{2}[\phi_{(a}^{+C}, \bar{\phi}_{C+b)}] \phi^{++}\right) \\ &- \frac{4}{3}(\theta^+)_\alpha^{3a} \text{Tr}\left(F_\beta^\alpha \lambda_a^{+\beta} + ig[\phi_a^{+B}, \bar{\phi}_{BC}] \lambda^{C\alpha}\right) + \frac{1}{3}(\theta^+)^4 \mathcal{L}. \quad (4.2.3) \end{aligned}$$

Notice that the $(\theta^+)^0$ component is nothing but the scalar operator $\text{Tr}(\phi^{++} \phi^{++})$, whereas the $(\theta^+)^4$ component is the on-shell Lagrangian.

Next we describe how to use supersymmetric Ward identities in order to constrain form factors, slightly extending the usual procedure for amplitudes. Ward identities associated with a certain symmetry generator s which leaves the vacuum invariant

³A quick reminder of harmonic superspace [79, 80] conventions, following closely [11, 81]. We introduce the harmonic projections of the θ_α^A and $\bar{\theta}_A^{\dot{\alpha}}$ superspace coordinates and of the supersymmetry charges Q_A^α , \bar{Q}_α^A , as $\theta_\alpha^{+a} := \theta_\alpha^A u_A^{+a}$, $\bar{\theta}_{-a}^{\dot{\alpha}} := \bar{\theta}_A^{\dot{\alpha}} \bar{u}_{-a}^A$, and $Q_{\pm a}^\alpha := \bar{u}_{\pm a}^A Q_A^\alpha$, $\bar{Q}_\alpha^{\pm a} := u_A^{\pm a} \bar{Q}_\alpha^A$ with the harmonic $SU(4)$ u and \bar{u} normalised as in Section 3 of [11].

are obtained in a standard way [82–85] by expanding the identity

$$0 = \langle 0|[s, \Phi(1) \cdots \Phi(n) \mathcal{O}]|0\rangle, \quad (4.2.4)$$

or

$$0 = \langle 0|\Phi(1) \cdots \Phi(n) [s, \mathcal{O}]|0\rangle + \sum_{i=1}^n \langle 0|\Phi(1) \cdots [s, \Phi(i)] \cdots \Phi(n) \mathcal{O}|0\rangle. \quad (4.2.5)$$

For instance, by considering s to be the momentum generator \mathcal{P} and using $[\mathcal{P}_\mu, \mathcal{O}(x)] = -i\partial_\mu \mathcal{O}(x)$ as well as the first equation of (4.2.2), we obtain

$$-i \langle 0|\Phi(1) \cdots \Phi(n) \partial_\mu \mathcal{O}(x)|0\rangle + \left(\sum_{i=1}^n p_i\right) \langle 0|\Phi(1) \cdots \Phi(n) \mathcal{O}(x)|0\rangle = 0. \quad (4.2.6)$$

Fourier transforming x to q and integrating by parts one obtains

$$\left(q - \sum_{i=1}^n p_i\right) F(q; 1, \dots, n) = 0, \quad (4.2.7)$$

where

$$F(q; 1, \dots, n) := \int d^4x e^{-iqx} \langle 1 \cdots n | \mathcal{O}(x) | 0 \rangle. \quad (4.2.8)$$

From this it follows that

$$F(q; 1, \dots, n) = C \cdot \delta^{(4)}\left(q - \sum_{i=1}^n p_i\right). \quad (4.2.9)$$

C can be fixed by further integrating both sides of (4.2.9) with a d^4q measure and using (4.2.8), which leads to $C = \langle 0|\Phi(1) \cdots \Phi(n) \mathcal{O}(0)|0\rangle = \langle 1 \cdots n | \mathcal{O}(0) | 0 \rangle$.

Similarly, we now consider Ward identities for the harmonic projections $Q_{\pm a}^\alpha$, $a = 1, 2$, of the Q -supersymmetry generators. We obtain

$$0 = \langle 0|\Phi(1) \cdots \Phi(n) [Q_\pm, \mathcal{T}(x, \theta^+)]|0\rangle + \sum_{i=1}^n \langle 0|\Phi(1) \cdots [Q_\pm, \Phi(i)] \cdots \Phi(n) \mathcal{T}(x, \theta^+)|0\rangle. \quad (4.2.10)$$

We now have to discuss how supersymmetry acts on the chiral part of $\mathcal{T}(x, \theta^+)$ as well as on the states.

In general the supersymmetry algebra closes only up to gauge transformations and equations of motion,⁴ however we consider here gauge-invariant operators such

⁴We would like to thank Paul Heslop for a useful conversation on these issues.

as \mathcal{T} which, furthermore, are made only of a subset of all fields, namely ϕ^{AB} , λ_α^A and $F_{\alpha\beta}$. It is an important fact that the algebra of the Q -generators closes off shell on the chiral part of \mathcal{T} [11], and hence these generators can be realised as differential operators. Of course, representing the \bar{Q} -generators in terms of differential operators is, in general, problematic, because the full supersymmetry algebra closes only on shell.

Moreover, for the chiral operator $\mathcal{T}(x, \theta^+)$ we have broken \bar{Q}^- since we have set $\theta^- = 0$ and hence we do not have a representation for this operator. For the Q_\pm -variation of $\mathcal{T}(x, \theta^+)$ we have,

$$[Q_-, \mathcal{T}(x, \theta^+)] = 0, \quad [Q_+, \mathcal{T}(x, \theta^+)] = i \frac{\partial}{\partial \theta^+} \mathcal{T}(x, \theta^+). \quad (4.2.11)$$

Note that since we consider the chiral part of the stress-tensor multiplet we have set $\bar{\theta} = 0$ and hence we have dropped $\bar{\theta}$ dependent terms in the realisation of Q and \bar{Q} . Then the first relation is obvious since $\mathcal{T}(x, \theta^+)$ is independent of θ^- . This also makes manifest the fact that all component operators of $\mathcal{T}(x, \theta^+)$ are annihilated by Q_{-a}^α [11]. On the other hand, Q_{+a}^α relates different components of the supermultiplet, as the second relation in (4.2.11) shows.

We define the super form factor as the super Fourier transform of the matrix element $\langle 1 \cdots n | \mathcal{T}(x, \theta^+) | 0 \rangle$, i.e.

$$\mathcal{F}_\mathcal{T}(q, \gamma_+; 1, \dots, n) := \int d^4x d^4\theta^+ e^{-i(qx + i\theta_+^{\alpha a} \gamma_{+a}^\alpha)} \langle 1 \cdots n | \mathcal{T}(x, \theta^+) | 0 \rangle, \quad (4.2.12)$$

where γ_{+a}^α is the Fourier-conjugate variable to $\theta_+^{\alpha a}$. Note that there is no γ_{-a}^α variable, since $\theta_-^{\alpha a}$ has been set to zero in order to define the chiral part of the stress-tensor multiplet. The Ward identities (4.2.10) can then be recast as

$$\begin{aligned} \left(\sum_{i=1}^n \lambda_i \eta_{-,i} \right) \mathcal{F}_\mathcal{T}(q, \gamma_+; 1, \dots, n) &= 0, \\ \left(\sum_{i=1}^n \lambda_i \eta_{+,i} - \gamma_+ \right) \mathcal{F}_\mathcal{T}(q, \gamma_+; 1, \dots, n) &= 0, \end{aligned} \quad (4.2.13)$$

where we have also introduced

$$\eta_{\pm a,i} := \bar{u}_{\pm a}^A \eta_{A,i} . \quad (4.2.14)$$

In arriving at (4.2.13) we have used (4.2.11) as well as the second relation in (4.2.2).

Next, we observe that (4.2.13) are solved by

$$\mathcal{F}_{\mathcal{T}}(q, \gamma_+; 1, \dots, n) = \delta^{(4)}\left(q - \sum_{i=1}^n \lambda_i \tilde{\lambda}_i\right) \delta^{(4)}\left(\gamma_+ - \sum_{i=1}^n \eta_{+,i} \lambda_i\right) \delta^{(4)}\left(\sum_{i=1}^n \eta_{-,i} \lambda_i\right) R, \quad (4.2.15)$$

for some function R which in principle depends on all bosonic and fermionic variables.

The simplest example is that of the MHV form factor, where the function R has a particularly simple expression derived in [60], namely

$$R^{\text{MHV}} = \frac{1}{\langle 12 \rangle \cdots \langle n1 \rangle} . \quad (4.2.16)$$

Notice that for an N^k MHV form factor, R has fermionic degree $4k$.

We can further constrain R by using some of the \bar{Q} -supersymmetries. More precisely, an inspection of the supersymmetry transformations of the fields reveals that a \bar{Q}^- transformation on the chiral part of the stress-tensor multiplet produces operators which are part of the full stress-tensor multiplet but not of its chiral truncation. Also, since $[Q_-, \mathcal{T}(x, \theta^+)] = 0$ we cannot realise \bar{Q}^- such that its anticommutator with Q_- gives a translation. One could of course still write a Ward identity for \bar{Q}^- , but this would involve operators of the full multiplet.

On the other hand, the \bar{Q}^+ -supersymmetry charge moves in the opposite direction of Q_+ across the different components of $\mathcal{T}(x, \theta^+)$, and is therefore realised as $\bar{Q}_{\dot{\alpha}}^+ = -\theta^{+\alpha} \partial / \partial x^{\dot{\alpha}\alpha}$.

We should stress at this point that the supersymmetry algebra on component fields closes only up to equations of motion and gauge transformations (the latter drop out since we consider gauge invariant operators). An important exception is the

subalgebra formed by the Q 's alone which does close off-shell for the fields appearing in $\mathcal{T}(x, \theta^+)$ [11]. Now we use the fact that matrix elements of terms proportional to equations of motion vanish at tree level, to argue that for our tree-level form factors the algebra formed by Q_+ and \bar{Q}^+ does close and, therefore, can be realised in the fashion described above. Thus, we can consider the \bar{Q}^+ Ward identity, which gives, after integrating by parts and using the third relation of (4.2.2),

$$\left(\sum_{i=1}^n \tilde{\lambda}_i \frac{\partial}{\partial \eta_{+,i}} - q \frac{\partial}{\partial \gamma_+} \right) \mathcal{F}_{\mathcal{T}}(q, \gamma_+; 1, \dots, n) = 0. \quad (4.2.17)$$

Acting on (4.2.15), we obtain the following relation for R ,

$$\delta^{(4)}\left(q - \sum_{i=1}^n \lambda_i \tilde{\lambda}_i\right) \delta^{(4)}\left(\gamma_+ - \sum_{i=1}^n \eta_{+,i} \lambda_i\right) \delta^{(4)}\left(\sum_{i=1}^n \eta_{-,i} \lambda_i\right) \left[\left(\sum_{i=1}^n \tilde{\lambda}_i \frac{\partial}{\partial \eta_{+,i}} - q \frac{\partial}{\partial \gamma_+} \right) R \right] = 0. \quad (4.2.18)$$

Notice that (4.2.18) implies a realisation of the supersymmetry generators on the form factor as

$$Q_{+a}^\alpha = \sum_{i=1}^n \lambda_i^\alpha \eta_{+,a,i} - \gamma_{+a}^\alpha, \quad Q_{-a}^\alpha = \sum_{i=1}^n \lambda_i^\alpha \eta_{-,a,i}, \quad (4.2.19)$$

whereas for $\bar{Q}_{\dot{\alpha}}^{+a}$,

$$\bar{Q}_{\dot{\alpha}}^{+a} = \sum_{i=1}^n \tilde{\lambda}_{i,\dot{\alpha}} \frac{\partial}{\partial \eta_{+,a,i}} - q_{\alpha\dot{\alpha}} \frac{\partial}{\partial \gamma_{\alpha+a}}. \quad (4.2.20)$$

4.2.2 Examples

In the previous section we have derived the general form of the supersymmetric form factor defined in (4.2.12). This expression is given in (4.2.15), and was obtained by solving Ward identities related to translations and Q_{\pm} -supersymmetries. The use of \bar{Q}^+ supersymmetry led to the constraint (4.2.18) on the function R . For the sake of illustration, we now present a few examples of component form factors derived from (4.2.15).

Form factor of $\text{Tr}(\phi^{++}\phi^{++})$

Our first example is the form factor of $\text{Tr}(\phi^{++}\phi^{++})$, which appears as the $(\theta^+)^0$ -term in the expansion of $\mathcal{T}(x, \theta^+)$ in (4.2.3). In this case, since

$$\int d^4\theta^+ e^{i\theta^+{}^\alpha\gamma_{+a}^\alpha} = (\gamma_+)^4, \quad (4.2.21)$$

we need to extract the $(\gamma_+)^4$ component of (4.2.15). This gives

$$\int d^4x e^{-iqx} \langle 1 \cdots n | \text{Tr}(\phi^{++}\phi^{++})(x) | 0 \rangle = \delta^{(4)}(q - \sum_{i=1}^n \lambda_i \tilde{\lambda}_i) \delta^{(4)}\left(\sum_{i=1}^n \eta_{-a,i} \lambda_i^\alpha\right) R, \quad (4.2.22)$$

or

$$\langle 1 \cdots n | \text{Tr}(\phi^{++}\phi^{++})(0) | 0 \rangle = \delta^{(4)}\left(\sum_{i=1}^n \eta_{-a,i} \lambda_i^\alpha\right) R. \quad (4.2.23)$$

Notice that with the help of (4.2.23) we can rewrite the supersymmetric form factor $\mathcal{F}_{\mathcal{T}}(q, \gamma_+; 1, \dots, n)$ as

$$\mathcal{F}_{\mathcal{T}}(q, \gamma_+; 1, \dots, n) = \delta^{(4)}(q - \sum_{i=1}^n \lambda_i \tilde{\lambda}_i) \delta^{(4)}\left(\gamma_+ - \sum_{i=1}^n \eta_{+,i} \lambda_i\right) \langle 1 \cdots n | \mathcal{T}(0, 0) | 0 \rangle, \quad (4.2.24)$$

since $\mathcal{T}(0, 0) := \text{Tr}(\phi^{++}\phi^{++})(0)$. In other words, the function R appearing in the $\mathcal{T}(x, \theta^+)$ form factor can be calculated from the form factor of its lowest component⁵ $\text{Tr}(\phi^{++}\phi^{++})(0)$. Similar considerations apply to form factors of other half BPS operators such as $\text{Tr}(\phi^{++})^n$ with $n > 2$.

Form factor of the on-shell Lagrangian

As a second important example, we now consider the form factor for the on-shell Lagrangian, whose expression is [11]

$$\mathcal{L} = \text{Tr} \left[-\frac{1}{2} F_{\alpha\beta} F^{\alpha\beta} + \sqrt{2} g \lambda^{\alpha A} [\phi_{AB}, \lambda_\alpha^B] - \frac{1}{8} g^2 [\phi^{AB}, \phi^{CD}] [\phi_{AB}, \phi_{CD}] \right]. \quad (4.2.25)$$

⁵One could arrive at (4.2.24) in a much more straightforward way by noticing that $\mathcal{T}(x, \theta_\alpha^{+a}) = \exp(i\mathcal{P}x) \exp(iQ_{+a}^\alpha \theta_\alpha^{+a}) \mathcal{T}(0, 0) \exp(-i\mathcal{P}x) \exp(-iQ_{+a}^\alpha \theta_\alpha^{+a})$ and using the invariance of the vacuum under supersymmetry and translations.

Notice that it contains the self-dual part of $\text{Tr}(F^2)$. The on-shell Lagrangian appears as the $(\theta^+)^4$ coefficient of the expansion of $\mathcal{T}(x, \theta^+)$ in (4.2.3). The corresponding Fourier transform gives

$$\int d^4\theta^+ e^{-i\theta^+{}^\alpha \gamma_{+a}^\alpha (\theta^+)^4} = 1, \quad (4.2.26)$$

i.e. we have to take the $\mathcal{O}(\gamma^0)$ component of (4.2.15). This is simply

$$\langle 1 \cdots n | \mathcal{L}(0) | 0 \rangle = \delta^{(8)} \left(\sum_{i=1}^n \eta_i \lambda_i \right) \cdot R. \quad (4.2.27)$$

It is interesting to note that for an MHV form factor, (4.2.27) is formally identical to the tree-level MHV superamplitude, except for a delta function of momentum conservation which now imposes $\sum_i p_i = q$ rather than the usual momentum conservation of the particles. This allows us to make an interesting observation for the limit $q \rightarrow 0$ in which this form factor reduces simply to the corresponding scattering amplitude. Actually, it turns out that any form factor with the on-shell Lagrangian \mathcal{L} inserted reduces to the corresponding scattering amplitude in the $q \rightarrow 0$ limit, since the insertion of the action corresponds to differentiating the path-integral for the amplitude with respect to the coupling [86–88].

Another observation is that for the case of a gluonic state with MHV helicity configuration, (4.2.27) agrees with the Higgs plus multi-gluon or “ ϕ -MHV” amplitude considered in [89]. Indeed, if we have a gluonic state, we can effectively replace the on-shell Lagrangian (4.2.25) with its first term, the square of the self-dual field strength.

Why is the maximally non-MHV form factor so simple?

The simplest tree-level form factor is the MHV form factor, e.g.

$$\langle 1^+ 2^+ \cdots i^- \cdots j^- \cdots (n-1)^+ n^+ | \text{Tr}(F_{\text{SD}}^2)(0) | 0 \rangle = \frac{\langle ij \rangle^4}{\langle 12 \rangle \langle 23 \rangle \cdots \langle n 1 \rangle}. \quad (4.2.28)$$

Interestingly, there are non-MHV form factors whose expression is also remarkably simple. Consider for example that of the self-dual field strength with an all negative-

helicity gluons state – we refer to this as the “maximally non-MHV” form factor. The result for this quantity is [89]

$$\langle 1^- \cdots n^- | \text{Tr}(F_{\text{SD}}^2)(0) | 0 \rangle = \frac{q^4}{[1\ 2][2\ 3] \cdots [n\ 1]} . \quad (4.2.29)$$

In the following we wish to show that the simplicity of (4.2.29) is determined by the supersymmetric Ward identity discussed earlier, and is linked to that of the MHV super form factor (4.2.16).

Recall from (4.2.24) that the super form factor of the chiral part of the stress-tensor multiplet $\mathcal{T}(x, \theta^+)$ has the form

$$\mathcal{F}_{\mathcal{T}} = \delta^{(4)}\left(q - \sum_{i=1}^n \lambda_i \tilde{\lambda}_i\right) \delta^{(4)}\left(\gamma_+ - \sum_{i=1}^n \eta_{+,i} \lambda_i\right) \mathcal{F}_{\phi^2} , \quad (4.2.30)$$

where

$$\mathcal{F}_{\phi^2} := \langle 1 \cdots n | \text{Tr}(\phi^{++} \phi^{++})(0) | 0 \rangle = \delta^{(4)}\left(\sum_{i=1}^n \eta_{-,i} \lambda_i\right) R . \quad (4.2.31)$$

For the MHV helicity configuration, the function R^{MHV} is given in (4.2.16),

$$\mathcal{F}_{\phi^2}^{\text{MHV}} = \frac{\delta^{(4)}\left(\sum_{i=1}^n \eta_{-,i} \lambda_i\right)}{\langle 12 \rangle \cdots \langle n1 \rangle} . \quad (4.2.32)$$

We can now use this fact and perform a Grassmann Fourier transform in order to derive the maximally non-MHV super form factor,

$$\mathcal{F}_{\phi^2}^{\text{N}^{\text{max}}\text{MHV}} = \prod_{i=1}^n \int d^4 \tilde{\eta}_i e^{i \eta_{i,A} \tilde{\eta}_i^A} \frac{\delta^{(4)}\left(\sum_{i=1}^n \tilde{\eta}_i^+ \tilde{\lambda}_i\right)}{[12] \cdots [n1]} . \quad (4.2.33)$$

Thus, the maximally non-MHV super form factor for the chiral part of the stress-tensor multiplet is

$$\mathcal{F}_{\mathcal{T}}^{\text{N}^{\text{max}}\text{MHV}} = \delta^{(4)}\left(q - \sum_{i=1}^n \lambda_i \tilde{\lambda}_i\right) \delta^{(4)}\left(\gamma_+ - \sum_{i=1}^n \eta_{+,i} \lambda_i\right) \mathcal{F}_{\phi^2}^{\text{N}^{\text{max}}\text{MHV}} . \quad (4.2.34)$$

We now focus on the component corresponding to the self-dual field strength, which

can be obtained from the coefficient of $(\gamma_+)^0$. This is given by⁶

$$\begin{aligned}
& \delta^{(4)} \left(\sum_{i=1}^n \eta_{+,i} \lambda_i \right) \prod_{i=1}^n \int d^4 \tilde{\eta}_i e^{i \eta_i \tilde{\eta}_i} \frac{\delta^{(4)} \left(\sum_{i=1}^n \tilde{\eta}_i^+ \tilde{\lambda}_i \right)}{[12] \cdots [n1]} \\
= & \delta^{(4)} \left(\sum_{i=1}^n \eta_{+,i} \lambda_i \right) \frac{\sum_{i<j} [ij] \sum_{k<l} [kl]}{[12] \cdots [n1]} \eta_1^4 \cdots \eta_i^3 \cdots \eta_j^3 \cdots \eta_k^3 \cdots \eta_l^3 \cdots \eta_n^4 \\
= & \frac{\sum_{i<j} \langle ij \rangle [ij] \sum_{k<l} \langle kl \rangle [kl]}{[12] \cdots [n1]} \eta_1^4 \cdots \eta_n^4 \\
= & \frac{q^4}{[12] \cdots [n1]} \eta_1^4 \cdots \eta_n^4 .
\end{aligned} \tag{4.2.35}$$

Equation (4.2.35) shows that there is a non-vanishing maximally non-MHV form factor for the self-dual field strength, whose expression is precisely given by (4.2.29).

4.2.3 Form factor of the complete stress-tensor multiplet

In this section we consider the form factor of the the full, non-chiral stress-tensor multiplet $\mathcal{T}(x, \theta^+, \tilde{\theta}_-)$. We can write this as⁷

$$\begin{aligned}
\mathcal{T}(x, \theta^+, \tilde{\theta}_-) & := \text{Tr}(W^{++} W^{++}) \\
& = e^{i\theta^+ Q_+ + i\tilde{\theta}_- \bar{Q}^-} \text{Tr}(\phi^{++} \phi^{++})(x) e^{-i\theta^+ Q_+ - i\tilde{\theta}_- \bar{Q}^-} \\
& = \text{Tr}(\phi^{++} \phi^{++}) + (\theta^+)^4 \mathcal{L} + (\tilde{\theta}_-)^4 \tilde{\mathcal{L}} + (\theta^+ \sigma^\mu \tilde{\theta}_-) (\theta^+ \sigma^\nu \tilde{\theta}_-) T_{\mu\nu} + \cdots ,
\end{aligned} \tag{4.2.36}$$

where we have indicated only some terms of the full multiplet.

The right-hand side of (4.2.36) is an expansion in the chiral as well as anti-chiral variables θ^+ and $\tilde{\theta}_-$. We can parallel this feature in the states by using a non-chiral description as in [90] with fermionic variables η_+ and $\tilde{\eta}_-$. With this choice, the

⁶In the following equation we omit a trivial delta function of momentum conservation.

⁷Notice that the second equality is true only up to equations of motion because the non-chiral algebra closes only on shell. In the following we will work at tree level and hence this point will not affect our considerations.

supersymmetry algebra is realised on states as

$$\begin{aligned}\langle i|Q_+ &= \langle i|\lambda_i\eta_{+,i}, & \langle i|Q_- &= \langle i|\lambda_i\frac{\partial}{\partial\tilde{\eta}_i^-}, \\ \langle i|\bar{Q}^- &= \langle i|\tilde{\lambda}_i\tilde{\eta}_i^-, & \langle i|\bar{Q}^+ &= \langle i|\tilde{\lambda}_i\frac{\partial}{\partial\eta_{+,i}}.\end{aligned}\quad (4.2.37)$$

This non-chiral representation can be obtained via a simple Fourier transform of half of the chiral superspace variables. In terms of the Nair description of states, this amounts to introducing a new super wavefunction,

$$\begin{aligned}\Phi(p, \eta_+, \tilde{\eta}^-) &:= \int d^2\eta_- e^{i\eta_-\tilde{\eta}^-} \Phi(p, \eta) \\ &= g^+(p)(\tilde{\eta}^-)^2 + \dots + \phi^{++}(\eta_+)^2(\tilde{\eta}^-)^2 + \phi^{--} + \dots + g^-(p)(\eta_+)^2.\end{aligned}\quad (4.2.38)$$

As a result, operators and superstates live in a non-chiral superspace. The non-chiral form factor in this representation is defined as

$$\mathcal{F}(q, \gamma_+, \tilde{\gamma}^-; 1, \dots, n) := \int d^4x d^4\theta^+ d^4\tilde{\theta}_- e^{-i(qx + \theta^+\gamma_+ + \tilde{\theta}_-\tilde{\gamma}^-)} \langle 1 \dots n | \mathcal{T}(x, \theta^+, \tilde{\theta}_-) | 0 \rangle. \quad (4.2.39)$$

In order to write down Ward identities for (4.2.39), we consider the action of supersymmetry generators on the operator $\mathcal{T}(x, \theta^+, \tilde{\theta}_-)$:

$$\begin{aligned}[Q_+, \mathcal{T}(x, \theta^+, \tilde{\theta}_-)] &= i\frac{\partial}{\partial\theta^+}\mathcal{T}(x, \theta^+, \tilde{\theta}_-), & [Q_-, \mathcal{T}(x, \theta^+, \tilde{\theta}_-)] &= -\tilde{\theta}_-\frac{\partial}{\partial x}\mathcal{T}(x, \theta^+, \tilde{\theta}_-), \\ [\bar{Q}^-, \mathcal{T}(x, \theta^+, \tilde{\theta}_-)] &= -\frac{\partial}{\partial\tilde{\theta}_-}\mathcal{T}(x, \theta^+, \tilde{\theta}_-), & [\bar{Q}^+, \mathcal{T}(x, \theta^+, \tilde{\theta}_-)] &= i\theta^+\frac{\partial}{\partial x}\mathcal{T}(x, \theta^+, \tilde{\theta}_-).\end{aligned}\quad (4.2.40)$$

Following closely the derivation of the Ward identities described in the previous section, we arrive at the following relations for each supersymmetry generator,

$$Q_+ : \quad (\eta_+\lambda - \gamma_+)\mathcal{F} = 0, \quad Q_- : \quad \left(q\frac{\partial}{\partial\tilde{\gamma}^-} - \lambda\frac{\partial}{\partial\tilde{\eta}^-}\right)\mathcal{F} = 0, \quad (4.2.41)$$

$$\bar{Q}^- : \quad (\tilde{\eta}^-\tilde{\lambda} - \tilde{\gamma}^-)\mathcal{F} = 0, \quad \bar{Q}^+ : \quad \left(q\frac{\partial}{\partial\gamma_+} - \tilde{\lambda}\frac{\partial}{\partial\eta_+}\right)\mathcal{F} = 0, \quad (4.2.42)$$

and hence the form factor in (4.2.39) takes the form

$$\mathcal{F} = \delta^{(4)}\left(q - \sum_{i=1}^n \lambda_i \tilde{\lambda}_i\right) \delta^{(4)}\left(\gamma_+ - \sum_{i=1}^n \eta_{+,i} \lambda_i\right) \delta^{(4)}\left(\tilde{\gamma}^- - \sum_{i=1}^n \tilde{\eta}_i^- \tilde{\lambda}_i\right) \mathcal{F}_{\phi^2}^{\text{nc}}, \quad (4.2.43)$$

for some function $\mathcal{F}_{\phi^2}^{\text{nc}}$.

A useful observation is that $\mathcal{F}_{\phi^2}^{\text{nc}}$ can be obtained from the corresponding function introduced in (4.2.30) for the chiral form factor via a half-Fourier transform on the η and $\tilde{\eta}$ variables, as

$$\mathcal{F}_{\phi^2}^{\text{nc}}(\lambda, \tilde{\lambda}, \eta_+, \tilde{\eta}^-) = \prod_{i=1}^n \int d^2\eta_{-,i} e^{i\eta_{-,i}\tilde{\eta}_i^-} \mathcal{F}_{\phi^2}(\lambda, \tilde{\lambda}, \eta_+, \eta_-). \quad (4.2.44)$$

In the remaining part of this section we would like to show a few applications of this formulation.

To begin with, we specialise to the MHV case, for which we have

$$\begin{aligned} \mathcal{F}_{\phi^2}^{\text{MHV,nc}} &= \prod_{i=1}^n \int d^2\eta_{-,i} e^{i\eta_{-,i}\tilde{\eta}_i^-} \frac{\delta^{(4)}(\sum_{i=1}^n \eta_{-,i}\lambda_i)}{\langle 12 \rangle \cdots \langle n1 \rangle} \\ &= \frac{\langle kl \rangle^2}{\langle 12 \rangle \cdots \langle n1 \rangle} \prod_{i \neq k,l}^n (\tilde{\eta}_i^-)^2 + \cdots \end{aligned} \quad (4.2.45)$$

The MHV form factor of $\text{Tr}(\phi^+)^2$ is then obtained by extracting the coefficient of $(\gamma_+)^4(\tilde{\gamma}^-)^4$ in (4.2.43), and thus it is immediately seen to give the correct answer. The form factor with an insertion of the chiral Lagrangian \mathcal{L} (which includes $\text{Tr}(F_{\text{SD}}^2)$) is obtained by taking the coefficient of $(\gamma_+)^0(\tilde{\gamma}^-)^4$:

$$\mathcal{F}_{\mathcal{L}}^{\text{MHV}} = \delta^{(4)}\left(\sum_{i=1}^n \eta_{+,i}\lambda_i\right) \mathcal{F}_{\phi^2}^{\text{MHV}} = \frac{\langle kl \rangle^4}{\langle 12 \rangle \cdots \langle n1 \rangle} \left(\eta_{+,k}^2 \eta_{+,l}^2 \prod_{i \neq k,l}^n (\tilde{\eta}_i^-)^2 \right) + \cdots \quad (4.2.46)$$

as expected. Finally, in order to obtain the form factor with $\tilde{\mathcal{L}}$ (which includes $\text{Tr}(F_{\text{ASD}}^2)$), we extract the coefficient of $(\gamma_+)^4(\tilde{\gamma}^-)^0$:

$$\begin{aligned} \mathcal{F}_{\tilde{\mathcal{L}}}^{\text{MHV}} &= \delta^{(4)}\left(\sum_{i=1}^n \tilde{\eta}_i^- \tilde{\lambda}_i\right) \mathcal{F}_{\phi^2}^{\text{MHV}} = \frac{\sum_{i<j} \langle ij \rangle [ij] \sum_{k<l} \langle kl \rangle [kl]}{\langle 12 \rangle \cdots \langle n1 \rangle} \prod_{i=1}^n (\tilde{\eta}_i^-)^2 \\ &= \frac{q^4}{\langle 12 \rangle \cdots \langle n1 \rangle} \prod_{i=1}^n (\tilde{\eta}_i^-)^2, \end{aligned} \quad (4.2.47)$$

which is indeed also correct.

4.3 Supersymmetric methods

In this section we take a brief survey of various methods that can be used to calculate form factors of the complete stress-tensor multiplet, at tree and loop level. These are simple but interesting extensions of well-known techniques for scattering amplitudes – MHV diagrams [4], on-shell recursion relations [5, 21] and (generalised) unitarity [2, 24, 91, 92] – thus we will limit ourselves to highlighting the peculiarities we encounter when dealing with form factors. The non-supersymmetric versions of these methods have been considered earlier in Section 2 and in [60].

A preliminary observation is that the form factor of the complete stress-tensor multiplet operator $\mathcal{T}(x, \theta^+, \tilde{\theta}_-)$ can be expressed in terms of that of its lowest bosonic component $\text{Tr}(\phi^{++}\phi^{++})$, as we have shown in (4.2.43), namely

$$\mathcal{F} = \delta^{(4)}\left(q - \sum_{i=1}^n \lambda_i \tilde{\lambda}_i\right) \delta^{(4)}\left(\gamma_+ - \sum_{i=1}^n \eta_{+,i} \lambda_i\right) \delta^{(4)}\left(\tilde{\gamma}^- - \sum_{i=1}^n \tilde{\eta}_i^- \tilde{\lambda}_i\right) \mathcal{F}_{\phi^2}^{\text{nc}}, \quad (4.3.1)$$

where $\mathcal{F}_{\phi^2}^{\text{nc}} := \langle 1 \cdots n | \text{Tr}(\phi^{++}\phi^{++})(0) | 0 \rangle$ and the superstate $\langle 1 \cdots n |$ is here in the non-chiral representation. One can then switch instantly to the chiral representation via a half-Fourier transform from the $\tilde{\eta}^-$ to the η_+ variables. Hence, we only need to devise methods to calculate the form factor $\langle 1 \cdots n | \text{Tr}(\phi^{++}\phi^{++})(0) | 0 \rangle$ using a chiral representation for the external state. This is the problem we address in the following.⁸

4.3.1 Supersymmetric MHV rules

We begin with a lightning illustration of super MHV rules. Here, the super MHV form factor,

$$\mathcal{F}^{\text{MHV}}(1, 2, \dots, n; q) = \frac{\delta^{(4)}\left(q - \sum_i \lambda_i \tilde{\lambda}_i\right) \delta^{(4)}\left(\sum_i \lambda_i \eta_{i,-}\right)}{\langle 1 2 \rangle \langle 2 3 \rangle \cdots \langle n 1 \rangle}, \quad (4.3.2)$$

⁸To simplify our notation, we will drop from now on the subscript in \mathcal{F}_{ϕ^2} .

is continued off shell with the standard prescription (4.1.4) of [4], and used as a vertex in addition to the standard MHV vertices. Form factors have a single operator insertion, hence we only draw diagrams with a single form factor MHV vertex. As an example, consider the NMHV tree-level super form factor. It can be computed by summing over all diagrams in Figure 4.5(a), whose expression is

$$\begin{aligned} \mathcal{F}_{\text{NMHV}}^{(0)} &= \sum_{i=1}^n \sum_{j=i+1}^{i+n-2} \int d^4 P_{ij} \int d^4 \eta_P \mathcal{A}_{\text{MHV}}^{(0)}(i, \dots, j, P_{ij}) \frac{1}{P_{ij}^2} \mathcal{F}_{\text{MHV}}^{(0)}(j+1, \dots, i-1, -P_{ij}; q) \\ &= \mathcal{F}_{\text{MHV}}^{(0)} \sum_{i=1}^n \sum_{j=i+1}^{i+n-2} \frac{\langle i-1 \ i \rangle \langle j \ j+1 \rangle}{\langle i-1 \ P_{ij} \rangle \langle P_{ij} \ i \rangle \langle j \ P_{ij} \rangle \langle P_{ij} \ j+1 \rangle} \frac{1}{P_{ij}^2} \delta^{(4)} \left(\sum_{k=i}^j \langle P_{ij} \ k \rangle \eta_k^A \right) \end{aligned} \quad (4.3.3)$$

We have also calculated tree-level N²MHV super form factor up to six points and checked that the results are all independent of the choice of reference spinor. We have also re-derived the split-helicity form factors, and checked numerical agreement with the results presented in Section 4.1.2.

As an additional example, consider the one-loop MHV super form factor. Following [77], this can be computed by summing over all diagrams in Figure 4.5(b), and is given by

$$\begin{aligned} \mathcal{F}_{\text{MHV}}^{(1)} &= \sum_{i=1}^n \sum_{j=i}^{i+n-1} \int \frac{d^D L_1}{L_1^2 + i\varepsilon} \frac{d^D L_2}{L_2^2 + i\varepsilon} \int d^4 \eta_{L_1} \int d^4 \eta_{L_2} \\ &\quad \mathcal{A}_{\text{MHV}}^{(0)}(i, \dots, j, L_1, L_2) \mathcal{F}_{\text{MHV}}^{(0)}(-L_2, -L_1, j+1, \dots, i-1; q) . \end{aligned} \quad (4.3.4)$$

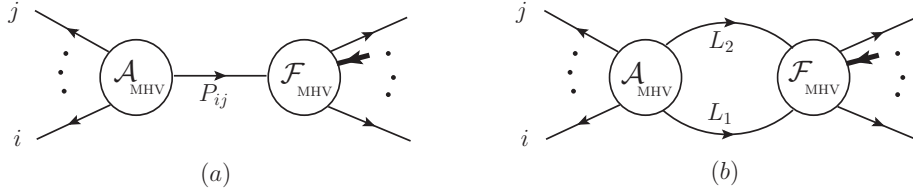


Figure 4.5: (a) *MHV diagram for a tree-level NMHV form factor.* (b) *MHV diagram for a one-loop MHV form factor.*

Finally, we note that the MHV vertex expansion may be proved at tree level along the lines of [93], namely by using a BCFW recursion relation with an all-line shift and showing that this is identical to the MHV diagram expansion.

4.3.2 Supersymmetric recursion relations

Now we consider a simple extension of the supersymmetric version [94, 95] of the BCFW recursion relation [5, 21]. We choose to work with an $[i, j\rangle$ shift, $\tilde{\lambda}_i \rightarrow \tilde{\lambda}_i + z\tilde{\lambda}_j$, $\lambda_j \rightarrow \lambda_j - z\lambda_i$, $\eta_i \rightarrow \eta_i + z\eta_j$. Factorisation requires that each term in the recursion relation must contain one form factor and one amplitude. Hence, for each kinematic channel we need to sum over two diagrams, with the form factor appearing either on the left-hand or right-hand side, see Figure 4.6. The result one obtains by summing over these two classes of diagrams has the form

$$\begin{aligned} \mathcal{F}(0) &= \sum_{a,b} \int d^4 P d^4 \eta_P \mathcal{F}_L(z=z_{ab}) \frac{1}{P_{ab}^2} \mathcal{A}_R(z=z_{ab}) \\ &+ \sum_{c,d} \int d^4 P d^4 \eta_P \mathcal{A}_L(z=z_{cd}) \frac{1}{P_{cd}^2} \mathcal{F}_R(z=z_{cd}) . \end{aligned} \quad (4.3.5)$$

One point deserves a special attention, namely the large- z behaviour of the form

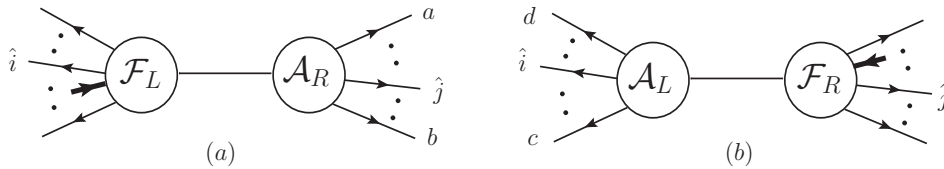


Figure 4.6: *The two recursive diagrams discussed in the text.*

factor. Recall that in order to have a recursion relation without boundary terms we need $\mathcal{F}(\dots \hat{p}_i, \dots, \hat{p}_j, \dots) \rightarrow 0$ as $z \rightarrow \infty$. We discuss this important point in Appendix B, where we prove that the condition mentioned above is indeed satisfied. We would also like to point out that the basic seeds in the form factor recursion relation are the two-point form factor, together with the three-point amplitudes.

4.3.3 Supersymmetric unitarity-based method

Supersymmetric generalised unitarity, as well as supersymmetric MHV rules, are easily applied to form factors. Consider for example a two-particle cut, depicted in Figure 4.7. On one side of the cut we have a tree-level form factor, on the other a tree scattering amplitude. For the case of a one-loop supersymmetric MHV form factor, the two-particle cut is equal to

$$\mathcal{F}_{\text{MHV}}^{(1)} \Big|_{s_{a+1, b-1}\text{-cut}} = \int d\text{LIPS}(l_1, l_2; P) \int d^4 \eta_{l_1} \int d^4 \eta_{l_2} \quad (4.3.6)$$

$$\mathcal{F}_{\text{MHV}}^{(0)}(-l_2, -l_1, b, \dots, a; q) \mathcal{A}_{\text{MHV}}^{(0)}(l_1, l_2, (a+1) \dots, (b-1)) ,$$

where the Lorentz-invariant phase-space measure is

$$d\text{LIPS}(l_1, l_2; P) := d^D l_1 d^D l_2 \delta^+(l_1^2) \delta^+(l_2^2) \delta^D(l_1 + l_2 + P) . \quad (4.3.7)$$

The sum over all possible states which can propagate in the loop is automatically

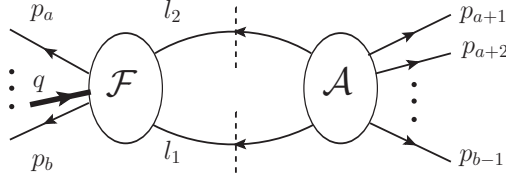


Figure 4.7: *A two-particle cut diagram for a one-loop form factor.*

performed by the fermionic integration. A simple calculation gives

$$\mathcal{F}_{\text{MHV}}^{(1)} \Big|_{s_{a+1, b-1}\text{-cut}} = \mathcal{F}_{\text{MHV}}^{(0)} \int d\text{LIPS}(l_1, l_2; P_{a+1, b-1}) \frac{\langle a a+1 \rangle \langle l_2 l_1 \rangle}{\langle a l_2 \rangle \langle l_2 a+1 \rangle} \frac{\langle b-1 b \rangle \langle l_1 l_2 \rangle}{\langle b-1 l_1 \rangle \langle l_1 b \rangle} , \quad (4.3.8)$$

which reproduces the result derived in [60] using component form factors and amplitudes.

It was shown in [96] that the expectation value of supersymmetric Wilson loops in momentum twistor space generates all planar amplitudes in $\mathcal{N} = 4$ SYM, and dual MHV rules in momentum twistor space were proposed in [97]. Inspired by these results, dual MHV rules directly formulated in dual momentum space were introduced in [98]. In these rules a lightlike closed polygon formed by linking the on-shell momenta of the external particles following their colour ordering plays an important role. Note that the same polygon appears in the amplitude/Wilson loop duality [9, 10, 99].

In this section we extend these rules to the calculation of form factors of the special operator considered in previous sections, namely the chiral part of the stress-tensor multiplet operator. It turns out that the rules for the amplitude have to be modified only slightly. More precisely, there are no new vertices to be introduced, and we only have to modify (super)momentum conservation of the particles in order to account for the (super)momentum injected by the operator. In the dual momentum picture, this implies the breaking of the closed null contour describing the particle's momenta.

The vertices of this open polygon in dual supermomentum space are labelled by (x_i, Θ_i) [8], with⁹

$$x_i - x_{i+1} := p_i = \lambda_i \tilde{\lambda}_i, \quad \Theta_i - \Theta_{i+1} := \lambda_i \eta_i, \quad (4.3.9)$$

with

$$x_i - x_{i+n} = \sum_{j=1}^n p_j = q, \quad \Theta_i - \Theta_{i+n} = \sum_{j=1}^n \lambda_j \eta_j = \gamma, \quad (4.3.10)$$

where q (γ) is the (super)momentum carried by the operator. Note that in the previous equation we have effectively injected the (super)momentum of the operator between on-shell states labelled by $i - 1$ and i and this is where the breaking of

⁹In order to avoid confusion with the variables θ 's introduced in earlier sections, we denote by Θ the variables living in dual super momentum space.

the polygon occurs. For each diagram an appropriate choice for the location of the breaking will have to be made. Furthermore, in this section we consider the chiral operator $\mathcal{T}(x, \theta^+)$ for which $\gamma_- = 0$, and hence $\Theta_{i;-} - \Theta_{i+n;-} = 0$. For amplitudes we have of course $q = 0$ and $\gamma = 0$ which would bring us back to a closed lightlike polygon.

In practice it is useful to convert the open polygon for form factors into a periodic configuration in dual momentum space with period q (γ) in the bosonic (fermionic) direction as in Figure 4.8. This is partially motivated by a duality observed at strong coupling in [63, 100] where form factors are related to the area of minimal surfaces ending on an infinite periodic sequence of null segments at the boundary of AdS . In [60] an attempt was made to map this geometric picture to weak coupling, in a way similar to the amplitude/Wilson loop duality [10, 99].

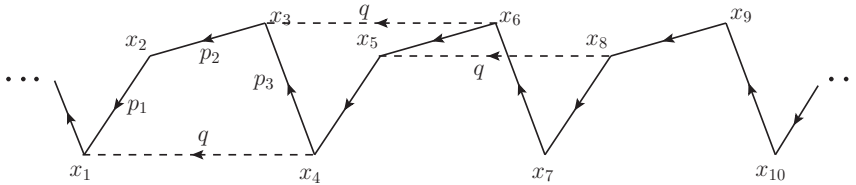


Figure 4.8: *The kinematic configuration in dual momentum space used to calculate three-point form factors using dual MHV rules.*

The emergence of a periodic configuration is also natural from a field-theoretic point of view once one takes into account that the operator insertion is a colour singlet, and hence does not interfere with the colour ordering of the external state. In other words, the (super)momentum carried by the operator can be inserted between any pair of particle momenta without spoiling the ordering. Precisely by resorting to a periodic configuration we can account for this property, as Figure 4.8 clearly shows.

One can also consider this periodic kinematic configuration in momentum twistor

space [101], as shown in Figure 4.9, with space-time points being mapped to lines in twistor space: $(x_i, \Theta_i) \sim \mathcal{Z}_{i-1} \wedge \mathcal{Z}_i$, where

$$\mathcal{Z}_i = (\lambda_i, \nu_i, \chi_i), \quad \nu_i = x_i \lambda_i = x_{i+1} \lambda_i, \quad \chi_i = \Theta_i \lambda_i = \Theta_{i+1} \lambda_i. \quad (4.3.11)$$

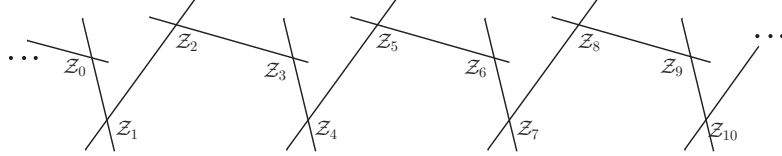


Figure 4.9: *The same kinematic configuration presented in Figure 4.8, in terms of momentum twistor space variables.*

4.3.4 Examples

In this section we want to explain the dual MHV rules by discussing a number of simple examples of tree-level and one-loop form factors. The dual MHV rules in dual momentum space for $\mathcal{N} = 4$ amplitudes are summarised for the reader's convenience in Appendix B, and we refer to [98] for full details.

The first example is that of an NMHV three-point form factor. The corresponding diagrams are shown in Figure 4.10, and are in one-to-one correspondence with three conventional MHV diagrams, depicted in Figure 4.11. Notice that the three diagrams in Figure 4.10 can be obtained by selecting the appropriate period in Figure 4.8.

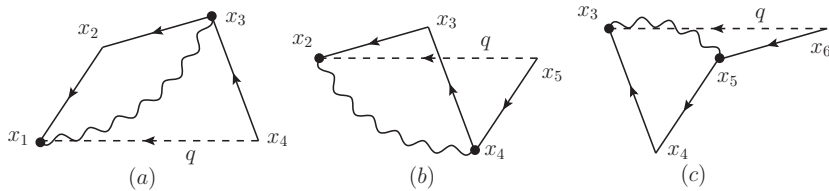


Figure 4.10: *Dual MHV diagrams for the three-point tree NMHV form factor.*

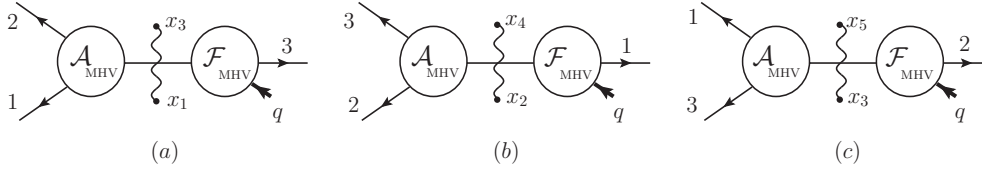


Figure 4.11: *Corresponding MHV diagrams for the three-point tree NMHV form factor.*

The extension to n -point NMHV form factors is immediate – we consider all dual MHV diagrams where one propagator connects two external vertices *within one period*. The final result is given by summing over all translationally inequivalent diagrams as

$$\mathcal{F}_{\text{NMHV}}^{(0)} = \mathcal{F}_{\text{MHV}}^{(0)} \sum_{i=1}^n \sum_{j=i+2}^{i+n-1} \frac{\langle i-1 \ i \rangle}{\langle i-1 \ \ell_{ij} \rangle \langle \ell_{ij} \ i \rangle} \frac{\langle j-1 \ j \rangle}{\langle j-1 \ \ell_{ij} \rangle \langle \ell_{ij} \ j \rangle} \frac{1}{x_{ij}^2} \int d^4 \eta_{ij} \delta^{0|8}(\ell_{ij} \eta_{ij} + \Theta_{ij}) , \quad (4.3.12)$$

where the spinor $|\ell_{ij}\rangle$ associated to the internal leg is defined as

$$|\ell_{ij}\rangle := |x_{ij}\rangle |\xi] , \quad (4.3.13)$$

and where $|\xi]$ is an arbitrary reference spinor. Notice that the particle labels of spinor variables i and $i+n$ are identified in this expression. Importantly, the fact that we are calculating a form factor rather than an amplitude – and the corresponding dependence on q and γ – is completely encoded in the periodic kinematic configuration as defined earlier. Furthermore, we observe that every diagram in the sum corresponds to a particular period (see Figures 4.10 and 4.11).

Notice that diagrams where a propagator connects two adjacent points give a vanishing result, and therefore are not included in the summation. On the other hand, diagrams where a propagator connects two points separated by exactly one period or more are non-vanishing, and have to be excluded since there is no corresponding conventional MHV diagram. For instance, among the three-point diagrams in Figure 4.10 we do not include the diagram with a propagator connecting points x_1 and x_4 .

This is an example of a more general fact: *diagrams where a single propagator connects points x_i and x_j with $|i - j| \geq n$ have to be discarded.* This applies to any loop order. The reason for this rule is that there are no corresponding supersymmetric MHV diagrams.

As an aside we mention that (4.3.12) can also be written in terms of momentum twistor variables as

$$\mathcal{F}_{\text{NMHV}}^{(0)} = \mathcal{F}_{\text{MHV}}^{(0)} \sum_{i=1}^n \sum_{j=i+2}^{i+n-1} [*, i-1, i, j-1, j], \quad (4.3.14)$$

where \mathcal{Z}_* is the reference momentum twistor, chosen as

$$\mathcal{Z}_* = (0, \xi, 0), \quad (4.3.15)$$

and $[*, i-1, i, j-1, j]$ is defined in Appendix B.

The case of one-loop MHV form factors is similar to the tree-level NMHV case. The n -point one-loop MHV form factor is given by

$$\begin{aligned} \mathcal{F}_{\text{MHV}}^{(1)} &= \mathcal{F}_{\text{MHV}}^{(0)} \int d^4 x_I d^8 \Theta_I \sum_{i=1}^n \sum_{j=i+1}^{i+n-1} \frac{\langle i-1 \ i \rangle}{\langle i-1 \ \ell_{iI} \rangle \langle \ell_{iI} \ i \rangle} \frac{\langle j-1 \ j \rangle}{\langle j-1 \ \ell_{Ij} \rangle \langle \ell_{Ij} \ j \rangle} \quad (4.3.16) \\ &\quad \frac{1}{\langle \ell_{iI} \ell_{Ij} \rangle \langle \ell_{Ij} \ell_{iI} \rangle} \frac{1}{x_{iI}^2} \int d^4 \eta_{iI} \delta^{0|8}(\ell_{iI} \eta_{iI} + \Theta_{iI}) \frac{1}{x_{Ij}^2} \int d^4 \eta_{Ij} \delta^{0|8}(\ell_{Ij} \eta_{Ij} + \Theta_{Ij}) \\ &+ \mathcal{F}_{\text{MHV}}^{(0)} \int d^4 x_I d^8 \Theta_I \sum_{i=1}^n \frac{\langle i-1 \ i \rangle}{\langle i-1 \ \ell_{iI'} \rangle \langle \ell_{iI'} \ \ell_{iI} \rangle \langle \ell_{iI} \ i \rangle} \frac{1}{\langle \ell_{iI} \ell_{i+nI} \rangle \langle \ell_{i+nI} \ell_{iI} \rangle} \\ &\quad \frac{1}{x_{iI}^2} \int d^4 \eta_{iI} \delta^{0|8}(\ell_{iI} \eta_{iI} + \Theta_{iI}) \frac{1}{x_{i+nI}^2} \int d^4 \eta_{i+nI} \delta^{0|8}(\ell_{i+nI} \eta_{i+nI} + \Theta_{i+nI}) \\ &\quad \int d^4 x_{I'} d^8 \Theta_{I'} \delta^4(x_{I'} - x_{i+nI}) \delta^{0|8}(\Theta_{I'} - \Theta_{i+nI}). \end{aligned}$$

Notice that we have treated a special class of diagrams differently, corresponding to the last three lines in (4.3.16). These are diagrams where the two propagators have momenta x_{iI} and x_{i+nI} . An example of such a diagram in the case of a three-point form factor is shown in Figure 4.12.

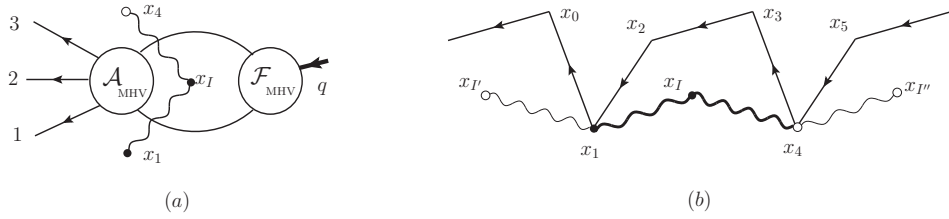


Figure 4.12: A special diagram with two propagators with momenta x_{iI} and x_{i+nI} . In the dual MHV diagram there are two propagators with momenta x_{1I} and x_{4I} , and two vertices, x_1 and x_I . Such diagrams correspond to the last three lines of (4.3.16).

The three-point dual MHV diagrams at one loop are shown in Figure 4.13. The diagrams in Figure 4.13 (g)-(i) are of the special class described earlier in Figure 4.12. Note that in the case of loop diagrams we also have to include diagrams where

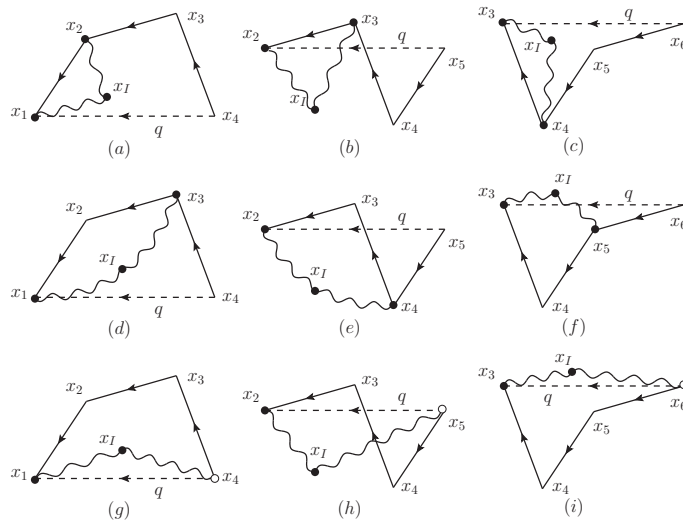


Figure 4.13: Dual MHV diagrams for the three-point MHV form factor at one loop.

two adjacent points or two points separated by exactly one period are connected by two or more propagators (see Figure 4.13 diagrams (a)-(c) and (g)-(i) respectively). We should also stress that all diagrams where two points x_i and x_j with $|i - j| > n$ are connected must be discarded. Generalisations to non-MHV form factors are straightforward.

Finally we compare the dual MHV diagrams with the periodic Wilson line diagrams studied in [60]. We can see that an identical truncation was necessary in order to obtain the correct result: in a single MHV diagram the external vertices which are connected to propagators must reside within one period, and the whole form factor is obtained by summing over all translationally inequivalent diagrams.

4.3.5 Higher-loop diagrams

At higher loops, the situation becomes more involved. To illustrate the main novelty we consider the two-point MHV form factor at two loops.¹⁰

As prototypical examples, we consider two particular diagrams, depicted in Figures 4.14 and 4.15. In the first diagram, the form factor MHV vertex is inserted in the exterior part of the diagram, whereas in the second situation it is inserted in the interior. On the right-hand side of each figure we also draw the corresponding dual MHV diagram. Let us start with the first, simpler situation. There is no subtlety in defining the internal region momenta x_I and x_J . The momenta in the propagators in the outer loop are x_{2I} , x_{3J} and x_{1J} , and it is straightforward to write down the two-loop dual MHV integrand. In the notation of Appendix B, there are two internal vertices, two external vertices at x_1 and x_2 (with x_1 being a two-point vertex) and four propagators, as shown by dark bullets and dark wavy lines in Figure 4.14 (b).

Consider now the second, more subtle situation drawn in Figure 4.15. In order to assign region momenta consistently to all regions in this diagram, we need to

¹⁰Incidentally, we recall that while at one loop it has been proved that (four-dimensional) MHV diagrams reproduce complete amplitudes [102], there is no such statement at two loops and beyond. However, MHV diagrams at two loops and beyond can be used effectively to compute unregulated integrands of amplitudes (and form factors, as demonstrated here) which have recently attracted great interest in their own right [103].

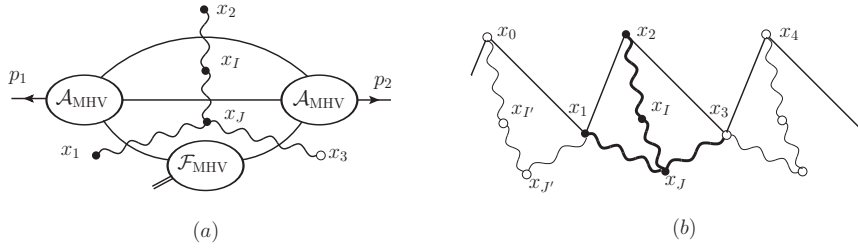


Figure 4.14: (a) First MHV diagram for a two-loop, two-point MHV form factor. (b) The corresponding dual MHV diagram.

introduce an additional loop momentum $x_{J'}$ such that $x_J - x_{J'} = q$, in exactly the same way as $x_1 - x_3 = q$. Similarly, one can also introduce $x_{I'}$ such that $x_{I'} - x_I = q$. The dual MHV diagram is shown in Figure 4.15(b).

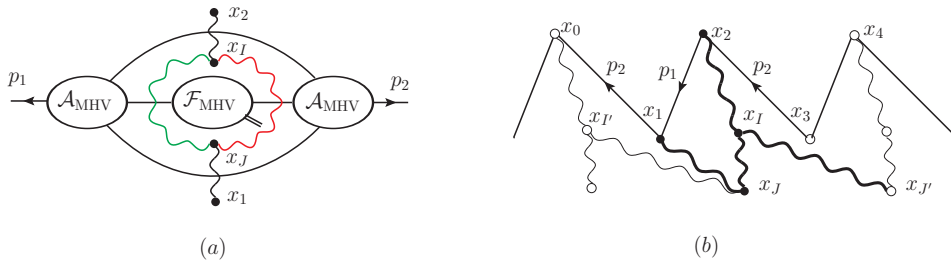


Figure 4.15: (a) Second MHV diagram for a two-loop, two-point MHV form factor. (b) The corresponding dual MHV diagram.

As before, we consider only translationally inequivalent diagrams within one period. Each such diagram will have two one-point external vertices, two three-point internal vertices and four propagators, as shown by dark bullets and dark wavy lines

in Figure 4.15(b). The expression of this dual MHV diagram is then

$$\begin{aligned}
& \int d^4 x_I d^8 \Theta_I \frac{1}{\langle \ell_{I2} \ell_{IJ} \rangle \langle \ell_{IJ} \ell_{I'J'} \rangle \langle \ell_{I'J'} \ell_{I2} \rangle} \int d^4 x_J d^8 \Theta_J \frac{1}{\langle \ell_{J1} \ell_{J'J'} \rangle \langle \ell_{J'J'} \ell_{JI} \rangle \langle \ell_{JI} \ell_{J1} \rangle} \\
& \frac{\langle 12 \rangle}{\langle 1 \ell_{2I} \rangle \langle \ell_{2I} 2 \rangle} \frac{\langle 21 \rangle}{\langle 2 \ell_{1J} \rangle \langle \ell_{1J} 1 \rangle} \\
& \frac{1}{x_{I2}^2} \int d^4 \eta_{I2} \delta^{0|8}(\ell_{I2} \eta_{I2} + \Theta_{I2}) \frac{1}{x_{J1}^2} \int d^4 \eta_{J1} \delta^{0|8}(\ell_{J1} \eta_{J1} + \Theta_{J1}) \\
& \frac{1}{x_{IJ}^2} \int d^4 \eta_{IJ} \delta^{0|8}(\ell_{IJ} \eta_{IJ} + \Theta_{IJ}) \frac{1}{x_{I'J'}^2} \int d^4 \eta_{I'J'} \delta^{0|8}(\ell_{I'J'} \eta_{I'J'} + \Theta_{I'J'}) \\
& \int d^4 x_{I'} d^8 \Theta_{I'} \delta^4(x_{I'} + x_{13}) \delta^{0|8}(\Theta_{I'} + \Theta_{13}) \int d^4 x_{J'} d^8 \Theta_{J'} \delta^4(x_{J'} - x_{13}) \delta^{0|8}(\Theta_{J'} - \Theta_{13}) .
\end{aligned} \tag{4.3.17}$$

Notice in the last line of (4.3.17) the delta functions which enforce the periodicity of the super region momenta $x_{I'}$ and $x_{J'}$. One can check that (4.3.17) is indeed equivalent to the result of the conventional MHV diagram in Figure 4.15(a).

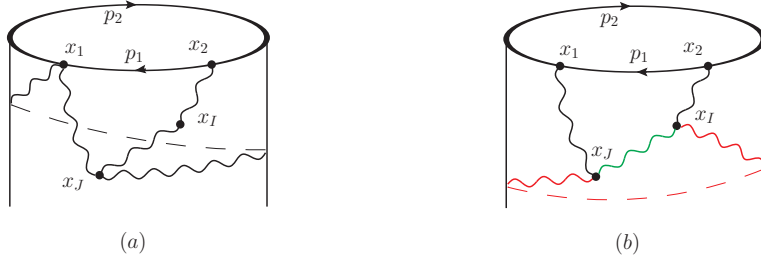


Figure 4.16: (a) Cylinder picture for the MHV diagram in Figure 4.14. (b) Cylinder picture for the MHV diagram in Figure 4.15. The period of the cylinder is q .

The dual MHV rules for form factors described above can be understood more naturally if we put the periodic configuration on a cylinder of period q , see Figure 4.16. In particular, Figure 4.16(b) corresponds to the MHV diagram in Figure 4.15. The two coloured propagators connecting x_I and x_J form a loop with winding momentum q , which exactly correspond to the coloured lines in the MHV diagram in Figure 4.15(a). We would like to stress a general feature of the rules we have described before, namely that no *single* propagator can stretch for one or more than one period around the cylinder.

The dual MHV rules can be applied to generic form factors. As in the case of amplitudes, in order to calculate an N^k MHV form factor at L loops, we need to sum over all allowed diagrams with

$$\#(\text{internal vertices}) = L , \quad \#(\text{propagators}) = k + 2L . \quad (4.3.18)$$

It would be very interesting to map the dual MHV rules described here to a dual Wilson line picture for form factors. We leave this question for future work.

Chapter 5

The Sudakov Form Factor in ABJM

This chapter summarises the results of [17] regarding the computation of the two-loop Sudakov form factor in three-dimensional $N = 6$ superconformal Chern-Simons theory via generalised unitarity. As an intermediate step, we derive the non-planar part of the one-loop four-point amplitude in terms of box integrals. Our result for the Sudakov form factor is given by a single non-planar tensor integral with uniform degree of transcendentality, and is in agreement with the known infrared divergences of two-loop amplitudes in ABJM theory. We also discuss a number of interesting properties satisfied by related three-dimensional integral functions.

5.1 The complete one-loop amplitude

5.1.1 Results

In this section we present our result for the complete four-point amplitude at one loop in ABJM. As mentioned earlier, this amplitude will be needed in order to construct the two-particle cuts of the two-loop form factor. The one-loop four-point amplitude is given by the sum of a planar and non-planar contribution¹:

$$\tilde{\mathcal{A}}^{(1)}(\bar{1}, 2, \bar{3}, 4) = \mathcal{A}_{\text{P}}^{(1)}(\bar{1}, 2, \bar{3}, 4) + \mathcal{A}_{\text{NP}}^{(1)}(\bar{1}, 2, \bar{3}, 4), \quad (5.1.1)$$

where

$$\mathcal{A}_{\text{P}}^{(1)}(\bar{1}, 2, \bar{3}, 4) = i N \mathcal{A}^{(0)}(\bar{1}, 2, \bar{3}, 4) I(1, 2, 3, 4) \left([1, 2, 3, 4] + [1, 4, 3, 2] \right), \quad (5.1.2)$$

and

$$\begin{aligned} \mathcal{A}_{\text{NP}}^{(1)}(\bar{1}, 2, \bar{3}, 4) = & -2i \mathcal{A}^{(0)}(\bar{1}, 2, \bar{3}, 4) \left[\left(I(1, 2, 3, 4) - I(4, 2, 3, 1) \right) [1, 2][3, 4] \right. \\ & \left. - \left(I(2, 3, 4, 1) - I(1, 3, 4, 2) \right) [1, 4][3, 2] \right]. \end{aligned} \quad (5.1.3)$$

Note that the double-trace structure $[1, 2]$ is

$$[1, 2] = \delta_{i_2}^{\bar{i}_1} \delta_{i_1}^{i_2}. \quad (5.1.4)$$

The complete one-loop amplitude can also be written in the following way,

$$\begin{aligned} \frac{\tilde{\mathcal{A}}^{(1)}(\bar{1}, 2, \bar{3}, 4)}{\mathcal{A}^{(0)}(\bar{1}, 2, \bar{3}, 4)} = & i \left\{ I(1, 2, 3, 4) \left[N \left([1, 2, 3, 4] + [1, 4, 3, 2] \right) - 2[1, 2][3, 4] - 2[1, 4][3, 2] \right] \right. \\ & \left. + 2 \left[I(4, 2, 3, 1)[1, 2][3, 4] - I(1, 3, 4, 2)[1, 4][3, 2] \right] \right\}. \end{aligned} \quad (5.1.5)$$

¹We work here in ABJM rather than ABJ, so there is the one gauge group rank N .

5.1.2 Symmetry properties of the one-loop amplitude

Before discussing the derivation of (5.1.1), it is instructive to prove that $\mathcal{A}_P^{(1)}$ and $\mathcal{A}_{NP}^{(1)}$ are antisymmetric under the swap $\bar{1} \leftrightarrow \bar{3}$. In order to show this one needs to use (3.3.43) and the following relations satisfied by the one-loop box (3.3.19):

$$I(a, b, c, d) = -I(b, c, d, a) , \quad I(a, b, c, d) = -I(c, b, a, d) . \quad (5.1.6)$$

These relations state that by cyclically shifting the labels of the external legs of the box function 3.3.19 by one unit one picks a minus sign; and similarly if one swaps two non-adjacent legs. Both relations are straightforward to prove using the definition 3.3.19 of the box function. One then finds,

$$\begin{aligned} I(3, 2, 1, 4) - I(4, 2, 1, 3) &= I(2, 3, 4, 1) - I(1, 3, 4, 2) , \\ I(2, 1, 4, 3) - I(3, 1, 4, 2) &= I(1, 2, 3, 4) - I(4, 2, 3, 1) . \end{aligned} \quad (5.1.7)$$

Using (5.1.7) we get

$$\begin{aligned} \mathcal{A}_P^{(1)}(\bar{1}, 2, \bar{3}, 4) &= -\mathcal{A}_P^{(1)}(\bar{3}, 2, \bar{1}, 4) , \\ \mathcal{A}_{NP}^{(1)}(\bar{1}, 2, \bar{3}, 4) &= -\mathcal{A}_{NP}^{(1)}(\bar{3}, 2, \bar{1}, 4) . \end{aligned} \quad (5.1.8)$$

Notice the presence of a minus sign between the two non-planar colour structure $[1, 2][3, 4]$ and $[1, 4][3, 2]$ appearing in the non-planar one-loop amplitude (5.1.3).

5.1.3 Derivation of the complete one-loop amplitude from cuts

We now briefly outline the strategy for the derivation of the complete one-loop amplitude (5.1.1), which is very similar to that in $\mathcal{N} = 4$ SYM, see for example [104]. We consider the two-particle cuts of the complete one-loop amplitude, which are obtained

by merging two tree-level amplitudes summed over all possible colour structures and internal particle species. We will see that each cut can be re-expressed in terms of cuts of sums of box functions. The sum over internal species is (partially) performed via an integration over the Grassmann variables η_{ℓ_1} and η_{ℓ_2} associated to the cut momenta. If one of the particles crossing is bosonic and the other is fermionic we also have to add to this the same expression with $\ell_1 \leftrightarrow \ell_2$ – this is necessary only for the s - and t -cuts. For instance, the s -cut integrand of the one-loop amplitude is²

$$\tilde{\mathcal{A}}^{(1)}(\bar{1}, 2, \bar{3}, 4)|_{s\text{-cut}} = \frac{1}{2} \int d^3\eta_{\ell_1} d^3\eta_{\ell_2} \tilde{\mathcal{A}}^{(0)}(\bar{1}, 2, -\bar{\ell}_2, -\ell_1) \times \tilde{\mathcal{A}}^{(0)}(\bar{3}, 4, \bar{\ell}_1, \ell_2) + \ell_1 \leftrightarrow \ell_2. \quad (5.1.9)$$

The one-loop amplitude has cuts in the s -, t - and u -channels, for which we find the following integrands:

$$\begin{aligned} \tilde{\mathcal{A}}^{(1)}(\bar{1}, 2, \bar{3}, 4)|_{s\text{-cut}} &= \frac{i}{2} \mathcal{A}^{(0)}(\bar{1}, 2, \bar{3}, 4) c_s \mathcal{S}_{12} I(1, 2, 3, 4)|_{s\text{-cut}}, \quad (5.1.10) \\ \tilde{\mathcal{A}}^{(1)}(\bar{1}, 2, \bar{3}, 4)|_{t\text{-cut}} &= \frac{i}{2} \mathcal{A}^{(0)}(\bar{1}, 2, \bar{3}, 4) c_t \mathcal{S}_{23} I(1, 2, 3, 4)|_{t\text{-cut}}, \\ \tilde{\mathcal{A}}^{(1)}(\bar{1}, 2, \bar{3}, 4)|_{u\text{-cut}} &= \frac{i}{2} \mathcal{A}^{(0)}(\bar{1}, 2, \bar{3}, 4) c_u \mathcal{S}_{13} I(3, 1, 2, 4)|_{u\text{-cut}}, \end{aligned}$$

where the colour factors c_s , c_t , c_u are

$$\begin{aligned} c_s &= N[1, 2, 3, 4] + N[1, 4, 3, 2] - 2[1, 2][3, 4], \\ c_t &= N[1, 2, 3, 4] + N[1, 4, 3, 2] - 2[1, 4][3, 2], \\ c_u &= 2[1, 2][3, 4] - 2[1, 4][3, 2], \end{aligned} \quad (5.1.11)$$

and we recall that by $\mathcal{A}^{(0)}(\bar{1}, 2, \bar{3}, 4)$ we denote the colour-ordered four-point amplitude. Furthermore, we indicate by $\mathcal{S}_{ab} I(a, b, c, d)|_{s_{ab}\text{-cut}}$, the s_{ab} -cut of the one-loop box function $I(a, b, c, d)$ in (3.3.19), symmetrised in the cut loop momenta ℓ_1 and ℓ_2 ,

²For convenience we include here a factor of $\frac{1}{2}$ in the definition of the (symmetrised) cuts. In practice it means that we take the average of the two contributions in the s - and t -cuts, and multiply the u -cut with a symmetry factor as two identical (super)particles cross the cut.

which are defined such that $\ell_1 + \ell_2 = p_a + p_b$,

$$\begin{aligned}
\mathcal{S}_{12}I(1, 2, 3, 4)|_{s\text{-cut}} &= \frac{s\text{Tr}(\ell_1 p_1 p_4)}{(\ell_1 - p_1)^2(\ell_1 + p_4)^2} + \ell_1 \leftrightarrow \ell_2, \\
\mathcal{S}_{23}I(1, 2, 3, 4)|_{t\text{-cut}} &= \frac{(-t)\text{Tr}(\ell_1 p_1 p_2)}{(\ell_1 - p_1)^2(\ell_1 + p_2)^2} + \ell_1 \leftrightarrow \ell_2, \\
\mathcal{S}_{13}I(3, 1, 2, 4)|_{u\text{-cut}} &= \frac{u\text{Tr}(\ell_2 p_3 p_4)}{(\ell_2 - p_3)^2(\ell_2 + p_4)^2} + \ell_1 \leftrightarrow \ell_2.
\end{aligned} \tag{5.1.12}$$

We should stress here that despite the simplified notation the cut momenta ℓ_1 and ℓ_2 are different for the three distinct channels under considerations. For instance, $\ell_1 + \ell_2 = p_1 + p_2$ for the s -cut, while $\ell_1 + \ell_2 = p_2 + p_3$ in the t -cut and $\ell_1 + \ell_2 = p_1 + p_3$ in the u -cut. Recall that the symmetrisation in the cut momenta in the s - and t -channel coefficients originates from summing over all possible particle species that can propagate on the cut legs, while in the u cut there is a single configuration allowed, and the result turns out to be automatically symmetric in ℓ_1 and ℓ_2 .

Next we merge the cuts into box functions. For the planar structures $[1, 2, 3, 4]$ and $[1, 4, 3, 2]$ this is immediate as the only function consistent with the s - and t -cuts in 5.1.10 and vanishing u -cut is $I(1, 2, 3, 4)$. Hence, the corresponding planar amplitude is

$$i\mathcal{A}^{(0)}(\bar{1}, 2, \bar{3}, 4) N([1, 2, 3, 4] + [1, 4, 3, 2]) I(1, 2, 3, 4), \tag{5.1.13}$$

thus arriving at the expression 5.1.2 for the planar part of the full one-loop amplitude.³ For the non-planar terms $[1, 2][3, 4]$ and $[1, 4][3, 2]$ we need to use the results of Appendix B.3.2 and in particular B.3.13, which we reproduce here,

$$\mathcal{S}_{ab}I(a, b, c, d)|_{s_{ab}\text{-cut}} = \mathcal{S}_{ab}I(a, b, d, c)|_{s_{ab}\text{-cut}}. \tag{5.1.14}$$

Firstly, we note that an immediate consequence of this result is that

$$\mathcal{S}_{23}I(2, 3, 4, 1)|_{t\text{-cut}} - \mathcal{S}_{23}I(2, 3, 1, 4)|_{t\text{-cut}} = 0, \tag{5.1.15}$$

³Note that at the level of the integral we can simply replace $\mathcal{S}_{12}I(1, 2, 3, 4)$ by $2I(1, 2, 3, 4)$.

in other words the combination $I(2, 3, 4, 1) - I(2, 3, 1, 4)$, symmetrised in the loop momenta ℓ_1 and ℓ_2 , with $\ell_1 + \ell_2 = p_2 + p_3$, has a vanishing t -channel cut as expected for the coefficient of the $[1, 2][3, 4]$ colour structure (see 5.1.11). For the same combination we find, using $I(2, 3, 4, 1) = -I(1, 2, 3, 4)$, the symmetrised s -cut as

$$-\mathcal{S}_{12}I(1, 2, 3, 4)|_{s\text{-cut}}, \quad (5.1.16)$$

and similarly, for the symmetrised u -cut we obtain

$$\mathcal{S}_{13}I(3, 1, 4, 2)|_{u\text{-cut}} = \mathcal{S}_{13}I(3, 1, 2, 4)|_{u\text{-cut}}, \quad (5.1.17)$$

where we have used $I(2, 3, 1, 4) = -I(3, 1, 4, 2)$ and B.3.13, which allows us to swap the last two legs on the symmetrised u -cut. Comparing with 5.1.10 and 5.1.11 we can uniquely fix the coefficient of the non-planar structure $[1, 2][3, 4]$:

$$2i\mathcal{A}^{(0)}(\bar{1}, 2, \bar{3}, 4) [1, 2][3, 4] \left[I(2, 3, 4, 1) - I(2, 3, 1, 4) \right], \quad (5.1.18)$$

or, using the first relation of 5.1.6,

$$-2i\mathcal{A}^{(0)}(\bar{1}, 2, \bar{3}, 4) [1, 2][3, 4] \left[I(1, 2, 3, 4) - I(4, 2, 3, 1) \right]. \quad (5.1.19)$$

One can proceed similarly for the coefficient of the other non-planar structure $[1, 4][3, 2]$, arriving at the result quoted earlier in 5.1.3. Note that in that result we use the freedom to rename loop momenta in order to eliminate the various symmetrisations introduced by the operation \mathcal{S}_{ab} above.

5.2 The Sudakov form factor at one and two loops

We now move on to the form factors of gauge-invariant, single-trace scalar operators

$$\mathcal{O} = \text{Tr} \left(\phi^{A_1} \bar{\phi}_{B_1} \phi^{A_2} \bar{\phi}_{B_2} \dots \phi^{A_L} \bar{\phi}_{B_L} \right) \chi_{A_1 \dots A_L}^{B_1 \dots B_L}, \quad (5.2.1)$$

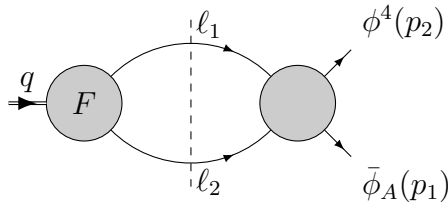


Figure 5.1: *The q^2 cut of the Sudakov form factor. Note that the amplitude on the right-hand side of the cut is summed over all possible colour orderings.*

where I and J are indices of the $\mathbf{4}$ and $\bar{\mathbf{4}}$ representation of the R -symmetry group $SU(4)$. The operators 5.2.1 are half BPS if χ is a symmetric traceless tensor in all the A_i and B_i indices separately (see for example [68, 105]). For $L = 2$, the relevant operator is

$$\mathcal{O}^A_B = \text{Tr} \left(\phi^A \bar{\phi}_B - \frac{\delta^A_B}{4} \phi^K \bar{\phi}_K \right). \quad (5.2.2)$$

In the rest of this chapter we will focus on the Sudakov form factor

$$\langle (\bar{\phi}_4)_{i_1}^{\bar{i}_1}(p_1) (\phi^A)_{i_2}^{i_2}(p_2) | \text{Tr}(\bar{\phi}_4 \phi^A)(0) | 0 \rangle := [1, 2] F(q^2), \quad (5.2.3)$$

where $q := p_1 + p_2$ and $A \neq 4$, and we recall that $[1, 2] := \delta_{i_2}^{\bar{i}_1} \delta_{i_1}^{i_2}$. At tree level,

$$F^{(0)}(q^2) = 1. \quad (5.2.4)$$

We will now derive this quantity at one and two loops.

5.2.1 One-loop form factor in ABJM

At one loop it is possible to determine the integrand of the form factor from a single unitarity cut in the q^2 channel. As shown in Figure 5.1, on one side of the cut there is the Sudakov form factor and on the other side the complete four-point amplitude, both at tree level. The colour-ordered tree amplitude is given in 3.3.17. Let us work out the colour factor first. It is given by

$$\delta_{i_1}^{\bar{i}_2} \delta_{i_2}^{i_1} (\delta_{i_2}^{\bar{i}_1} \delta_{i_1}^{i_2} \delta_{i_2}^{\bar{i}_1} \delta_{i_1}^{i_2} - \delta_{i_2}^{\bar{i}_1} \delta_{i_1}^{i_2} \delta_{i_2}^{\bar{i}_1} \delta_{i_1}^{i_2}) = (N' - N) \delta_{i_2}^{\bar{i}_1} \delta_{i_1}^{i_2}. \quad (5.2.5)$$

Obviously, the one-loop form factor vanishes identically in ABJM theory, because in this case $N' = N$.

We now consider the kinematic part. Since the operator is built solely out of scalars, only the four-point scalar amplitude can appear in the cut. To match the particles of the tree amplitude in Figure 5.1, we pick the $(\eta_1)^1(\eta_{\ell_1})^3(\eta_{\ell_2})^2(\eta_2)^0$ component from the $\delta^{(6)}(Q)$ to write the q^2 cut of the one-loop form factor as:

$$\frac{\delta^{(6)}(Q)|_{(\eta_1)^1(\eta_{\ell_1})^3(\eta_{\ell_2})^2(\eta_2)^0}}{\langle 1 2 \rangle \langle 2 \ell_1 \rangle} = \frac{\langle \ell_1 \ell_2 \rangle^2 \langle 1 \ell_1 \rangle}{\langle 1 2 \rangle \langle 2 \ell_1 \rangle} = \frac{\langle 1 2 \rangle \langle 1 \ell_1 \rangle}{\langle 2 \ell_1 \rangle} = -\frac{\text{Tr}(\ell_1 p_1 p_2)}{2(\ell_1 \cdot p_2)}, \quad (5.2.6)$$

which can be immediately lifted to a full integral as it is the only possible cut of the form factor. Thus we get,

$$F^{(1)}(q^2) = (N' - N) \int \frac{d^D \ell_1}{i\pi^{D/2} \ell_1^2 (\ell_1 - p_2)^2 (\ell_1 - p_1 - p_2)^2} \text{Tr}(\ell_1 p_1 p_2). \quad (5.2.7)$$

The integral in 5.2.7 is a linear triangle and is of $\mathcal{O}(\epsilon)$. Hence, we conclude that the one-loop Sudakov form factor in ABJ theory vanishes in strictly three dimensions. Moreover, the three-dimensional integrand vanishes in ABJM theory but is non-vanishing for $N \neq N'$ and can (and does) participate in unitarity cuts at two loops. Note, that the vanishing of the one-loop form factors in ABJ(M) is consistent with the infrared finiteness of one-loop amplitudes in ABJ(M).

5.2.2 Two-loop form factor in ABJM

Next, we come to the computation of the two-loop Sudakov form factor. In order to construct an ansatz for its integrand we will make use of two-particle cuts, and fix potential remaining ambiguities with various three-particle cuts described in detail in Section 5.2.2.

Three-particle cuts are very useful because they receive contributions from planar as well as non-planar integral functions at the same time, and thus are particularly

constraining. A special feature of ABJM theory is that all amplitudes with an odd number of external particles vanish and, as a consequence, all cuts involving such amplitudes are identically zero [106]. In our case this observation will be important for triple cuts, where three- and five-particle amplitudes would appear.

A particular type of such cuts, first considered in [106] in the context of loop amplitudes in ABJM, involves three adjacent cut loop momenta meeting at a three-point vertex. The vanishing of these cuts imposes strong constraints on the form of the loop integrands. We will discuss and exploit this later in this section, where we will also make the intriguing observation that integral functions with numerators satisfying such constraints are transcendental.

Two-particle cuts

We begin by considering the cut shown in Figure 5.2, which contains a tree-level Sudakov form factor merged with the integrand of the complete one-loop, four-point amplitude. The internal particle assignment is fixed and is determined by the particular operator we consider. The integrand of this cut is given by, schematically,

$$\int d^3\eta_{\ell_1} d^3\eta_{\ell_2} F^{(0)}(\bar{\ell}_2, \ell_1)[\ell_2, \ell_1] \tilde{\mathcal{A}}^{(1)}(\bar{1}, 2, -\bar{\ell}_1, -\ell_2) , \quad (5.2.8)$$

where $\tilde{\mathcal{A}}^{(1)}$ is the complete one-loop amplitude, given in 5.1.1, and we recall that the colour factor $[a, b]$ is defined in 5.1.4.

We begin by working out the colour structures that will appear in the result. Firstly we consider the planar amplitude 5.1.2 and combine it with the part of the non-planar amplitude 5.1.3 containing $I(1, 2, -\ell_1, -\ell_2)$. Intriguingly, by contracting this with the tree-level form factor (given in 5.2.3 and 5.2.4) we obtain a vanishing result:

$$\left(N([1, 2, \ell_1, \ell_2] + [1, \ell_2, \ell_1, 2]) - 2[1, 2][\ell_1, \ell_2] \right) [\ell_2, \ell_1] = 0 . \quad (5.2.9)$$

We now consider the remaining contributions arising from the non-planar one-loop amplitude 5.1.3. There are two possible colour contractions to consider,

$$c_{\text{NP}}^{(1)} := 2 [1, 2][\ell_1, \ell_2][\ell_2, \ell_1] = 2 N^2 [1, 2] , \quad (5.2.10)$$

and

$$c_{\text{NP}}^{(2)} := 2 [\ell_1, 2][1, \ell_2][\ell_2, \ell_1] = 2 [1, 2] . \quad (5.2.11)$$

Note that 5.2.11 is subleading in the large N limit, and can be discarded in the large- N limit. Moreover, the corresponding coefficient actually vanishes which implies that the two-loop form factor does not have non-planar corrections.

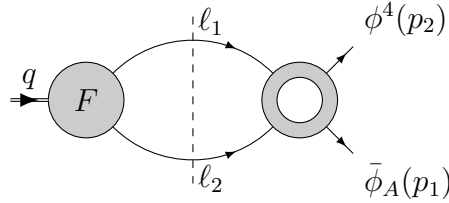


Figure 5.2: *Tree-level form factor glued to the complete one-loop amplitude.*

We now need to determine the coefficient of $c_{\text{NP}}^{(1)}$. On the two-particle cut $\ell_1^2 = \ell_2^2 = 0$ its integrand is given by the appropriate component tree-level amplitude 5.2.6 times a particular box integral 5.1.3:

$$\mathcal{C}_1^{(\text{NP})}|_{s\text{-cut}} := \frac{1}{2} \frac{\langle 12 \rangle \langle 1\ell_1 \rangle}{\langle 2\ell_1 \rangle} I(-\ell_2, 2, -\ell_1, 1) + \ell_1 \leftrightarrow \ell_2 . \quad (5.2.12)$$

Recall that we have to symmetrise in order to include all particle species in the sum over intermediate on-shell states. Since $I(-\ell_2, 2, -\ell_1, 1)$ is antisymmetric under

$\ell_1 \leftrightarrow \ell_2$ the complete cut-integrand can be written as⁴

$$\begin{aligned} \mathcal{C}_1^{(\text{NP})}|_{s\text{-cut}} &:= \frac{1}{2} \left(\frac{\langle 12 \rangle \langle 1\ell_1 \rangle}{\langle 2\ell_1 \rangle} - \frac{\langle 12 \rangle \langle 1\ell_2 \rangle}{\langle 2\ell_2 \rangle} \right) I(-\ell_2, 2, -\ell_1, 1) \\ &= -\frac{1}{2} \int \frac{d^D \ell_3}{i\pi^{D/2}} \frac{q^2 (\text{Tr}(p_1 p_2 \ell_1 \ell_3) - q^2 \ell_3^2)}{\ell_3^2 (\ell_1 - \ell_3)^2 (p_1 - \ell_3)^2 (\ell_3 - \ell_1 + p_2)^2} . \end{aligned} \quad (5.2.13)$$

Summarising, two-particle cuts indicate that the two-loop form factor is expressed in terms of a single crossed triangle with a particular numerator, represented in Figure 5.3,

$$\mathbf{XT}(q^2) = q^2 \int \frac{d^D \ell_1 d^D \ell_3}{(i\pi^{D/2})^2} \frac{\text{Tr}(p_1 p_2 \ell_1 \ell_3) - q^2 \ell_3^2}{\ell_1^2 \ell_2^2 \ell_3^2 (\ell_1 - \ell_3)^2 (p_1 - \ell_3)^2 (\ell_3 - \ell_1 + p_2)^2} , \quad (5.2.14)$$

so that

$$\mathcal{C}_1^{(\text{NP})} = -\frac{1}{2} \mathbf{XT}(q^2) . \quad (5.2.15)$$

For future convenience we will define

$$\mathbf{xt} := \frac{q^2 \left[\text{Tr}(p_1 p_2 \ell_1 \ell_3) - q^2 \ell_3^2 \right]}{\ell_1^2 \ell_2^2 \ell_3^2 (\ell_1 - \ell_3)^2 (p_1 - \ell_3)^2 (\ell_3 - \ell_1 + p_2)^2} . \quad (5.2.16)$$

The result of the evaluation of $\mathbf{XT}(q^2)$ is quoted in (5.2.25) and shows that this quantity has maximal degree of transcendentality. Before evaluating $\mathbf{XT}(q^2)$, we use triple cuts in order to confirm the correctness of the ansatz obtained from two-particle cuts.

⁴Similarly as done earlier for the complete one-loop amplitude, we include a factor of 1/2 in the symmetrisation.

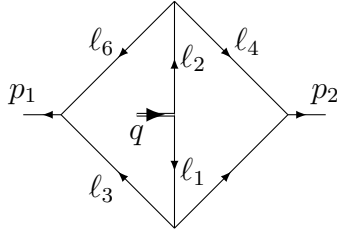


Figure 5.3: *The crossed triangle integral arising from gluing a tree form factor with the complete one-loop four-point amplitude. The cross in the middle represents the momentum $q = p_1 + p_2$. We call these integrals “crossed triangles” because they have the topology of the master integral (A.3.8). Note however that the latter integral is non-transcendental, while the particular numerator in (5.2.14) makes this integral transcendental.*

Three-vertex cuts

To confirm the uplift of the two-particle cut to the integral (5.2.14), we will study additional cuts. We begin by considering three-point vertex cuts involving three adjacent legs meeting at a three-point vertex. These cuts were first examined in [106], where it was observed that they must vanish since there are no three-particle amplitudes in ABJM theory. Calling k_1 , k_2 and k_3 the momenta meeting at the vertex, we have

$$k_1 + k_2 + k_3 = 0, \quad k_1^2 = k_2^2 = k_3^2 = 0. \quad (5.2.17)$$

The conditions (5.2.17) imply that all spinors associated to these momenta are proportional, thus

$$\langle k_1 k_2 \rangle = \langle k_2 k_3 \rangle = \langle k_3 k_1 \rangle = 0. \quad (5.2.18)$$

In our case, consider for instance the three-point vertex cut with momenta ℓ_2 , ℓ_4 and $\ell_6 := \ell_2 - \ell_4$ (see Figure 5.3 for the labelling of the momenta). Importantly, the form factor is expected to vanish as the three momenta belonging to a three-point vertex

become null. By rewriting the numerator of (5.2.14) using only cut momenta, it is immediately seen that it vanishes, since

$$\begin{aligned} \text{Tr}[p_1 p_2 (p_1 - \ell_2)(p_1 - \ell_6)] - q^2 (p_1 - \ell_6)^2 &= -\text{Tr}[p_1 p_2 (p_1 - \ell_2) \ell_6] - q^2 (p_1 - \ell_6)^2 \\ &= -\text{Tr}(p_1 p_2 p_1 \ell_6) + 4(p_1 \cdot p_2)(p_1 \cdot \ell_6) = 0, \end{aligned} \quad (5.2.19)$$

where we have used $\langle \ell_2 \ell_6 \rangle = 0$ to set $\text{Tr}(p_1 p_2 \ell_2 \ell_6) = 0$. It is easy to see that all other three-vertex cuts of the integral (5.2.14) vanish in a similar fashion because of the particular form of its numerator.

Important consequences of these specific properties of the numerator of the integral function (5.2.14) are that the result is transcendental as we will show below and is free of unphysical infrared divergences related to internal three-point vertices. These divergences appear in three-dimensional integrals with internal three-vertices even if the external kinematics is massive (unlike in four dimensions) and it appears that master integrals with appropriate numerators to cancel these peculiar infrared divergences are a preferred basis for amplitudes and form factors in ABJM. Related discussions in the context of ABJM amplitudes have appeared in [106, 107]. Note that for form factors we do not have dual conformal symmetry for the integral functions.

Three-particle cuts

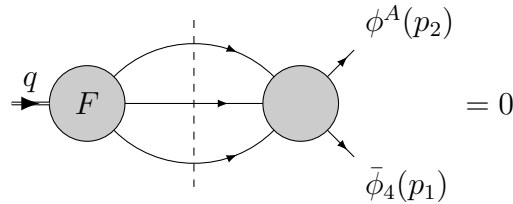


Figure 5.4: *The (vanishing) three-particle cut of the two-loop Sudakov form factor.*

The remaining cut we will study is a triple cut, illustrated in Figure 5.4. These cuts may potentially detect additional integral functions which have no two-particle cuts, and are thus very important. Moreover, such cuts are sensitive to both planar and non-planar topologies. In this triple cut, a tree-level amplitude is connected to a tree-level form factor by three cut propagators. Due to the vanishing of amplitudes with an odd number of external legs in the ABJM theory, the triple cut in question vanishes. We will now check that the triple cut of the two-loop crossed triangle \mathbf{XT} of (5.2.14), which we have detected using two-particle cuts, is indeed equal to zero.

To this end, we note that there are two possible ways to triple-cut \mathbf{T} , shown in Figures 5.2.2. The cut loop momenta are called ℓ_2 , ℓ_5 and ℓ_3 and satisfy

$$\ell_2 + \ell_5 + \ell_3 = p_1 + p_2, \quad \ell_2^2 = \ell_5^2 = \ell_3^2 = 0. \quad (5.2.20)$$

We observe that these two cuts cannot be converted into one another by a simple relabelling of the cut momenta because of the the presence of non-trivial numerators. The A-cut of the non-planar integrand is:

$$\mathbf{XT}|_{3\text{-p cut A}} = -q^2 \frac{\langle 1 2 \rangle}{\langle \ell_3 \ell_5 \rangle \langle \ell_5 2 \rangle \langle 1 \ell_3 \rangle}. \quad (5.2.21)$$

After a similar calculation, the B-cut turns out to be identical to the A-cut:

$$\mathbf{XT}|_{3\text{-p cut B}} = \mathbf{XT}|_{3\text{-p cut A}} = -q^2 \frac{\langle 1 2 \rangle}{\langle \ell_3 \ell_5 \rangle \langle \ell_5 2 \rangle \langle 1 \ell_3 \rangle}. \quad (5.2.22)$$

A quick way to establish the vanishing of the triple cuts consists in symmetrising in the particle momenta p_1 and p_2 , which is allowed since the Sudakov form factor is a function of q^2 . This symmetrisation gives

$$-\frac{q^2 \langle 1 2 \rangle}{\langle \ell_3 \ell_5 \rangle} \left[\frac{1}{\langle \ell_5 2 \rangle \langle 1 \ell_3 \rangle} - \frac{1}{\langle \ell_5 1 \rangle \langle 2 \ell_3 \rangle} \right] = -\frac{q^4}{\langle 1 | \ell_5 | 2 \rangle \langle 1 | \ell_3 | 2 \rangle}. \quad (5.2.23)$$

This expression is symmetric in ℓ_5 and ℓ_3 . In evaluating the triple cut one has to introduce a jacobian proportional to $\epsilon(\ell_2, \ell_3, \ell_5)$ [106] which effectively makes this triple cut vanish upon integration.

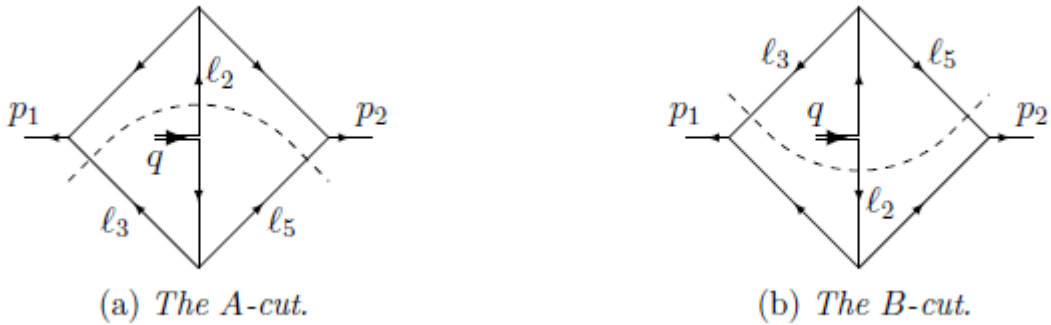


Figure 5.5: *The two triple cuts of the crossed triangle, with $\ell_2 + \ell_3 + \ell_5 = q$. In the second figure we have relabelled the loop momenta in order to merge the two contributions.*

Results and comparison to the two-loop amplitudes

Combining the information from the unitarity cuts discussed above, we conclude that the two-loop Sudakov form factor in ABJM is given by a single non-planar integral, as

$$F_{\text{ABJM}}(q^2) = -2 \left(\frac{N}{k} \right)^2 \left(-\frac{1}{2} \right) \mathbf{XT}(q^2), \quad (5.2.24)$$

where $\mathbf{XT}(q^2)$ is defined in (5.2.14) and we have reintroduced the dependence on the Chern-Simons level k . The integral $\mathbf{XT}(q^2)$ can be computed by reduction to master integrals using integration by parts identities. The details of the reductions are provided in Appendix A. The expansion of the result in the dimensional regularisation parameter ϵ can then be found using the expressions for the the master integrals (A.3.5)–(A.3.8). Plugging these masters into the reduction (A.3.9), we arrive at

$$\mathbf{XT}(q^2) = \left(\frac{-q^2 e^{\gamma_E}}{\mu^2} \right)^{-2\epsilon} \left[\frac{\pi}{\epsilon^2} + \frac{2\pi \log 2}{\epsilon} - 4\pi \log^2 2 - \frac{2\pi^3}{3} + \mathcal{O}(\epsilon) \right], \quad (5.2.25)$$

where γ_E is the Euler-Mascheroni constant. One comment is in order here. We have derived (5.2.25) in a normalisation where the the loop integration measure is written as $d^D l / (i\pi^{D/2})$. This should be converted to the standard one $d^D l / (2\pi)^D$. At two

loops, this implies that (5.2.25) has to be multiplied by a factor of $-1/(4\pi)^D$. The result in the standard normalisation is then

$$\mathcal{F}_{\text{ABJM}}(q^2) = -\frac{1}{(4\pi)^3} \left(\frac{N}{k}\right)^2 \left(\frac{-q^2 e^{\gamma_E}}{4\pi\mu^2}\right)^{-2\epsilon} \left[\frac{\pi}{\epsilon^2} + \frac{2\pi \log 2}{\epsilon} - 4\pi \log^2 2 - \frac{2\pi^3}{3} + \mathcal{O}(\epsilon) \right], \quad (5.2.26)$$

We note that $\mathcal{F}(q^2)$ can be expressed more compactly by introducing a new scale

$$\mu'^2 := 8\pi e^{-\gamma_E} \mu^2, \quad (5.2.27)$$

in terms of which we get

$$\mathcal{F}_{\text{ABJM}}(q^2) = \frac{1}{64\pi^2} \left(\frac{N}{k}\right)^2 \left(\frac{-q^2}{\mu'^2}\right)^{-2\epsilon} \left[-\frac{1}{\epsilon^2} + 6 \log^2 2 + \frac{2\pi^2}{3} \right] + \mathcal{O}(\epsilon), \quad (5.2.28)$$

which is our final result.

We now discuss two consistency checks that confirm the correctness of (5.2.28). Firstly, we recall that the Sudakov form factor captures the infrared divergences of scattering amplitudes. We now check that (5.2.28) matches the infrared poles of the four-point amplitude evaluated in [74, 108]. Here we quote its expression as given in [108]:

$$\mathcal{A}_4^{(2)} = -\frac{1}{16\pi^2} \mathcal{A}_4^{(0)} \left[\frac{(-s/\mu'^2)^{-2\epsilon}}{4\epsilon^2} + \frac{(-t/\mu'^2)^{-2\epsilon}}{4\epsilon^2} - \frac{1}{2} \log^2 \left(\frac{-s}{-t} \right) - 4\zeta_2 - 3 \log^2 2 \right], \quad (5.2.29)$$

where μ' is related to μ in the same way as in (5.2.27). Hence, the Sudakov form factor (5.2.28) is in perfect agreement with the form of the infrared divergences of (5.2.29). Secondly, we have also checked that the expansion of our result in terms of master integrals (i.e. the expansion of the two-loop non-planar triangle **XT** defined in (5.2.14)) is identical to that obtained from the Feynman diagram based result of [109]. This implies that the cut-based calculation of this presented here and the Feynman diagram calculation of [109] agree to all orders in ϵ – even if we have been using cuts in strictly three dimensions.

5.3 Maximally transcendental integrals in 3d

As discussed in section 5.2.2, the integrand \mathbf{xT} that appears in the Sudakov form factor in ABJM has a particular numerator such that all the cuts which isolate a three-point vertex vanish. We have observed in this example that this property ensures that the integral \mathbf{XT} has a uniform (and maximal) degree of transcendentality – failure to obey the triple-cut condition, for instance by altering the form of the numerator, would result in the appearance of new terms with lower degree of transcendentality. In this section we present further integrals that vanish in these three-particle cuts and have maximal degree of transcendentality. These integrals are expected to appear in the form factor of ABJ theory where cancellations between colour factors such as that in (5.2.9), do not occur.

We begin by considering the following planar integral function:

$$\begin{aligned} \mathbf{LT}(q^2) &= \int \frac{d^D \ell_1 d^D \ell_3}{(i\pi^{D/2})^2} \frac{-q^2 [\text{Tr}(p_1 \ell_3 p_2 \ell_1) - (\ell_1 - p_1)^2 (\ell_3 - p_2)^2]}{\ell_1^2 (p_1 + p_2 - \ell_1)^2 \ell_3^2 (p_1 + p_2 - \ell_3)^2 (\ell_1 - \ell_3)^2 (\ell_3 - p_2)^2} \quad (5.3.1) \\ &= \left(\frac{-q^2 e^{\gamma_E}}{\mu^2} \right)^{-2\epsilon} \left[-\frac{\pi}{4\epsilon^2} - \frac{\pi \log 2}{\epsilon} + 2\pi \log^2 2 - \frac{5\pi^3}{8} + \mathcal{O}(\epsilon) \right], \end{aligned}$$

which is shown in Figure 5.3(a).

It is easy to see that the three vertex cut $\{\ell_1, \ell_3, \ell_5\}$ vanishes, since on this cut the numerator can be placed in the form

$$\langle \ell_1 1 \rangle \langle \ell_3 2 \rangle \langle 1 2 \rangle \langle \ell_3 \ell_1 \rangle, \quad (5.3.2)$$

after using a Schouten identity. (5.3.2) vanishes because $\langle \ell_3 \ell_1 \rangle = 0$ on this cut.

A further property of (5.3.1) emerges when we consider particular triple cuts involving two adjacent massless legs, which in three dimensions are associated with soft gluon exchange [106]. With reference to Figure 5.3(a), we cut the three momenta ℓ_3 , ℓ_6 and ℓ_4 . The cut conditions $\ell_3^2 = \ell_6^2 = \ell_4^2 = 0$ together with the masslessness of

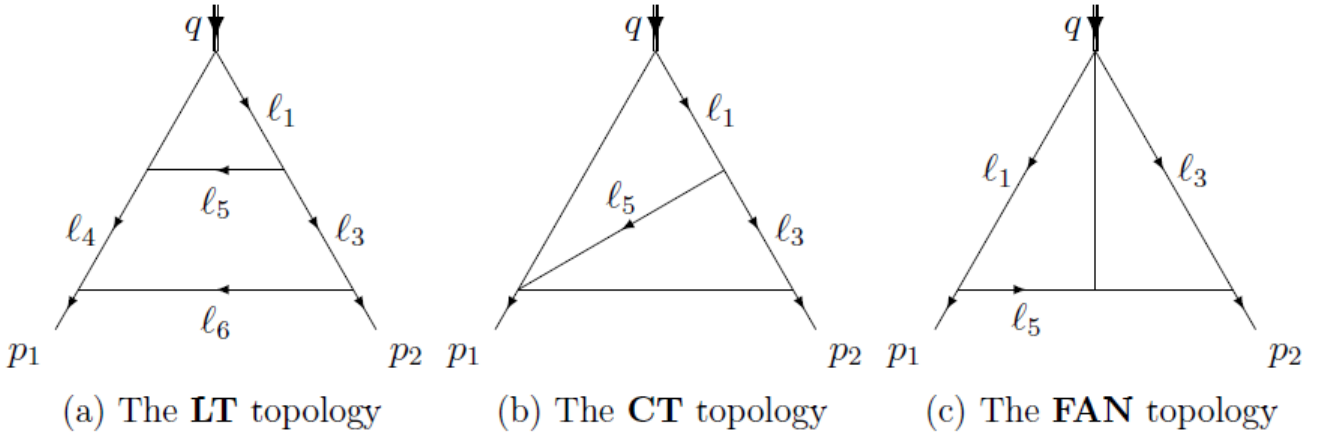


Figure 5.6: *The three maximally transcendental integrals considered in (5.3.1), (5.3.6) and (5.3.7)*

p_1 and p_2 can only be satisfied if ℓ_6 becomes soft, that is

$$\ell_6 \rightarrow 0, \quad \ell_4 \rightarrow p_1, \quad \ell_3 \rightarrow p_2. \quad (5.3.3)$$

In this limit, the second term of (5.3.1) vanishes since $\ell_3 - p_2 = \ell_6 \rightarrow 0$. The first term becomes

$$-q^2 \frac{\text{Tr}(p_1 \ell_3 p_2 \ell_1)}{8\epsilon(\ell_3, p_1, p_2)} \rightarrow -q^2 \frac{2|\ell_1|1}{4\langle 12 \rangle}, \quad (5.3.4)$$

where $8\epsilon(\ell_3, p_1, p_2)$ is the Jacobian.⁵ After restoring the remaining propagators we are left with

$$\frac{2\epsilon(\ell_1, p_1, p_2)}{\ell_1^2(\ell_1 - p_2)^2(q - \ell_1)^2}, \quad (5.3.5)$$

which reproduces the one-loop integrand of the one-loop form factor, given earlier in (5.2.7).

Other examples of integrals with different topologies that satisfy the three-particle cut condition are depicted in Figures 5.3(b) and 5.3(c). The definitions of the integrals

⁵This Jacobian arises from re-writing the δ -functions of the cut momenta, $\ell_3^2 = \ell_4^2 = 0$, in terms of p_1, p_2 and ℓ_6 .

as well as their values are listed below:

$$\begin{aligned}
\mathbf{CT}(q^2) &= \int \frac{d^D \ell_1 d^D \ell_3}{(i\pi^{D/2})^2} \frac{\text{Tr}(p_1, p_2, \ell_3, \ell_1)}{\ell_1^2 (p_1 + p_2 - \ell_1)^2 \ell_3^2 (\ell_1 - \ell_3)^2 (\ell_3 - p_2)^2} \\
&= \left(\frac{-q^2 e^{\gamma_E}}{\mu^2} \right)^{-2\epsilon} \left[-\frac{\pi}{4\epsilon^2} + \frac{7\pi^3}{24} + \mathcal{O}(\epsilon) \right],
\end{aligned} \tag{5.3.6}$$

$$\begin{aligned}
\mathbf{FAN}(q^2) &= \int \frac{d^D \ell_1 d^D \ell_3}{(i\pi^{D/2})^2} \frac{\text{Tr}(p_1, p_2, \ell_3, \ell_1)}{\ell_1^2 \ell_3^2 (p_1 + p_2 - \ell_1 - \ell_3)^2 (\ell_1 - p_1)^2 (\ell_3 - p_2)^2} \\
&= \left(\frac{-q^2 e^{\gamma_E}}{\mu^2} \right)^{-2\epsilon} \left[-\frac{\pi}{4\epsilon^2} + \frac{7\pi^3}{24} + \mathcal{O}(\epsilon) \right].
\end{aligned} \tag{5.3.7}$$

Note that the ϵ expansion of (5.3.6) and (5.3.7) agree up to $\mathcal{O}(1)$. It is simple to show that these integrals satisfy the properties discussed earlier, for example by setting $\{\ell_1, \ell_3, \ell_5\}$ on shell in **CT** and $\{\ell_1, p_1, \ell_5\}$ in **FAN** and similarly for all other possible three-vertex cuts.

The reductions of the integrals considered in this section in terms of scalar master integrals through IBP identities can be found in Appendix A.

Chapter 6

Massive Amplitudes on the Coulomb Branch

In this chapter we present previously unpublished work on loop-level amplitudes on the Coulomb Branch of $\mathcal{N} = 4$ sYM. We exploit a convenient choice of parametrization for massive momenta to compute one-loop amplitudes with massive external states for the first time. We find that both gauge invariance and five-dimensional momentum conservation lead to a constrained basis of massive box integrals. A basis may also be derived at two loops, although these integrals remain to be computed.

6.1 One-Loop 4-Point Integrand from Unitarity

In this section we compute the one-loop four point amplitude with two massive external particles in transverse polarisation. A natural approach is to consider cuts of the four-point super-amplitude. First we consider the s -channel cut with both massive particles on the same side:

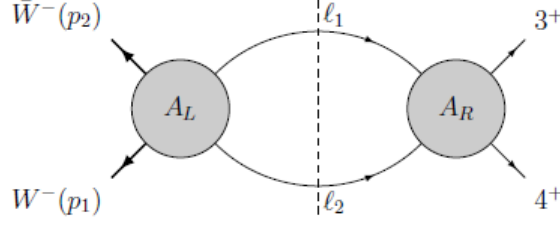


Figure 6.1: *The massless s-cut.*

$$\mathcal{A}|_{\text{s-cut}} = \int d^4\ell \, d^8\eta \, \mathcal{A}_L \mathcal{A}_R. \quad (6.1.1)$$

We can split the R-symmetry indices to write the fermionic delta function factor in the integrand as:

$$\begin{aligned} \delta_{12,L} \times \delta_{12,R} = & \left[\delta_L^{(4)}(\dots + |\ell_1\rangle\eta_{\ell_1 a} + |\ell_2\rangle\eta_{\ell_2 a}) + \frac{m\langle 1^\perp 2^\perp \rangle}{\langle 1^\perp q \rangle \langle q 2^\perp \rangle} \delta_L^{(2)}(\langle q^{i^\perp} \rangle \eta_{ia}) \right] \\ & \times \left[1 - \frac{[1^\perp q][q 2^\perp]}{m[1^\perp 2^\perp]} \delta^{(2)}(\mu_i \eta_{ia}) \right] \times \delta_R^{(4)}(|\ell_1\rangle\eta_{\ell_1 a} + |\ell_2\rangle\eta_{\ell_2 a} + \dots) \end{aligned} \quad (6.1.2)$$

for $R = 1, 2$ and similarly for $R = 3, 4$. Note that since the massive legs are all external the $\delta^{(2)}$ terms are independent of loop momenta; therefore, we can pull the $\delta_R^{(4)}$ associated with the massless amplitude on the right hand side of the cut through the other delta functions thus factoring out the tree amplitude. We then find:

$$\mathcal{A}|_{\text{s-cut}} = \mathcal{A}^{(0)} s_{12}^\perp \frac{\text{tr}(\ell_1 \ell_2 p_3 p_4)}{(\ell_1 \cdot p_4)(\ell_2 \cdot p_3)((\ell_1 - p_2)^2 + m^2)} \quad (6.1.3)$$

where $s_{ij}^\perp = 2(p_i^\perp \cdot p_j^\perp)$. This reduces by standard methods to

$$\mathcal{A}|_{\text{s-cut}} = \mathcal{A}^{(0)} s_{12}^\perp (t + m^2) \frac{1}{(\ell_1 \cdot p_4)((\ell_1 - p_2)^2 + m^2)} \quad (6.1.4)$$

corresponding to the cut of a 2-mass hard box integral with one massive internal leg. In the t -channel there are two different assignments of massive legs which must be considered separately.

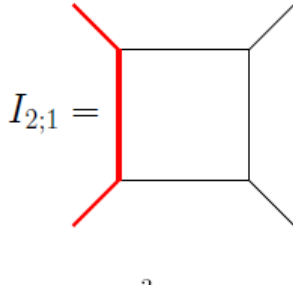


Figure 6.2: *The integral arising from the s -cut. The thick lines represent massive propagators.*

Now that there are massive legs in the cut, we must reconsider the terms involving combinations of lower-order δ s; however, since each $\delta^{(2)}$ contributes only one loop power of η , it is easy to see that these do not contribute. Thus, for the first diagram with adjacent momenta we reproduce the result of the massless s -cut and extract the integral $I_{2;1}$. We shall leave the second cut for now, and consider the problematic case of two internal massive lines.

Here, we must finally consider all η components of the superamplitude. Since the k -functions are not the simple ratios of the two mass case, we cannot simply extract a factor of the tree amplitude; more problematically, we must consider all combinations of fermionic delta functions appearing in the cut. As both k -functions and the arguments of the $\delta^{(2)}$ depend on the reference momentum q , these give rise to a large slew of terms containing lightcone propagators arising from such cross terms which resist simplification. The simplest of these comes from the term proportional to

$$\begin{aligned} & \delta_R^{(4)}(|\ell_1\rangle\eta_{\ell_1} + |\ell_2\rangle\eta_{\ell_2} + \dots)\bar{K}_L\delta_L^{(2)}(\langle qi^\perp\rangle\eta_{ia})\frac{[q\ell_1][q\ell_2]}{[\ell_1\ell_2]}\delta_R^{(2)}(\mu_i\eta_{ia}) \\ & = m^2\frac{\langle q\ell_2\rangle}{[\ell_1\ell_2]}\left(\frac{\langle\ell_1\ell_2\rangle}{\langle q\ell_2\rangle} + \frac{\langle\ell_11\rangle}{\langle q1\rangle} + \frac{\langle\ell_12\rangle}{\langle q2\rangle}\right). \end{aligned} \quad (6.1.5)$$

All this is very messy, and how to interpret these lightcone integrals is not clear. Fortunately, we do not have to, as described in the next section.

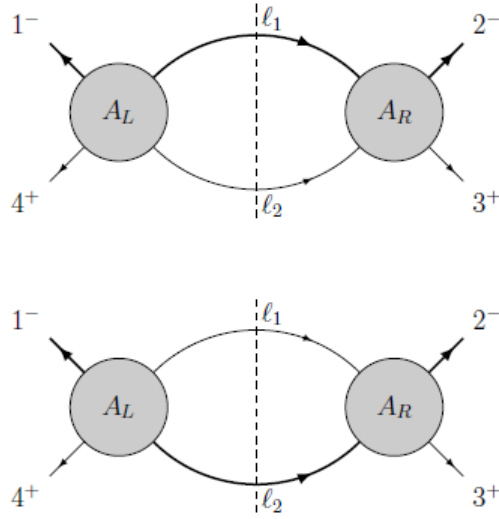


Figure 6.3: *The two cuts in the t -channel, with differing configurations of internal masses.*

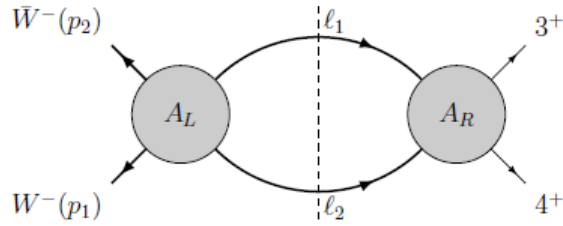


Figure 6.4: *The cut in the s -channel with massive cut propagators.*

6.1.1 Three-Vertex Cuts and the Basis of Integrals

Unitarity on the level of superamplitudes runs into problems with lightcone integrals, but it does give us some clues as to what integral functions can contribute. Are the integrals glimpsed in the massless s -cut and t -cut all that can appear? The answer, it turns out, is, yes. Recall the transverse momentum conservation condition $\sum_i m_i = 0$. This implies that there are always an even number of massive particles in any amplitude. Therefore, we can write down the full set of massive box functions and

by taking cuts around the corners exclude any with an odd number of masses at any vertex. For the 4-point amplitude, this leaves us with the following three topologies:

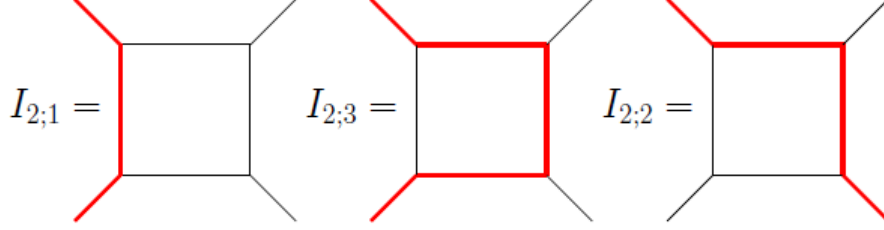


Figure 6.5: *The three integrals contributing to the 4-point 2-mass amplitude.*

6.1.2 Coefficients

Since we have identified a basis of box integrals, we can simply extract the coefficients from quadruple cuts. Since the three-point amplitudes are merely those of the massless theory with appropriately perped momenta;

$$A_3^{(0)}(W_1^-, W_2^-, g_3^+) = \frac{\langle 1^\perp 2^\perp \rangle^3}{\langle 2^\perp 3 \rangle \langle 3 1^\perp \rangle}. \quad (6.1.6)$$

we can immediately write down the answer:

$$c_n = (p_1^\perp \cdot p_2^\perp)(p_2^\perp \cdot p_3)A_4^{(0)} \quad (6.1.7)$$

which is the same for all configurations of internal masses. Hence:

$$A_4^{(1)}(W_1^-, W_2^-, g_3^+, g_4^+) = (s^\perp - m^2)(t^\perp - m^2)A_4^{(0)}(I_{2;3}(s, t) + I_{2;1}(s, t)) \quad (6.1.8)$$

$$A_4^{(1)}(W_1^-, g_2^+, W_3^-, g_4^+) = (s^\perp - m^2)(t^\perp - m^2)A_4^{(0)}(I_{2;2}(s, t) + I_{2;2}(t, s)) \quad (6.1.9)$$

Note the different integrals which appear for the split helicity and non-split helicity case, and that these integrals come with different divergences in the $1/\epsilon$ expansion.

6.2 Higher Point Amplitudes

Applying the same criteria, we find no new integrals beyond six points. The full set of one loop integrals is given below:

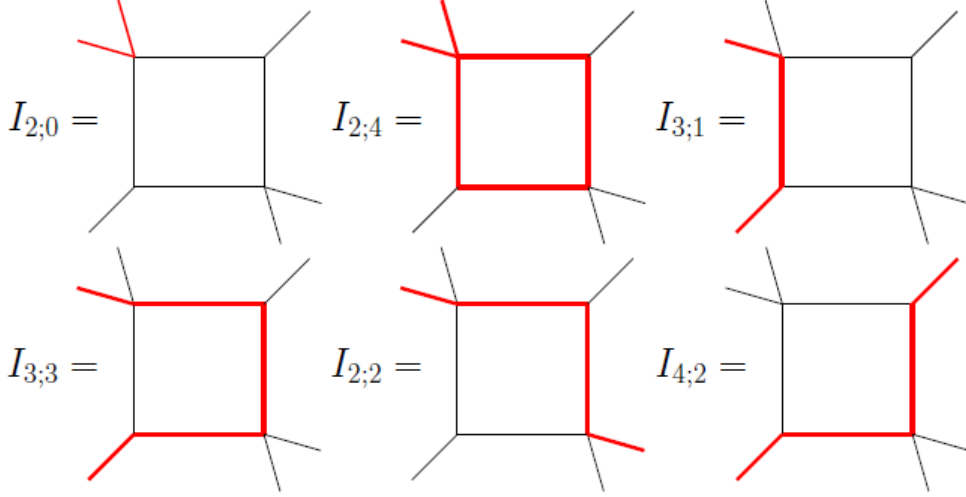


Figure 6.6: *The Basis of one-loop massive integrals on the Coulomb Branch. Bold lines indicate massive legs.*

The values of all these integrals can be found in A.

To find the coefficients, it is now most advantageous to go to a particular q -frame. Setting $q \rightarrow p_3$ we can write the Coulomb Branch tree-level W -gluon amplitude in the form of the Parke-Taylor amplitude with appropriately perped momenta, eg.

$$A(W_1^-, \bar{W}_2^-, g_3^+, g_4^+) = \frac{\langle 1^+ 2^+ \rangle^3}{\langle 2^+ 3 \rangle \langle 3 4 \rangle \langle 4 1^+ \rangle} \quad (6.2.1)$$

while the four-point UHV amplitude takes the intriguing form

$$A_4^{\text{UHV}} = \frac{m^4 (s - m^2)}{(t - m^2)^2 (u - m^2)}. \quad (6.2.2)$$

It should be noted that this choice of frame is *not* compatible with the linear orthogonality condition required for the factorised form of the Superamplitude; one can have either a simple superspace structure or simple component amplitudes.

With this form of the tree amplitude, it is easy to see that the contributions from cuts containing only MHV and $\overline{\text{MHV}}$ vertices, as at four points, are identical to those in the conformal case with appropriately perped momenta. The cuts containing UHV amplitudes require more care, as these at first sight appear to contribute lightcone integrals. We illustrate their vanishing for the five-point case

$$c_{15;\text{UHV}} = \frac{s_{15} - m^2}{[(\ell_1 - p_5)^2 - m^2][(\ell_1 - p_1)^2 - m^2]^2} \frac{(\langle \ell_1 2 \rangle [\ell_3 3] \langle \ell_3 \ell_4 \rangle)^3}{\langle 2 \ell_2 \rangle \langle \ell_1 \ell_2 \rangle [3 \ell_2] [\ell_2 \ell_3] \langle \ell_3 \rangle \langle 4 \ell_4 \rangle}. \quad (6.2.3)$$

Note the three lightcone propagators which appear as a factor. However, exploiting the kinematics we can write:

$$c_{\text{UHV}} \propto A^{\text{tree}} \langle \ell_4 | p_4 | \ell_3 \rangle = 0 \quad (6.2.4)$$

and similarly for the contribution with a $\overline{\text{UHV}}$ corner. Therefore we see that the full one-loop amplitude has no lightcone contributions and is given purely in terms of the Feynman integrals, with q -dependence captured by the coefficients alone.

6.3 The Two-Loop Integrand

We may also use the vertex condition to deduce which integrals may appear at two loops and higher. For instance, for the four-point amplitude with adjacent massive legs, we find the following integrals:

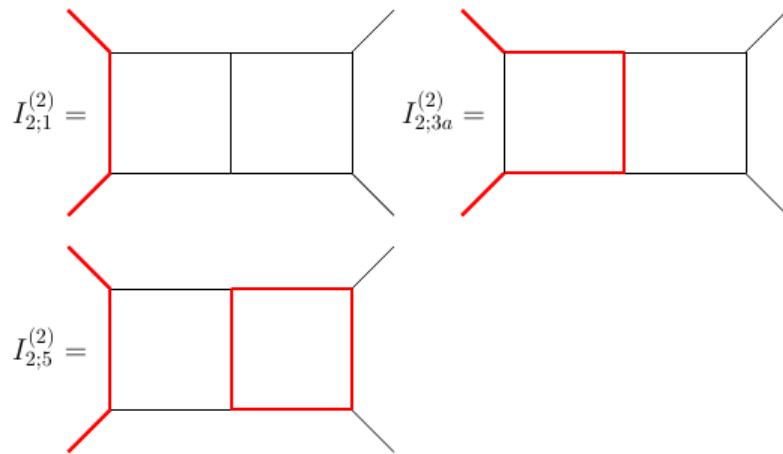


Figure 6.7: *The integrals appearing at four points, at two loops.*

Unfortunately, their values are not known beyond an expansion for small masses. It would be very interesting to see if the BDS ansatz and its violation holds on the Coulomb branch.

Appendix A

A Menagerie of Integral Functions

In this appendix, we state the values of various integral functions which appear in this thesis, and review the computation of the integrals described in 5.3.

A.1 Massless Scalar Box Functions

The zero-mass box in $4 + \epsilon$ dimensions is given by

$$F^{0m}(s, t) = \frac{1}{\epsilon^2} \left[\left(\frac{s}{\mu^2} \right)^{-\epsilon} + \left(\frac{t}{\mu^2} \right)^{-\epsilon} \right] + \log^2 \left(\frac{s}{t} \right) + \pi^2. \quad (\text{A.1.1})$$

The two-mass easy box function is given

$$\begin{aligned} F^{2m\epsilon}(s, t, P^2, Q^2) &= \int \frac{d^d \ell}{(2\pi)^d} \frac{1}{\ell^2 (\ell - P)^2 (\ell - P - q)^2 (\ell + p)^2} \\ &= \frac{1}{\epsilon^2} \left[\left(\frac{-s}{\mu^2} \right)^{-\epsilon} + \left(\frac{-t}{\mu^2} \right)^{-\epsilon} - \left(\frac{P^2}{\mu^2} \right)^{-\epsilon} - \left(\frac{Q^2}{\mu^2} \right)^{-\epsilon} \right] \\ &\quad + \text{Li}_2(1 - aP^2) + \text{Li}_2(1 - aQ^2) - \text{Li}_2(1 - as) - \text{Li}_2(1 - at) \end{aligned} \quad (\text{A.1.2})$$

where the invariants $s = (p + P)^2$ and $t = (P + q)^2$ and a is the combination

$$a = \frac{P^2 + Q^2 - s - t}{P^2 Q^2 - st}. \quad (\text{A.1.3})$$

The expression to all orders in ϵ is

$$\begin{aligned}
F^{2me}(s, t, P^2, Q^2) &= \frac{1}{\epsilon^2} \left[\left(\frac{-s}{\mu^2} \right)^{-\epsilon} + \left(\frac{-t}{\mu^2} \right)^{-\epsilon} - \left(\frac{P^2}{\mu^2} \right)^{-\epsilon} - \left(\frac{Q^2}{\mu^2} \right)^{-\epsilon} \right. \\
&+ \left(\frac{a}{1-aP^2} \right)^\epsilon {}_2F_1 \left(\epsilon, \epsilon; 1+\epsilon; \frac{1}{1-aP^2} \right) + \left(\frac{a}{1-aQ^2} \right)^\epsilon {}_2F_1 \left(\epsilon, \epsilon; 1+\epsilon; \frac{1}{1-aQ^2} \right) \\
&\left. - \left(\frac{a}{1-s} \right)^\epsilon {}_2F_1 \left(\epsilon, \epsilon; 1+\epsilon; \frac{1}{1-as} \right) - \left(\frac{a}{1-at} \right)^\epsilon {}_2F_1 \left(\epsilon, \epsilon; 1+\epsilon; \frac{1}{1-at} \right) \right]
\end{aligned} \tag{A.1.4}$$

A.2 Scalar Triangles

The two-loop ladder triangle is given by

$$\begin{aligned}
\text{LT}(q^2, \epsilon) &= \int \frac{d^d \ell_1 d^d \ell_3}{(2\pi)^d} \frac{1}{\ell_1^2 \ell_3^2 (\ell_1 - q)^2 (\ell_1 - \ell_3)^2 (\ell_3 - p_1)^2 (\ell_3 - q)^2} \\
&= (-q^2)^{-2\epsilon} e^{\gamma\epsilon} \frac{1}{\epsilon} \left[\frac{1}{2\epsilon} G(2, 2) + G_3(2 + \epsilon, 1, 1) \right. \\
&\quad \left. - 2G(2, 1) \left(\frac{1}{\epsilon} G_3(2, 1, 1 + \epsilon) + G_3(1, 1, 1) \right) \right] \\
&= (-q^2)^{-2\epsilon} \left[\frac{1}{\epsilon^4} + \frac{5\pi^2}{24\epsilon^2} + \frac{29}{6\epsilon} \zeta_3 + \frac{3}{32} \pi^4 + \mathcal{O}(\epsilon) \right]
\end{aligned} \tag{A.2.1}$$

on

where the epsilon expansion has been taken around $d = 4$ and

$$\begin{aligned}
G(x, y) &= \frac{\Gamma(x + y + \epsilon - 2) \Gamma(2 - \epsilon - x) \Gamma(2 - \epsilon - y)}{\Gamma(x) \Gamma(y) \Gamma(4 - x - y - 2\epsilon)} \\
G_3(x, y, z) &= \frac{\Gamma(2 - x - z - \epsilon) \Gamma(2 - y - z - \epsilon) \Gamma(-2 + x + y + z + \epsilon)}{\Gamma(x) \Gamma(y) \Gamma(4 - x - y - z - 2\epsilon)}.
\end{aligned} \tag{A.2.2}$$

The crossed triangle is given

$$CT(q^2, \epsilon) = (-q^2)^{-2\epsilon} \left[\frac{1}{\epsilon^4} - \frac{\pi^2}{\epsilon^2} - \frac{83}{3\epsilon} \zeta_3 - \frac{59}{120} \pi^4 + \mathcal{O}(\epsilon) \right] \tag{A.2.3}$$

A.3 Transcendental Integrals In Three Dimensions

In order to compute the integrals found in 5.3, we reduce to master integrals using IBP relations as automated by the package FIRE [110]. To do this, we must write them full in terms of propagators. Defining these as follows

$$\begin{array}{ccccccc} P_1 & P_2 & P_3 & P_4 & P_5 & P_6 & P_7 \\ \hline \ell_1^2 & (\ell_1 - p_1 - p_2)^2 & \ell_3^2 & (\ell_1 + \ell_3 - p_1)^2 & (\ell_1 - \ell_3)^2 & (\ell_3 - p_2)^2 & (\ell_1 - p_1)^2 \end{array}$$

the crossed triangle can be written as

$$\begin{aligned} \mathbf{XT}(q^2) = \frac{q^2}{2} & \left(\mathbf{1}^- \mathbf{2}^- \mathbf{6}^+ + \mathbf{1}^- \mathbf{3}^- \mathbf{6}^+ - \mathbf{1}^- - \mathbf{1}^- \mathbf{6}^+ \mathbf{7}^- + \mathbf{2}^- \mathbf{4}^- \mathbf{6}^+ \right. \\ & - \mathbf{2}^- \mathbf{5}^- \mathbf{6}^+ - \mathbf{2}^- \mathbf{6}^+ \mathbf{7}^- - \mathbf{4}^- \mathbf{6}^+ \mathbf{7}^- \\ & + \mathbf{5}^- \mathbf{6}^+ \mathbf{7}^- + \mathbf{5}^- \mathbf{6}^+ \mathbf{7}^- + \mathbf{6}^+ \mathbf{7}^- \mathbf{7}^- \\ & \left. - q^2 \mathbf{3}^- \mathbf{6}^+ - q^2 \mathbf{4}^- \mathbf{6}^+ \mathbf{7}^- \right) G_{NP}(1, 1, 1, 1, 1, 0, 0) \end{aligned} \quad (\text{A.3.1})$$

where $G_{NP}(1, 1, 1, 1, 1, 0, 0)$ is the scalar integral with the crossed triangle topology.

Replacing P_4 with $(\ell_3 - p_1 - p_2)^2$ the ladder triangle takes the form

$$\begin{aligned} \mathbf{LT}(q^2) = \frac{q^2}{2} & \left(-\mathbf{1}^- \mathbf{3}^- \mathbf{6}^+ + \mathbf{1}^- - \mathbf{2}^- \mathbf{4}^- \mathbf{6}^- + \mathbf{2}^- \right. \\ & + \mathbf{3}^- \mathbf{6}^+ \mathbf{7}^- + q^2 \mathbf{1}^- \mathbf{6}^+ + \mathbf{2}^- \mathbf{6}^+ + q^2 \mathbf{3}^- \mathbf{6}^+ \\ & \left. + q^2 \mathbf{4}^- \mathbf{6}^+ - q^2 \mathbf{6}^+ \mathbf{7}^- - q^2 - q^4 \mathbf{6}^+ \right) G_P(1, 1, 1, 1, 1, 0, 0). \end{aligned} \quad (\text{A.3.2})$$

The integral \mathbf{CT} can be expressed using the same propagators as the ladder as

$$\begin{aligned} \mathbf{CT}(q^2) = & \left(\frac{1}{2} \mathbf{1}^- \mathbf{2}^- \mathbf{6}^+ - \frac{1}{2} \mathbf{1}^- \mathbf{4}^- + \frac{q^2}{2} \mathbf{1}^- \mathbf{4}^- \mathbf{6}^+ - \frac{q^2}{2} \mathbf{2}^- \mathbf{4}^- \mathbf{4}^- \mathbf{6}^+ + \frac{1}{2} \mathbf{2}^- \mathbf{4}^- \right. \\ & + \frac{q^2}{2} \mathbf{2}^- \mathbf{4}^- \mathbf{6}^+ - \frac{1}{2} \mathbf{3}^- \mathbf{4}^- \mathbf{6}^+ \mathbf{7}^- + \frac{q^2}{2} \mathbf{2}^- \mathbf{3}^- \mathbf{6}^+ + \frac{1}{2} \mathbf{4}^- \mathbf{4}^- \mathbf{6}^+ \mathbf{7}^- - \frac{q^2}{2} \mathbf{4}^- \mathbf{4}^- \mathbf{6}^+ \\ & \left. - \frac{q^2}{2} \mathbf{4}^- \mathbf{5}^- \mathbf{6}^+ - \frac{q^2}{2} \mathbf{4}^- - \frac{q^2}{2} \mathbf{4}^- \mathbf{6}^+ \mathbf{7}^- - \frac{q^2}{2} \mathbf{4}^- \mathbf{6}^+ \right) G_P(1, 1, 1, 1, 1, 0, 0) \end{aligned} \quad (\text{A.3.3})$$

To write **FAN** we use a different set of propagators

P_1	P_2	P_3	P_4	P_5	P_6	P_7
$(\ell_1 - p_1)^2$	ℓ_1^2	ℓ_3^2	$(\ell_3 - p_2)^2$	$(\ell_1 + \ell_3 - p_1 - p_2)^2$	$(\ell_3 + \ell_1)^2$	$(\ell_1 + p_2)^2$

so that

$$\begin{aligned}
\mathbf{FAN}(q^2) = & \frac{1}{2} \left(\mathbf{1}^- \mathbf{2}^- - \mathbf{1}^- \mathbf{3}^- + \mathbf{1}^- \mathbf{4}^- - \mathbf{1}^- \mathbf{7}^- - \mathbf{2}^- \mathbf{5}^- \right. \\
& + \mathbf{2}^- \mathbf{6}^- - \mathbf{2}^- \mathbf{7}^- + \mathbf{3}^- \mathbf{7}^- - q^2 \mathbf{3}^- - \mathbf{4}^- \mathbf{7}^- \\
& \left. + \mathbf{7}^- - \mathbf{6}^- \mathbf{7}^- + q^2 \mathbf{6}^- + \mathbf{7}^- \mathbf{7}^- - q^2 \mathbf{7}^- \right) G_{\mathbf{FAN}}(1, 1, 1, 1, 1, 0, 0) \quad (\text{A.3.4})
\end{aligned}$$

The master integrals that appear at two loops, in particular in the reduction of our result (5.2.24), are given in $D = 3 - 2\epsilon$ dimensions by the following expressions:

$$\mathbf{SUNSET}(q^2) = \text{---} \bigcirc \text{---} = - \left(\frac{-q^2}{\mu^2} \right)^{-2\epsilon} \frac{\Gamma(\frac{1}{2} - \epsilon)^3 \Gamma(2\epsilon)}{\Gamma(\frac{3}{2} - 3\epsilon)} \quad (\text{A.3.5})$$

$$\mathbf{TRI}(q^2) = \text{---} \bigcirc \text{---} = -(-q^2)^{-1} \left(\frac{-q^2}{\mu^2} \right)^{-2\epsilon} \frac{\Gamma(\frac{1}{2} - \epsilon)^2 \Gamma(-2\epsilon) \Gamma(\frac{3}{2} + \epsilon) \Gamma(2 + 2\epsilon)}{\epsilon(1 + 2\epsilon)^2 \Gamma(\frac{1}{2} - 3\epsilon)} \quad (\text{A.3.6})$$

$$\mathbf{GLASS}(q^2) = \text{---} \bigcirc \bigcirc \text{---} = (-q^2)^{-1} \left(\frac{-q^2}{\mu^2} \right)^{-2\epsilon} \frac{\Gamma(\frac{1}{2} - \epsilon)^4 \Gamma(\frac{1}{2} + \epsilon)^2}{\Gamma(1 - 2\epsilon)^2} \quad (\text{A.3.7})$$

$$\begin{aligned}
\mathbf{TrianX}(q^2) = & \text{---} \triangle \text{---} = (-q^2)^{-3} \left(\frac{-q^2}{\mu^2} \right)^{-2\epsilon} e^{-2\gamma_E \epsilon} \left[\frac{4\pi}{\epsilon^2} + \frac{\pi(3 + 8 \log 2)}{\epsilon} \right. \\
& - \frac{2\pi}{3} (81 + 4\pi^2 + 6 \log 2 (4 \log 2 - 9)) + \frac{\pi}{6} \left(-\pi^2 (7 + 40 \log 2) \right. \\
& \left. \left. + 8(69 + 6 \log 2 + 2 \log^2 2 (8 \log 2 - 27) - 113\zeta_3) \right) \epsilon + \mathcal{O}(\epsilon) \right], \quad (\text{A.3.8})
\end{aligned}$$

where we use the conventions of [111] for the integration measure. The first three of these integrals are planar and their expressions in all orders in ϵ can be easily obtained by first computing their Mellin-Barnes representations most conveniently using the

MB and `barnesroutines` packages by David Kosower. The expansion around $\epsilon = 0$ of the **TRI** and **GLASS** topologies has uniform degree of transcendentality, while this is not the case for the **SUNSET** and **TrianX** topologies. The reductions to master integrals are then given by:

$$\begin{aligned} \mathbf{XT}(q^2) &= \frac{7(D-3)(3D-10)(3D-8)}{2(D-4)^2(2D-7)} \mathbf{SUNSET}(q^2) \\ &+ (-q^2) \frac{5(D-3)(3D-10)}{2(D-4)(2D-7)} \mathbf{TRI}(q^2) + (-q^2)^3 \frac{D-4}{4(2D-7)} \mathbf{TrianX}(q^2). \end{aligned} \quad (\text{A.3.9})$$

$$\mathbf{LT}(q^2) = \frac{8-3D}{D-3} \mathbf{SUNSET}(q^2) + q^2 (\mathbf{GLASS}(q^2) - \mathbf{TRI}(q^2)), \quad (\text{A.3.10})$$

$$\mathbf{CT}(q^2) = \mathbf{FAN}(q^2) = \left(\frac{1}{4\epsilon} - \frac{3}{2} \right) \mathbf{SUNSET}(q^2). \quad (\text{A.3.11})$$

A.4 Massive Boxes in Four Dimensions

The fully massive box integral was computed by t'Hooft and Veltman in [112], and was given in a compact form in [113]. The results presented here for divergent integrals are taken from appropriate limits of those presented in [113]. The denominator in Feynman parametrization depends on the Cayley matrix

$$Y_{ij} = m_i^2 + m_j^2 + p_{ij}^2 \quad (\text{A.4.1})$$

and the final results often depend on the roots $r_{ij,l}$ of the equation

$$m_i^2 + Y_{ij}x + m_j^2x^2 = 0 \quad (\text{A.4.2})$$

which may be written

$$r_{ij,1} = (m_i/m_j)x_{ij}, \quad r_{ij,2} = (m_j/m_i)x_{ij}^{-1} \quad (\text{A.4.3})$$

where

$$x_{ij} = \frac{\sqrt{1 - 4m^2/p_{ij}^2} - 1}{\sqrt{1 - 4m^2/p_{ij}^2} + 1}. \quad (\text{A.4.4})$$

and we have also used the notation $x_{12} = x_s$, $x_{23} = x_t$. We also use the notation ¹

$$\mathcal{L}i_2(x_1, \dots, x_n) = \text{Li}_2 \left(1 - \prod_{i=1}^n x_i \right). \quad (\text{A.4.5})$$

The fully massive box is most concisely given by the formula

$$I(p_i, m_i) = \frac{1}{\sqrt{\det Y}} \sum_{k,l=1}^2 \left[(-1)^{k+1} \mathcal{L}i_2 \left(z_k, \frac{r_{23,l}}{r_{20,l}} \right) - \mathcal{L}i_2(-z_k, r_{03,l}) \right. \\ \left. - \mathcal{L}i_2 \left(-z_k r_{13,l}, \frac{r_{21,l}}{r_{20,l}} \right) + \mathcal{L}i_2(-z_k r_{13,l}, r_{01,l}) \right] \quad (\text{A.4.6})$$

where the z_k are defined in the following way

$$\det Y_{ij} = b^2 - 4ac \quad z_k = \frac{1}{2a} \left(-b \pm \sqrt{\det Y} \right) \quad (\text{A.4.7})$$

where $k = 1$ corresponds to $+$ and $k = 2$ to $-$. Finite integrals may be derived by taking appropriate limits of this expression.

The divergent integrals appearing in the four-point Coulomb Branch amplitudes are given by:

$$I_{2;1}(s, t) = \frac{1}{s(t - m^2)} \left[\frac{2}{\epsilon^2} + \frac{1}{\epsilon} \left[\log \left(\frac{m^2}{s} \right) + 2 \log \left(\frac{m^2}{t - m^2} \right) \right] \right. \\ \left. + 2 \log \left(\frac{m^2}{s} \right) \log \left(\frac{m^2}{t - m^2} \right) - \frac{5\pi^2}{6} \right], \quad (\text{A.4.8})$$

$$I_{2;2}(s, t) = \frac{1}{(s - m^2)(t - m^2)} \left[\frac{1}{\epsilon^2} + \frac{1}{\epsilon} \left[\log \left(\frac{m^2}{s - m^2} \right) + \log \left(\frac{m^2}{t - m^2} \right) \right] \right. \\ \left. + 2 \log \left(\frac{m^2}{s - m^2} \right) \log \left(\frac{m^2}{t - m^2} \right) \right], \quad (\text{A.4.9})$$

¹A natural analytic continuation can be made for complex masses.

$$I_{2;3}(s, t) = \frac{1}{m^2(t-m^2)} \frac{x_s}{1-x_s^2} \left[2\log(x_s) \left[-\frac{1}{\epsilon} - \log\left(\frac{m^2}{t-m^2}\right) + \log(1-x_s^2) \right] \right. \\ \left. + \text{Li}_2(x_s^2) + 2\text{Li}_2(1-x_2) - \frac{\pi^2}{6} \right], \quad (\text{A.4.10})$$

$$I_{4m}(s, t) = \frac{1}{m^2 s} \frac{x_t}{1-x_t^2} \log(x_t) \left[\frac{1}{\epsilon} + \log\left(\frac{m^2}{s}\right) \right]. \quad (\text{A.4.11})$$

The full n -point amplitudes with two massive legs also includes the divergent integrals:

$$I_{3;1} = \frac{1}{s(t-m^2) - (Q^2-m^2)(P^2-m^2)} \left[\left[\frac{1}{\epsilon} + 2\log\left(\frac{m^2}{m^2-P^2}\right) \right] \left(\log\left(\frac{m^2-P^2}{s}\right) - \log\left(\frac{m^2-t}{Q^2}\right) \right) \right. \\ \left. + 2\text{Li}_2\left(\frac{s-Q^2}{Q^2}\right) - \text{Li}_2\left(\frac{P^2-t}{m^2-t}\right) - 2\mathcal{L}i_2\left(\frac{m^2-P^2}{s}, \frac{Q^2}{m^2-t}\right) \right] \quad (\text{A.4.12})$$

$$I_{2;2} = \frac{1}{(m^2-s)(m^2-t) - (m^2-P^2)(m^2-Q^2)} \left[\frac{1}{\epsilon} \log\left(\frac{(m^2-P^2)(m^2-Q^2)}{(m^2-s)(m^2-t)}\right) \right. \\ + 2\text{Li}_2\left(1 - \frac{m^2-P^2}{m^2-s}\right) - 2\text{Li}_2\left(1 - \frac{m^2-P^2}{m^2-t}\right) \\ + 2\text{Li}_2\left(1 - \frac{m^2-Q^2}{m^2-t}\right) - 2\text{Li}_2\left(1 - \frac{m^2-Q^2}{m^2-s}\right) \\ + 2\text{Li}_2\left(1 - \frac{(m^2-Q^2)(m^2-P^2)}{(m^2-s)(m^2-t)}\right) + 2\log\left(\frac{m^2-s}{\mu^2}\right) \log\left(\frac{m^2-t}{\mu^2}\right) \\ - \log^2\left(\frac{m^2-P^2}{\mu^2}\right) - \log^2\left(\frac{m^2-Q^2}{\mu^2}\right) + \log\left(\frac{m^2-P^2}{m^2-t}\right) \log\left(\frac{m^2}{\mu^2}\right) \\ \left. + \log\left(\frac{m^2-Q^2}{\mu^2-s}\right) \log\left(\frac{m^2}{\mu^2}\right) \right] \quad (\text{A.4.13})$$

Appendix B

Material Ancillary to Chapters 4 and 5

B.1 Vanishing of form factors at large z

B.1.1 Bosonic form factors

In this appendix we consider a generic non-MHV bosonic form factor of the operator $\text{Tr}(\phi^2)$ and prove that, for a $[k, l]$ shift

$$\hat{\lambda}_k := \tilde{\lambda}_k + z\tilde{\lambda}_l, \quad \hat{\lambda}_l := \lambda_l - z\lambda_k, \quad (\text{B.1.1})$$

$F(z)$ vanishes as $z \rightarrow \infty$ if

$$(h_k, h_l) \text{ is equal to : } (0, +), (+, +), (-, +), (0, 0), (-, 0), (-, -). \quad (\text{B.1.2})$$

The proof is based on the MHV diagram expansion of form factors, and follows closely that for amplitudes presented in [5].

To begin with, it is immediate to see that an MHV form factor (4.1.3) with a $[k, l]$ shift vanishes as $z \rightarrow \infty$, with the only exception of the case $(h_k, h_l) = (+, 0)$.

Consider now a generic non-MHV form factor. Each MHV diagram contributing to its expansion is a product of MHV vertices, times propagators $1/L^2$. These propagators will either be independent of z , or vanish when $z \rightarrow \infty$. As in [5], the spinors $\lambda_L = L|\tilde{\xi}]$ associated to internal legs can also be made z -independent by choosing the reference spinor $\tilde{\xi}$ to be equal to $\tilde{\xi} = \tilde{\lambda}_l$. Thus, dangerous z -dependent terms can only arise from terms affected by the shifts in the external legs k and l .

For the cases where (h_k, h_l) is $(\pm, +)$ or $(0, +)$, only the denominators acquire z -dependence, and hence $F(z)$ vanishes at large z . By using anti-MHV diagrams we arrive at the same result for the case where (h_k, h_l) is equal to either $(-, -)$ or $(-, 0)$. The case $(h_k, h_l) = (0, 0)$ needs special attention. The case when k and l belong to the same MHV vertex has already been considered, and leads to a falloff of the diagram as $z \rightarrow \infty$. When k and l belong to different vertices, there will be at least one propagator depending on z , which will provide a factor of $1/z$ at large z . The vertex involving leg l behaves asymptotically as z^2/z^2 regardless of whether it is an MHV form factor or a conventional MHV vertex, while all other vertices are independent of z . We conclude that each MHV diagram falls off as $1/z$ at large z .

We mention here that the argument described above can also be applied to scattering amplitudes. Shifting two scalars makes the amplitude vanish as $z \rightarrow \infty$ provided that the scalars take the same $SU(4)$ indices.

B.1.2 Supersymmetric form factors

As we have shown in the previous appendix, the bosonic form factor vanishes at infinity for an $[i, j]$ shift if i and j are both scalars. Here we want to use supersymmetry to relate the large- z behaviour of generic supersymmetric form factors to that of form factors with legs i and j being both scalars. This will then prove the validity of the supersymmetric BCFW recursion relation for all supersymmetric form factors in

fashion similar to [95].

For supersymmetric non-chiral form factor $F(\lambda, \tilde{\lambda}, \eta_+, \tilde{\eta}^-)$, the $[i, j]$ shift is

$$\begin{aligned}\hat{\tilde{\lambda}}_i(z) &:= \tilde{\lambda}_i + z\tilde{\lambda}_j, & \hat{\lambda}_j &:= \lambda_j - z\lambda_i, \\ \hat{\eta}_{i,+} &:= \eta_{i,+} + z\eta_{j,+}, & \hat{\tilde{\eta}}_j^- &:= \tilde{\eta}_j^- - z\tilde{\eta}_i^-.\end{aligned}\quad (\text{B.1.3})$$

As in [95], we choose a particular transformation where

$$\bar{Q}_{\tilde{\zeta}} = \tilde{\zeta}_{\dot{\alpha}+} \bar{Q}^{\dot{\alpha}+}, \quad Q_{\xi} = \xi_{\alpha}^- Q_{\alpha}^-, \quad (\text{B.1.4})$$

where

$$\tilde{\zeta} = \frac{1}{[i\ j]} \left(-\tilde{\lambda}_i \eta_j + \tilde{\lambda}_j \eta_i \right), \quad \xi = \frac{1}{\langle i\ j \rangle} \left(-\lambda_i \tilde{\eta}_j + \lambda_j \tilde{\eta}_i \right). \quad (\text{B.1.5})$$

One can check that their action on the fermionic coordinates $\eta_{k,+}, \tilde{\eta}_k^-$ is

$$e^{\bar{Q}_{\tilde{\zeta}}} \eta_{k,+} := \eta'_{k,+} = \eta_{k,+} - \eta_{i,+} \frac{[kj]}{[ij]} + \eta_{j,+} \frac{[ki]}{[ij]}, \quad (\text{B.1.6})$$

$$e^{Q_{\xi}} \tilde{\eta}_k^- := \tilde{\eta}'_k^- = \tilde{\eta}_k^- - \tilde{\eta}_i^- \frac{\langle kj \rangle}{\langle ij \rangle} + \tilde{\eta}_j^- \frac{\langle ki \rangle}{\langle ij \rangle}, \quad (\text{B.1.7})$$

and in particular $e^{\bar{Q}_{\tilde{\zeta}}} \eta_{i,+} = e^{\bar{Q}_{\tilde{\zeta}}} \eta_{j,+} = e^{Q_{\xi}} \tilde{\eta}_i^- = e^{Q_{\xi}} \tilde{\eta}_j^- = 0$. Since the form factor is invariant under \bar{Q}^+ and Q_- transformations, i.e. $e^{\bar{Q}_{\tilde{\zeta}}} \mathcal{F} = e^{Q_{\xi}} \mathcal{F} = \mathcal{F}$ (see (4.2.41)),

we conclude that

$$\begin{aligned}& \mathcal{F}(\lambda_1, \tilde{\lambda}_1, \eta_{1,+}, \tilde{\eta}_1^-; \cdots; \lambda_i, \hat{\tilde{\lambda}}_i, \hat{\eta}_{i,+}, \hat{\tilde{\eta}}_i^-; \cdots; \hat{\lambda}_j, \tilde{\lambda}_j, \eta_{j,+}, \hat{\tilde{\eta}}_j^-; \cdots; \lambda_n, \tilde{\lambda}_n, \eta_{n,+}, \tilde{\eta}_n^-) \\ &= \mathcal{F}(\lambda_1, \tilde{\lambda}_1, \eta'_{1,+}, \tilde{\eta}'_1^-; \cdots; \lambda_i, \hat{\tilde{\lambda}}_i, 0, 0; \cdots; \hat{\lambda}_j, \tilde{\lambda}_j, 0, 0; \cdots; \lambda_n, \tilde{\lambda}_n, \eta'_{n,+}, \tilde{\eta}'_n^-). \quad (\text{B.1.8})\end{aligned}$$

Thus, we can always choose a supersymmetry transformation which sets i and j to be scalars. It is important to notice that under the $[i, j]$ shift, the transformed η'_+ and $\tilde{\eta}'^-$ variables are independent of z . The large- z behaviour of $\mathcal{F}(z)$ is therefore the same as that of the bosonic form factor with i and j being scalars. This case was considered in the previous appendix, and shown to fall off as $1/z$ at large z . Hence the statement is also true for the shifted supersymmetric form factor $\mathcal{F}(z)$. The proof

illustrated above concerned the large- z behaviour of the full non-chiral super form factor, but a very similar one applies to the form factor in chiral superspace, since the latter is related to the former by a half-Fourier transform in superspace.

B.2 Dual MHV rules

The momentum superspace is defined as

$$x_i - x_{i+1} = p_i = \lambda_i \tilde{\lambda}_i, \quad \theta_i - \theta_{i+1} = \lambda_i \eta_i, \quad (\text{B.2.1})$$

with the conventions

$$x_{ij} = x_i - x_j, \quad \theta_{ij} = \theta_i - \theta_j. \quad (\text{B.2.2})$$

We define the spinor $|\ell_{ij}\rangle$ as

$$|\ell_{ij}\rangle \equiv |x_{ij}\xi\rangle, \quad (\text{B.2.3})$$

where $|\xi\rangle$ is an arbitrary reference spinor.

The Feynman rules for dual MHV diagram are given as in Figure B.1. Originally this is used to calculate scattering amplitudes, here we use the same rules to calculate tree and one-loop super form factors.


The general dual MHV diagrams for NMHV tree and MHV one-loop are shown in figure B.2.

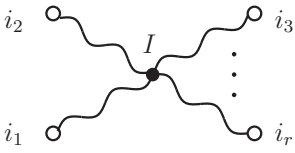
The dual diagram for NMHV tree case gives the

$$\frac{\langle i-1 \ i \rangle}{\langle i-1 \ \ell_{ij} \rangle \langle \ell_{ij} \ i \rangle} \frac{\langle j-1 \ j \rangle}{\langle j-1 \ \ell_{ij} \rangle \langle \ell_{ij} \ j \rangle} \frac{1}{x_{ij}^2} \int d^4 \eta_{ij} \delta^{0|8}(\ell_{ij} \eta_{ij} + \theta_{ij}), \quad (\text{B.2.4})$$

which can be easily translated in terms of the superconformally invariant R -function $R_{*,ij} = [* , i-1, i, j-1, j]$, which is

$$[i, j, k, l, m] \equiv \frac{\delta^{(4)}(\langle i \ j \ k \ l \rangle \chi_m + \text{cyclic terms})}{\langle i \ j \ k \ l \rangle \langle j \ k \ l \ m \rangle \langle k \ l \ m \ i \rangle \langle l \ m \ i \ j \rangle \langle m \ i \ j \ k \rangle}. \quad (\text{B.2.5})$$

(a)  $\frac{1}{x_{ij}^2} \int d^4 \eta_{ij} \delta^{0|8}(\ell_{ij} \eta_{ij} + \Theta_{ij})$

(b)  $g_{\text{YM}}^2 \int d^4 x_I d^8 \Theta_I \frac{1}{\langle \ell_{I i_1} \ell_{I i_2} \rangle \langle \ell_{I i_2} \ell_{I i_3} \rangle \cdots \langle \ell_{I i_{r-1}} \ell_{I i_r} \rangle \langle \ell_{I i_r} \ell_{I i_1} \rangle}$

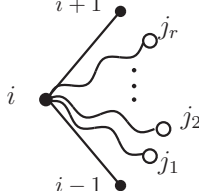
(c)  $\frac{\langle i-1 \ i \rangle}{\langle i-1 \ \ell_{ij_1} \rangle \langle \ell_{ij_1} \ell_{ij_2} \rangle \langle \ell_{ij_2} \ell_{ij_3} \rangle \cdots \langle \ell_{ij_{r-1}} \ell_{ij_r} \rangle \langle \ell_{ij_r} \ i \rangle}$

Figure B.1: Feynman rules for dual MHV diagrams. (a) Propagator. (b) Internal vertices. (c) External vertices.

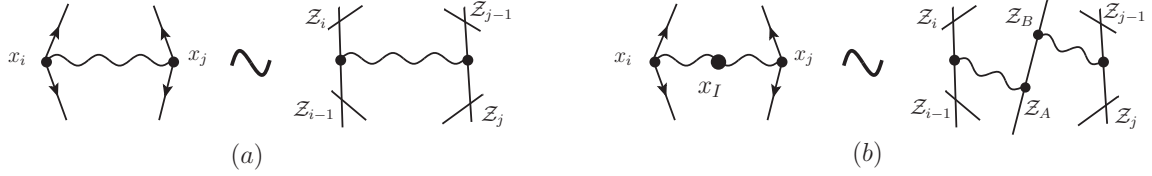


Figure B.2: Dual MHV diagrams for (a) NMHV tree, (b) MHV one-loop, and their diagrammatic correspondence between dual spacetime picture and momentum twistor picture.

The reference momentum twistor is chosen as $\mathcal{Z}_* = (0, \xi, 0)$.

Similarly, the MHV diagram for one-loop MHV case gives

$$g_{\text{YM}}^2 \int d^4 x_I d^8 \theta_I \frac{1}{\langle \ell_{iI} \ell_{Ij} \rangle \langle \ell_{Ij} \ell_{iI} \rangle} \frac{\langle i-1 \ i \rangle}{\langle i-1 \ \ell_{iI} \rangle \langle \ell_{iI} \ i \rangle} \frac{\langle j-1 \ j \rangle}{\langle j-1 \ \ell_{Ij} \rangle \langle \ell_{Ij} \ j \rangle} \frac{1}{x_{iI}^2} \int d^4 \eta_{iI} \delta^{0|8}(\ell_{iI} \eta_{iI} + \theta_{iI}) \frac{1}{x_{Ij}^2} \int d^4 \eta_{Ij} \delta^{0|8}(\ell_{Ij} \eta_{Ij} + \theta_{Ij}) , \quad (\text{B.2.6})$$

which is equivalent to the expression in terms of momentum twistor variables [101]

$$g_{\text{YM}}^2 \int d^{3|4} \mathcal{Z}_A \wedge d^{3|4} \mathcal{Z}_B [* , i-1, i, A, B'] [* , j-1, j, A, B''] , \quad (\text{B.2.7})$$

where

$$B' = (A, B) \cap (*, j-1, j) , \quad B'' = (A, B) \cap (*, i-1, i) . \quad (\text{B.2.8})$$

B.3 Properties of the box integral in ABJM

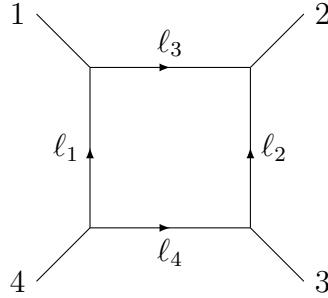


Figure B.3: *Four-point one-loop box.*

The box integral function (3.3.19) was constructed and used in [74], and has several interesting properties that have been exploited in the present work. This section presents and proves (some of) these properties.

B.3.1 Rotation by 90°

The first property we wish to discuss is what could be called a $\pi/2$ rotation symmetry. Focusing on the numerator of the box integrand,

$$N = s \text{Tr}(\ell_1 p_1 p_4) + \ell_1^2 \text{Tr}(p_1 p_2 p_4), \quad (\text{B.3.1})$$

we can eliminate ℓ_1 in favour of ℓ_3 and arrange to have only the external legs p_2, p_3, p_1 appear in the numerator. Using momentum conservation, we can re-write N as

$$N = (-t - u) \text{Tr}((\ell_3 + 1)p_1(-p_1 - p_2 - p_3)) + (\ell_3 + p_1) \text{Tr}(p_1 p_2(-p_1 - p_2 - p_3)) \quad (\text{B.3.2})$$

$$= - \left[t \text{Tr}(\ell_3 p_2 p_1) + \ell_3^2 \text{Tr}(p_2 p_3 p_4) \right] + \mathcal{R},$$

where

$$\mathcal{R} = s \text{Tr}(\ell_3 p_3 p_1) - u \text{Tr}(\ell_3 p_2 p_1) - 2(\ell_3 \cdot p_1) \text{Tr}(p_2 p_3 p_1). \quad (\text{B.3.3})$$

In three dimensions the loop momentum ℓ_3 can be expressed as a function of the external momenta p_1, p_2, p_3 as

$$\ell_3 = \alpha p_1 + \beta p_2 + \gamma p_3, \quad (\text{B.3.4})$$

where α, β, γ are arbitrary coefficients. When this identity is used in the expression for \mathcal{R} , we find that \mathcal{R} is identically zero in three dimensions. Hence

$$s \text{Tr}(\ell_1 p_1 p_4) + \ell_1^2 \text{Tr}(p_1 p_2 p_4) = -t \left(\text{Tr}(\ell_3 p_2 p_1) + \ell_3^2 \text{Tr}(p_2 p_3 p_4) \right). \quad (\text{B.3.5})$$

It is also interesting to write down explicitly the s - and t -cut of the one-loop box. Starting from the expression of the box integral

$$I(1, 2, 3, 4) := \int \frac{d^D \ell}{i\pi^{D/2}} \frac{N}{\ell^2 (\ell - p_1)^2 (\ell - p_1 - p_2)^2 (\ell + p_4)^2}, \quad (\text{B.3.6})$$

with N given in (B.3.1), we first consider the s -cut of this function. This gives

$$I(1, 2, 3, 4)|_{s\text{-cut}} = \frac{s \text{Tr}(\ell_1 p_1 p_4)}{\ell_3^2 \ell_4^2}, \quad (\text{B.3.7})$$

which upon using $\ell_3 = \ell_1 - p_1$ and $\ell_4 = -(\ell_1 + p_4)$ becomes

$$I(1, 2, 3, 4)|_{s\text{-cut}} = \frac{s\langle 41 \rangle}{\langle 4\ell_1 \rangle \langle \ell_1 1 \rangle}. \quad (\text{B.3.8})$$

Similarly the t -channel expression of the full integrand is

$$I(1, 2, 3, 4) = \frac{t \operatorname{Tr}(\ell_3 p_2 p_1) + \ell_3^2 \operatorname{Tr}(p_2 p_3 p_1)}{\ell_1^2 \ell_2^2 \ell_3^2 \ell_4^2}. \quad (\text{B.3.9})$$

The t -cut of $I(1, 2, 3, 4)$ is immediately written using the three-dimensional identity (B.3.5),

$$\begin{aligned} I(1, 2, 3, 4)|_{t\text{-cut}} &= -\frac{t \operatorname{Tr}(\ell_3 p_2 p_1)}{\ell_1^2 \ell_2^2} \\ &= \frac{t \langle 12 \rangle}{\langle 1 \ell_3 \rangle \langle \ell_3 2 \rangle}. \end{aligned} \quad (\text{B.3.10})$$

Finally, if we re-introduce the tree-level amplitude prefactor $\mathcal{A}^{(0)}(\bar{1}, 2, \bar{3}, 4) = 1/(\langle 12 \rangle \langle 23 \rangle)$, we can write down the two cuts of the one-loop amplitude,

$$\mathcal{A}^{(0)}(\bar{1}, 2, \bar{3}, 4) \times I(1, 2, 3, 4)|_{s\text{-cut}} = -\frac{\langle 34 \rangle}{\langle 4 \ell_1 \rangle \langle \ell_1 1 \rangle}, \quad (\text{B.3.11})$$

$$\mathcal{A}^{(0)}(\bar{1}, 2, \bar{3}, 4) \times I(1, 2, 3, 4)|_{t\text{-cut}} = \frac{\langle 23 \rangle}{\langle 1 \ell_3 \rangle \langle \ell_3 2 \rangle}. \quad (\text{B.3.12})$$

B.3.2 An identity for the s -channel cuts of $I(1, 2, 3, 4)$ and $I(1, 2, 4, 3)$

Here we discuss an intriguing property of the three-dimensional cuts of $I(1, 2, 3, 4)$. We consider the s -channel cut of this function and symmetrise it in the cut loop momenta ℓ_1 and ℓ_2 , where $\ell_1 + \ell_2 = p_1 + p_2$. The result we wish to show is that the symmmetrised three-dimensional cuts of $I(1, 2, 3, 4)$ and $I(1, 2, 4, 3)$ are in fact identical:

$$I(1, 2, 3, 4)|_{s\text{-cut}} + \ell_1 \leftrightarrow \ell_2 = I(1, 2, 4, 3)|_{s\text{-cut}} + \ell_1 \leftrightarrow \ell_2. \quad (\text{B.3.13})$$

In order to do so, we use (B.3.8) to write

$$\begin{aligned}
I(1, 2, 3, 4)|_{s\text{-cut}} + \ell_1 \leftrightarrow \ell_2 &= s\langle 41 \rangle \left(\frac{1}{\langle 4|\ell_1|1 \rangle} + \frac{1}{\langle 4|\ell_2|1 \rangle} \right) \\
&= s\langle 41 \rangle \left(\frac{\langle 4|\ell_1 + \ell_2|1 \rangle}{\langle 4|\ell_1|1 \rangle \langle 4|\ell_2|1 \rangle} \right) \\
&= \frac{s\langle 41 \rangle \langle 4|2|1 \rangle}{\langle 4|\ell_1|1 \rangle \langle 4|\ell_2|1 \rangle},
\end{aligned} \tag{B.3.14}$$

where in the last step momentum conservation was used. Again using (B.3.8) this time for the s -cut of $I(1, 2, 4, 3)$ one can write,

$$I(1, 2, 4, 3)|_{s\text{-cut}} = \frac{s\langle 31 \rangle}{\langle 3\ell_1 \rangle \langle \ell_1 1 \rangle}, \tag{B.3.15}$$

and hence

$$\begin{aligned}
I(1, 2, 4, 3)|_{s\text{-cut}} + \ell_1 \leftrightarrow \ell_2 &= s\langle 31 \rangle \left(\frac{\langle 3|\ell_1 + \ell_2|1 \rangle}{\langle 3|\ell_1|1 \rangle \langle 3|\ell_2|1 \rangle} \right) \\
&= \frac{\langle 31 \rangle \langle 3|2|1 \rangle}{\langle 3|\ell_1|1 \rangle \langle 3|\ell_2|1 \rangle}.
\end{aligned} \tag{B.3.16}$$

Next we compare (B.3.14) to (B.3.16):

$$\begin{aligned}
\frac{I(1, 2, 3, 4)|_{s\text{-cut}}}{I(1, 2, 4, 3)|_{s\text{-cut}}} &= \frac{\langle 41 \rangle \langle 4|2|1 \rangle \langle 3|\ell_1|1 \rangle \langle 3|\ell_2|1 \rangle}{\langle 31 \rangle \langle 3|2|1 \rangle \langle 4|\ell_1|1 \rangle \langle 4|\ell_2|1 \rangle} \\
&= \frac{\langle 1|4|2 \rangle \langle \ell_1|3|\ell_2 \rangle}{\langle 1|3|2 \rangle \langle \ell_1|4|\ell_2 \rangle} \\
&= 1,
\end{aligned} \tag{B.3.17}$$

thus proving (B.3.13).

Bibliography

- [1] R. Eden, P. Landshoff, D. Olive, and J. Polkinghorne. The Analytic S-matrix.
- [2] Zvi Bern, Lance J. Dixon, David C. Dunbar, and David A. Kosower. One loop n point gauge theory amplitudes, unitarity and collinear limits. *Nucl.Phys.*, B425:217–260, 1994.
- [3] Edward Witten. Perturbative gauge theory as a string theory in twistor space. *Commun.Math.Phys.*, 252:189–258, 2004.
- [4] Freddy Cachazo, Peter Svrcek, and Edward Witten. MHV vertices and tree amplitudes in gauge theory. *JHEP*, 0409:006, 2004.
- [5] Ruth Britto, Freddy Cachazo, Bo Feng, and Edward Witten. Direct proof of tree-level recursion relation in Yang-Mills theory. *Phys.Rev.Lett.*, 94:181602, 2005.
- [6] C.F. Berger, Z. Bern, L.J. Dixon, F. Febres Cordero, D. Forde, et al. An Automated Implementation of On-Shell Methods for One-Loop Amplitudes. *Phys.Rev.*, D78:036003, 2008.
- [7] Z. Bern, J.J.M. Carrasco, and Henrik Johansson. New Relations for Gauge-Theory Amplitudes. *Phys.Rev.*, D78:085011, 2008.

- [8] J.M. Drummond, J. Henn, G.P. Korchemsky, and E. Sokatchev. Dual superconformal symmetry of scattering amplitudes in N=4 super-Yang-Mills theory. *Nucl.Phys.*, B828:317–374, 2010.
- [9] Luis F. Alday and Juan Martin Maldacena. Gluon scattering amplitudes at strong coupling. *JHEP*, 0706:064, 2007.
- [10] Andreas Brandhuber, Paul Heslop, and Gabriele Travaglini. MHV amplitudes in N=4 super Yang-Mills and Wilson loops. *Nucl.Phys.*, B794:231–243, 2008.
- [11] Burkhard Eden, Paul Heslop, Gregory P. Korchemsky, and Emery Sokatchev. The super-correlator/super-amplitude duality: Part I. *Nucl.Phys.*, B869:329–377, 2013.
- [12] Nima Arkani-Hamed and Jaroslav Trnka. The Amplituhedron. 2013.
- [13] Nima Arkani-Hamed, Jacob L. Bourjaily, Freddy Cachazo, Alexander B. Goncharov, Alexander Postnikov, et al. Scattering Amplitudes and the Positive Grassmannian. 2012.
- [14] Vittorio Del Duca, Claude Duhr, and Vladimir A. Smirnov. An Analytic Result for the Two-Loop Hexagon Wilson Loop in N = 4 SYM. *JHEP*, 1003:099, 2010.
- [15] Oluf Tang Engelund and Radu Roiban. Correlation functions of local composite operators from generalized unitarity. *JHEP*, 1303:172, 2013.
- [16] Andreas Brandhuber, Omer Gurdogan, Robert Mooney, Gabriele Travaglini, and Gang Yang. Harmony of Super Form Factors. *JHEP*, 1110:046, 2011.
- [17] Andreas Brandhuber, mer Grdoan, Dimitrios Korres, Robert Mooney, and Gabriele Travaglini. Two-loop Sudakov Form Factor in ABJM. *JHEP*, 1311:022, 2013.

- [18] Lance J. Dixon. Calculating scattering amplitudes efficiently. 1996.
- [19] Stephen J. Parke and T.R. Taylor. An Amplitude for n Gluon Scattering. *Phys.Rev.Lett.*, 56:2459, 1986.
- [20] Frits A. Berends and W.T. Giele. Recursive Calculations for Processes with n Gluons. *Nucl.Phys.*, B306:759, 1988.
- [21] Ruth Britto, Freddy Cachazo, and Bo Feng. New recursion relations for tree amplitudes of gluons. *Nucl.Phys.*, B715:499–522, 2005.
- [22] Kasper Risager. A Direct proof of the CSW rules. *JHEP*, 0512:003, 2005.
- [23] R.E. Cutkosky. Singularities and discontinuities of Feynman amplitudes. *J.Math.Phys.*, 1:429–433, 1960.
- [24] Ruth Britto, Freddy Cachazo, and Bo Feng. Generalized unitarity and one-loop amplitudes in $N=4$ super-Yang-Mills. *Nucl.Phys.*, B725:275–305, 2005.
- [25] V.A. Smirnov. Feynman integral calculus. 2006.
- [26] Johannes M. Henn, Alexander V. Smirnov, and Vladimir A. Smirnov. Analytic results for planar three-loop four-point integrals from a Knizhnik-Zamolodchikov equation. *JHEP*, 1307:128, 2013.
- [27] Nima Arkani-Hamed, Jacob L. Bourjaily, Freddy Cachazo, and Jaroslav Trnka. Local Integrals for Planar Scattering Amplitudes. *JHEP*, 1206:125, 2012.
- [28] G. Passarino and M.J.G. Veltman. One Loop Corrections for $e^+ e^-$ Annihilation Into $\mu^+ \mu^-$ in the Weinberg Model. *Nucl.Phys.*, B160:151, 1979.
- [29] J. Gluza, K. Kajda, and T. Riemann. AMBRE: A Mathematica package for the construction of Mellin-Barnes representations for Feynman integrals. *Comput.Phys.Commun.*, 177:879–893, 2007.

- [30] Charalampos Anastasiou and Alejandro Daleo. Numerical evaluation of loop integrals. *JHEP*, 0610:031, 2006.
- [31] J.B. Tausk. Nonplanar massless two loop Feynman diagrams with four on-shell legs. *Phys.Lett.*, B469:225–234, 1999.
- [32] Steven Weinberg. Infrared photons and gravitons. *Phys.Rev.*, 140:B516–B524, 1965.
- [33] George F. Sterman and Maria E. Tejeda-Yeomans. Multiloop amplitudes and resummation. *Phys.Lett.*, B552:48–56, 2003.
- [34] Zvi Bern, Lance J. Dixon, and Vladimir A. Smirnov. Iteration of planar amplitudes in maximally supersymmetric Yang-Mills theory at three loops and beyond. *Phys.Rev.*, D72:085001, 2005.
- [35] Alfred H. Mueller. On the Asymptotic Behavior of the Sudakov Form-factor. *Phys.Rev.*, D20:2037, 1979.
- [36] John C. Collins. Algorithm to Compute Corrections to the Sudakov Form-factor. *Phys.Rev.*, D22:1478, 1980.
- [37] Ashoke Sen. Asymptotic Behavior of the Sudakov Form-Factor in QCD. *Phys.Rev.*, D24:3281, 1981.
- [38] Alexander M. Polyakov. Gauge Fields as Rings of Glue. *Nucl.Phys.*, B164:171–188, 1980.
- [39] Jean-Loup Gervais and A. Neveu. The Slope of the Leading Regge Trajectory in Quantum Chromodynamics. *Nucl.Phys.*, B163:189, 1980.
- [40] V.S. Dotsenko and S.N. Vergeles. Renormalizability of Phase Factors in the Nonabelian Gauge Theory. *Nucl.Phys.*, B169:527, 1980.

- [41] G.P. Korchemsky and A.V. Radyushkin. Renormalization of the Wilson Loops Beyond the Leading Order. *Nucl.Phys.*, B283:342–364, 1987.
- [42] A.I. Vainshtein, Valentin I. Zakharov, and Mikhail A. Shifman. Higgs Particles. *Sov.Phys.Usp.*, 23:429–449, 1980.
- [43] Luis F. Alday, Johannes M. Henn, Jan Plefka, and Theodor Schuster. Scattering into the fifth dimension of N=4 super Yang-Mills. *JHEP*, 1001:077, 2010.
- [44] Johannes M. Henn. Dual conformal symmetry at loop level: massive regularization. *J.Phys.*, A44:454011, 2011.
- [45] Johannes M. Henn. Scattering amplitudes on the Coulomb branch of N=4 super Yang-Mills. *Nucl.Phys.Proc.Suppl.*, 205-206:193–198, 2010.
- [46] G. Mack and Abdus Salam. Finite component field representations of the conformal group. *Annals Phys.*, 53:174–202, 1969.
- [47] Sidney R. Coleman and Roman Jackiw. Why dilatation generators do not generate dilatations? *Annals Phys.*, 67:552–598, 1971.
- [48] V.M. Braun, G.P. Korchemsky, and Dieter Mueller. The Uses of conformal symmetry in QCD. *Prog.Part.Nucl.Phys.*, 51:311–398, 2003.
- [49] Lars Brink, John H. Schwarz, and Joel Scherk. Supersymmetric Yang-Mills Theories. *Nucl.Phys.*, B121:77, 1977.
- [50] Marcus T. Grisaru, M. Rocek, and W. Siegel. ZERO VALUE FOR THE THREE LOOP BETA FUNCTION IN N=4 SUPERSYMMETRIC YANG-MILLS THEORY. 1988.
- [51] William E. Caswell and Daniela Zanon. Zero Three Loop Beta Function in the $N = 4$ Supersymmetric Yang-Mills Theory. *Nucl.Phys.*, B182:125, 1981.

- [52] L.V. Avdeev and O.V. Tarasov. The Three Loop Beta Function in the $N = 1$, $N = 2$, $N = 4$ Supersymmetric Yang-Mills Theories. *Phys.Lett.*, B112:356–358, 1982.
- [53] Stanley Mandelstam. Light Cone Superspace and the Ultraviolet Finiteness of the N=4 Model. *Nucl.Phys.*, B213:149–168, 1983.
- [54] Paul S. Howe, K.S. Stelle, and P.K. Townsend. The Relaxed Hypermultiplet: An Unconstrained N=2 Superfield Theory. *Nucl.Phys.*, B214:519, 1983.
- [55] Lars Brink, Olof Lindgren, and Bengt E.W. Nilsson. The Ultraviolet Finiteness of the N=4 Yang-Mills Theory. *Phys.Lett.*, B123:323, 1983.
- [56] Paul S. Howe, K.S. Stelle, and Peter C. West. A Class of Finite Four-Dimensional Supersymmetric Field Theories. *Phys.Lett.*, B124:55, 1983.
- [57] V.P. Nair. A Current Algebra for Some Gauge Theory Amplitudes. *Phys.Lett.*, B214:215, 1988.
- [58] Nathaniel Craig, Henriette Elvang, Michael Kiermaier, and Tracy Slatyer. Massive amplitudes on the Coulomb branch of N=4 SYM. *JHEP*, 1112:097, 2011.
- [59] Stefan Dittmaier. Weyl-van der Waerden formalism for helicity amplitudes of massive particles. *Phys.Rev.*, D59:016007, 1998.
- [60] Andreas Brandhuber, Gabriele Travaglini, and Gang Yang. Analytic two-loop form factors in N=4 SYM. *JHEP*, 1205:082, 2012.
- [61] Andreas Brandhuber, Bill Spence, Gabriele Travaglini, and Gang Yang. Form Factors in N=4 Super Yang-Mills and Periodic Wilson Loops. *JHEP*, 1101:134, 2011.

- [62] David J. Gross and Paul F. Mende. The High-Energy Behavior of String Scattering Amplitudes. *Phys.Lett.*, B197:129, 1987.
- [63] Juan Maldacena and Alexander Zhiboedov. Form factors at strong coupling via a Y-system. *JHEP*, 1011:104, 2010.
- [64] J.M. Drummond, J. Henn, G.P. Korchemsky, and E. Sokatchev. The hexagon Wilson loop and the BDS ansatz for the six-gluon amplitude. *Phys.Lett.*, B662:456–460, 2008.
- [65] Ofer Aharony, Oren Bergman, Daniel Louis Jafferis, and Juan Maldacena. N=6 superconformal Chern-Simons-matter theories, M2-branes and their gravity duals. *JHEP*, 0810:091, 2008.
- [66] Sean A. Hartnoll, Christopher P. Herzog, and Gary T. Horowitz. Building a Holographic Superconductor. *Phys.Rev.Lett.*, 101:031601, 2008.
- [67] Arthur E. Lipstein. Integrability of N = 6 Chern-Simons Theory. 2011.
- [68] J.A. Minahan and K. Zarembo. The Bethe ansatz for superconformal Chern-Simons. *JHEP*, 0809:040, 2008.
- [69] Dongmin Gang, Yu-tin Huang, Eunkyung Koh, Sangmin Lee, and Arthur E. Lipstein. Tree-level Recursion Relation and Dual Superconformal Symmetry of the ABJM Theory. *JHEP*, 1103:116, 2011.
- [70] Konstantin Wiegandt. Equivalence of Wilson Loops in $\mathcal{N} = 6$ super Chern-Simons matter theory and $\mathcal{N} = 4$ SYM Theory. *Phys.Rev.*, D84:126015, 2011.
- [71] Ilya Bakhmatov. On $AdS_4 \times CP^3 T-duality$. *Nucl.Phys.*, B847 : 38 – –53, 2011.
- [72] Andreas Brandhuber, Gabriele Travaglini, and Congkao Wen. All one-loop amplitudes in N=6 superconformal Chern-Simons theory. *JHEP*, 1210:145, 2012.

- [73] Yu-tin Huang and Arthur E. Lipstein. Amplitudes of 3D and 6D Maximal Superconformal Theories in Supertwistor Space. *JHEP*, 1010:007, 2010.
- [74] Wei-Ming Chen and Yu-tin Huang. Dualities for Loop Amplitudes of N=6 Chern-Simons Matter Theory. *JHEP*, 1111:057, 2011.
- [75] Till Bargheer, Florian Loebbert, and Carlo Meneghelli. Symmetries of Tree-level Scattering Amplitudes in N=6 Superconformal Chern-Simons Theory. *Phys.Rev.*, D82:045016, 2010.
- [76] Seiji Terashima. On M5-branes in N=6 Membrane Action. *JHEP*, 0808:080, 2008.
- [77] Andreas Brandhuber, Bill J. Spence, and Gabriele Travaglini. One-loop gauge theory amplitudes in N=4 super Yang-Mills from MHV vertices. *Nucl.Phys.*, B706:150–180, 2005.
- [78] Ruth Britto, Bo Feng, Radu Roiban, Marcus Spradlin, and Anastasia Volovich. All split helicity tree-level gluon amplitudes. *Phys.Rev.*, D71:105017, 2005.
- [79] A. Galperin, E. Ivanov, S. Kalitsyn, V. Ogievetsky, and E. Sokatchev. Unconstrained N=2 Matter, Yang-Mills and Supergravity Theories in Harmonic Superspace. *Class.Quant.Grav.*, 1:469–498, 1984.
- [80] A.S. Galperin, E.A. Ivanov, V.I. Ogievetsky, and E.S. Sokatchev. Harmonic superspace. 2001.
- [81] Burkhard Eden, Paul Heslop, Gregory P. Korchemsky, and Emery Sokatchev. The super-correlator/super-amplitude duality: Part II. *Nucl.Phys.*, B869:378–416, 2013.
- [82] Marcus T. Grisaru, H.N. Pendleton, and P. van Nieuwenhuizen. Supergravity and the S Matrix. *Phys.Rev.*, D15:996, 1977.

- [83] Marcus T. Grisaru and H.N. Pendleton. Some Properties of Scattering Amplitudes in Supersymmetric Theories. *Nucl.Phys.*, B124:81, 1977.
- [84] Michelangelo L. Mangano and Stephen J. Parke. Multiparton amplitudes in gauge theories. *Phys.Rept.*, 200:301–367, 1991.
- [85] Henriette Elvang, Daniel Z. Freedman, and Michael Kiermaier. SUSY Ward identities, Superamplitudes, and Counterterms. *J.Phys.*, A44:454009, 2011.
- [86] Kenneth A. Intriligator. Bonus symmetries of N=4 superYang-Mills correlation functions via AdS duality. *Nucl.Phys.*, B551:575–600, 1999.
- [87] B. Eden, Paul S. Howe, C. Schubert, E. Sokatchev, and Peter C. West. Extremal correlators in four-dimensional SCFT. *Phys.Lett.*, B472:323–331, 2000.
- [88] B. Eden, C. Schubert, and E. Sokatchev. Three loop four point correlator in N=4 SYM. *Phys.Lett.*, B482:309–314, 2000.
- [89] Lance J. Dixon, E.W. Nigel Glover, and Valentin V. Khoze. MHV rules for Higgs plus multi-gluon amplitudes. *JHEP*, 0412:015, 2004.
- [90] Yu-tin Huang. Non-Chiral S-Matrix of N=4 Super Yang-Mills. 2011.
- [91] Zvi Bern, Lance J. Dixon, David C. Dunbar, and David A. Kosower. Fusing gauge theory tree amplitudes into loop amplitudes. *Nucl.Phys.*, B435:59–101, 1995.
- [92] Zvi Bern, Lance J. Dixon, and David A. Kosower. Two-loop $g \rightarrow g$; g splitting amplitudes in QCD. *JHEP*, 0408:012, 2004.
- [93] Henriette Elvang, Daniel Z. Freedman, and Michael Kiermaier. Proof of the MHV vertex expansion for all tree amplitudes in N=4 SYM theory. *JHEP*, 0906:068, 2009.

- [94] Andreas Brandhuber, Paul Heslop, and Gabriele Travaglini. A Note on dual superconformal symmetry of the N=4 super Yang-Mills S-matrix. *Phys.Rev.*, D78:125005, 2008.
- [95] Nima Arkani-Hamed, Freddy Cachazo, and Jared Kaplan. What is the Simplest Quantum Field Theory? *JHEP*, 1009:016, 2010.
- [96] L.J. Mason and David Skinner. The Complete Planar S-matrix of N=4 SYM as a Wilson Loop in Twistor Space. *JHEP*, 1012:018, 2010.
- [97] Mathew Bullimore, L.J. Mason, and David Skinner. MHV Diagrams in Momentum Twistor Space. *JHEP*, 1012:032, 2010.
- [98] Andreas Brandhuber, Bill Spence, Gabriele Travaglini, and Gang Yang. A Note on Dual MHV Diagrams in N=4 SYM. *JHEP*, 1012:087, 2010.
- [99] J.M. Drummond, G.P. Korchemsky, and E. Sokatchev. Conformal properties of four-gluon planar amplitudes and Wilson loops. *Nucl.Phys.*, B795:385–408, 2008.
- [100] Luis F. Alday and Juan Maldacena. Comments on gluon scattering amplitudes via AdS/CFT. *JHEP*, 0711:068, 2007.
- [101] Andrew Hodges. Eliminating spurious poles from gauge-theoretic amplitudes. *JHEP*, 1305:135, 2013.
- [102] Andreas Brandhuber, Bill Spence, and Gabriele Travaglini. From trees to loops and back. *JHEP*, 0601:142, 2006.
- [103] Nima Arkani-Hamed, Jacob L. Bourjaily, Freddy Cachazo, Simon Caron-Huot, and Jaroslav Trnka. The All-Loop Integrand For Scattering Amplitudes in Planar N=4 SYM. *JHEP*, 1101:041, 2011.

- [104] Bo Feng, Yin Jia, and Rijun Huang. Relations of loop partial amplitudes in gauge theory by Unitarity cut method. *Nucl.Phys.*, B854:243–275, 2012.
- [105] Dongsu Bak and Soo-Jong Rey. Integrable Spin Chain in Superconformal Chern-Simons Theory. *JHEP*, 0810:053, 2008.
- [106] S. Caron-Huot and Yu-tin Huang. The two-loop six-point amplitude in ABJM theory. *JHEP*, 1303:075, 2013.
- [107] Marco S. Bianchi, Matias Leoni, Andrea Mauri, Silvia Penati, and Alberto Santambrogio. Scattering in ABJ theories. *JHEP*, 1112:073, 2011.
- [108] Marco S. Bianchi, Matias Leoni, Andrea Mauri, Silvia Penati, and Alberto Santambrogio. Scattering Amplitudes/Wilson Loop Duality In ABJM Theory. *JHEP*, 1201:056, 2012.
- [109] Donovan Young. Form Factors of Chiral Primary Operators at Two Loops in ABJ(M). *JHEP*, 1306:049, 2013.
- [110] A.V. Smirnov. Algorithm FIRE – Feynman Integral REduction. *JHEP*, 0810:107, 2008.
- [111] M. Czakon. Automatized analytic continuation of Mellin-Barnes integrals. *Comput.Phys.Commun.*, 175:559–571, 2006.
- [112] Gerard 't Hooft and M.J.G. Veltman. Scalar One Loop Integrals. *Nucl.Phys.*, B153:365–401, 1979.
- [113] A. Denner and S. Dittmaier. Scalar one-loop 4-point integrals. *Nucl.Phys.*, B844:199–242, 2011.